NEUROTOXIC AND GENETIC IMPACTS ON DOPAMINERGIC NEURON DEATH AND REGENERATION IN ZEBRAFISH (*DANIO RERIO)*

MICHAEL KALYN

Thesis submitted to the University of Ottawa
in partial fulfillment of the requirements for the
Doctorate in Philosophy degree in Biology

Department of Biology
Faculty Science
University of Ottawa

PREFACE

This thesis was written following the format of "a series of articles" in partial fulfillment of the Ph.D. requirements for the Biology Department at the University of Ottawa. Chapter 2 entitled "Comprehensive analysis of neurotoxin-induced ablation of dopaminergic neurons in zebrafish larvae" by Michael Kalyn, Khang Hua, David Wong, Suzita Moor and Marc Ekker has been published in the journal Biomedicines (2020) 8, 1. Chapter 3 entitled "Neuroprotective screening of natural phenolics in an MPTP-induced model of Parkinson's disease using zebrafish" by Michael Kalyn, Dana Elsaid and Marc Ekker is currently in preparation for submission. Chapter 4 entitled "Cerebroventricular microinjections of MPTP on adult zebrafish induces dopaminergic neuronal death, mitochondrial fragmentation and sensorimotor impairments" by Michael Kalyn and Marc Ekker has been published in the journal Frontiers in Neuroscience (2021) 15, 718244. Chapter 5 entitled "Differential roles of *nr4a2* (*nurr1*) paralogs in the brain and behavior of zebrafish" by Michael Kalyn, Rose Garvey, Jory Curry, Jan Mennigen, Hyojin Lee, and Marc Ekker is currently in preparation for submission. Contributions to other publications not within this thesis are listed in Appendix B.

ACKNOWLEDGMENTS

First and foremost I would like to extend my deepest gratitude to Dr. Marc Ekker for giving me the opportunity to work within his lab and for his continuous support and guidance throughout my Ph.D. I have won the lottery with Marc when it comes to supervisors. Marc is a world leading scientist in zebrafish research that is never too busy for his students. He has always encouraged opportunity, growth and professionalism inside and out of the lab and is a primary reason for my continued scientific invigoration. I am not only thankful for the opportunities given to present my work at international meetings, but for the overwhelming amounts of wisdom and inspiration you have provided me with over the years. I'm truly grateful for everything .

I would next like to thank all members of the Ekker lab, past and present, who have continued to motivate me with their passion for science and for making the lab a welcoming place to be each day. I am particularly thankful for Khang Hua, Simon Monis, Emily Yu, Rawan Merhi and Hellen Weishchutz Mendes who have become close friends and have always provided me with intangible advice about both research and life. I am also grateful for our amazing technician and even better human being, Vishal Saxena, who has watched my scientific career grow and supported it through and through. I thank you for your patience in experimental troubleshooting and for your guidance. You have become an amazing friend to me and I cherish the countless talks about life, movies and culture we have had over the years. I am also thankful for the assistance given to me by undergraduate honour's and research program students.

I would like to thank my Committee members, Dr. Marie-Andree Akimenko, Dr. Jan Mennigen and Dr. Bill Willmore who have dedicated much of their time to provide me with invaluable feedback and input. I would especially like to thank Jan for the opportunity to collaborate with him and his lab, for his constant support and for always having an open door policy about anything, research related or not. I am also thankful for ACVS for maintaining the zebrafish lines, to the science store and to all University of Ottawa staff that makes our research possible. Furthermore, I would like to extend my thanks to Andrew Ochalski and Jacky Liang from the Ottawa Core Histology Facility for microscopy training and consultation.

Most importantly, I would like to dedicate this work to my amazing family who never shied from encouraging my scientific career. I am incredibly fortunate to have this network of amazing support that continues to motivate me to be a better person every day. Thank you immensely to my loving parents, sister, brother in-law, niece and partner. None of this could have been accomplished without all of you.

STATEMENT OF CONTRIBUTIONS

The thesis titled “Neurotoxic and genetic impacts on dopaminergic neuron death and regeneration in zebrafish (*Danio rerio*)” is composed of four related studies. Three of the four were conducted in a collaboration with other researchers. Chapters 2 and 4 are published, chapters 3 and 5 are in preparation for submission.

Chapter 2: “Comprehensive analysis of neurotoxin-induced ablation of dopaminergic neurons in zebrafish larvae”. Dr. Marc Ekker and Dr. David Wong helped in the study conceptualization and manuscript review. Khang Hua helped with the data curation, analysis and manuscript revision. Zaid Karaki helped perform technical replicates. I conceptualized the study, performed all of the experiments, curated and analyzed the data and wrote the manuscript.

Chapter 3: “Neuroprotective screening of natural phenolics in an MPTP-model of Parkinson’s Disease using zebrafish”. Dr. Marc Ekker helped in with manuscript revisions. Dana Elsaid helped performed technical replicates of experiments. I conceptualized the study, performed the experiments, analyzed the data and wrote the manuscript.

Chapter 4: “Cerebroventricular microinjections of MPTP on adult zebrafish induces dopaminergic neuronal death, mitochondrial fragmentation and sensorimotor impairments”. Dr. Marc Ekker helped in the conceptualization of the study and manuscript revisions. I conceptualized the study, performed the experiments, analyzed the data and wrote the manuscript.

Chapter 5: Differential roles of *nr4a2* (*nurr1*) paralogs in the brain and behavior of zebrafish”. Dr. Marc Ekker helped conceptualize the study and with manuscript review. Vishal Saxena helped perform the CRISPR-Cas9 microinjections. Rose Garvey helped curate data for *nr4a2b* mutants. Jory Curry helped with light/dark behavior analysis. Dr. Hyojin Lee helped with

metabolism data analysis and discussion. Dr. Jan Mennigen provided metabolism feedback. I conceptualized the study, performed all experiments outside of light/dark behavioral and metabolic assays, analyzed the data and wrote the manuscript.

ABSTRACT

The neurotransmitter dopamine (DA) plays a critical role in regulating cognition, behavior and physiology in humans. Imbalances in DA or damage to the dopaminergic (DAnergic) system can be consequential to neurological health and lead to the progression of psychiatric and neurodegenerative disorders that include but are not limited to schizophrenia and Parkinson's disease (PD). PD, in particular, is associated with debilitating motor symptoms that result following a considerable loss of midbrain DAnergic neurons. This loss is likely correlated to a combinatory insult of environmental exposures and genetic predisposition, as the majority of cases are idiopathic in nature. To date there remains to be a curative treatment, thus much research has been done to generate models of sporadic PD through the use of neurotoxic exposures in addition to the search for plant-derived chemicals that confer neuroprotection prior to the onset of symptoms to improve the quality of life for those at risk.

Here, we established a model to mimic pathologies observed in sporadic PD using both larval and adult zebrafish. The larval model examined the neurotoxic impact of 1-methyl-4-phenyl-1,2,3,6-tetrahydropyridine (MPTP), 1-methyl-4-phenyl-pyridinium (MPP^+), 6-hydroxydopamine (6-OHDA), rotenone, and paraquat to delineate the optimal compound that exerts the largest degree of diencephalic DAnergic cell death and motor perturbance using Tg(*dat:eGFP*) transgenic zebrafish. Using this model, we also showed that between ascorbic acid (AA), ferulic acid (FA) and vanillic acid (VA), pretreatment of FA elicits that largest neuroprotective effect against MPTP-induced oxidative stress and neurodegeneration. The optimization of a reliable adult model to investigate mitochondrial impacts in vivo was then addressed through introducing MPTP into the cerebroventricular fluid of Tg(*dat:tom20 MLS:mCherry*) transgenic zebrafish. Gene expression

and immunostaining data suggest that MPTP induces DAnergic mitochondrial fragmentation through mitophagy activation.

Moreover, we sought to examine the genetic influence over DAnergic production and disorders by targeting *nr4a2* paralogs for CRISPR-Cas9 mediated mutagenesis. Despite a similar deleterious effect observed in DAnergic populations, *nr4a2a* and *nr4a2b* mutants each possess variable effects on neurotrophins, metabolism, other neurotransmitters and behavior. *nr4a2a* mutants more closely resemble PD pathologies, whereas *nr4a2b* mutants exhibit phenotypes reminiscent of psychiatric disorders. Throughout DAnergic regeneration, *nr4a2a* was also shown to mimic *shha* expression patterns suggestive of a predominant role over *nr4a2b* in differentiation. Further gene expression data may also indicate that *notch1a* drives the proliferative stages of DAnergic progenitors prior to the shift to *shha* signaling for differentiation.

In sum, we believe the sporadic and genetic models of DA deficiencies offer an opportunistic tool to study molecular mechanisms of DAnergic regeneration, potential therapeutics and to gain a better understanding of mitochondrial influence in neurological pathologies.

TABLE OF CONTENTS

LIST OF FIGURES

LIST OF TABLES

LIST OF ABBREVIATIONS

6-OHDA	6-hydroxydopamine
AA	ascorbic acid
AADC	aromatic amino acid decarboxylase
BBB	blood-brain barrier
bp	base pairs
BrdU	5-Bromo-2-deoxyuridine
Cas9	CRISPR-associated protein 9
cDNA	complementary deoxyribonucleic acid
CNS	central nervous system
CRISPR	clustered regularly interspaced short palindromic repeats
CVF	cerebroventricular fluid
CVMI	cerebroventricular microinjections
DA	dopamine
DAnergic	dopaminergic
DAT	dopamine transporter
dpf	day(s) post-fertilization
dpt	day(s) post-treatment
DMSO	dimethyl sulfoxide
Drp1	dynamin-related protein 1
DSB	double-strand break
eGFP	enhanced green fluorescent protein
ETC	electron transport chain
FA	ferulic acid
FIS1	mitochondrial fission 1 protein
GABA	gamma-aminobutyric acid
Gad	glutamic acid decarboxylase
hpf	hour(s) post-fertilization
KO	knockout
Kb	kilobases
LC_{50}	median lethal dose
L-DOPA	L-3,4-dihydroxyphenylalanine
MAO-B	monoamine oxidase B
mpf	month(s) post-fertilization
mpt	month(s) post-treatment
MPP+	1-methyl-4-phenyl-pyridinium
MPTP	1-methyl-4-phenyl-1,2,3,6-tetrahydropyridine
mRNA	messenger ribonucleic acid
Mfn1	mitofusin 1
Mfn2	mitofusin 2
NAc	nucleus accumbens
NHEJ	non-homologous end joining
NR4A2	nuclear orphan receptor 4 family 2 member A
OB	olfactory bulbs
Opa1	optic atrophy 1

Paraquat	methyl viologen dichloride hydrate
PCR	polymerase chain reaction
PD	Parkinson’s disease
PINK1	PTEN-induced putative kinase protein 1
PPv	periventricular pretectal nucleus
PT	posterior tuberculum
qRT-PCR	real-time quantitative reverse transcription polymerase chain reaction
ROS	reactive oxygen species
SEM	standard error of the mean
SNpc	substantia nigra pars compacta
SNP	single nucleotide polymorphism
Tel	telencephalon
Tg	transgenic
TH	tyrosine hydroxylase
UTR	untranslated region
VA	vanillic acid
vDC	ventral diencephalon
VMAT2	vesicular monoamine transporter 2
VTA	ventral tegmentum area
WT	wild-type

CHAPTER 1: GENERAL INTRODUCTION

1.1. Dopamine biosynthesis

Dopamine (DA) is a small catecholaminergic neurotransmitter that possesses an extensive influence over the periphery (PNS) and central nervous systems (CNS). DA has been at the fore-front of vertebrate neurological studies for decades due to its involvement within a wide array of both simple and complex behaviors that range from movement to pleasure to memory (Wise 2004). The biosynthesis of DA originates in the liver with the catalysis of tyrosine (from dietary phenylalanine) mediated through phenylalanine hydroxylase. Blood-borne tyrosine is subsequently transported into the brain, crossing the blood-brain-barrier (BBB), to then enter dopaminergic (DAnergic) neurons. Within the cytosol of DAnergic neurons, tyrosine hydroxylase (TH) adds an hydroxyl group to the *meta* position of tyrosine to facilitate the conversion into dihydroxyphenylalanine (L-DOPA). This step is hallmarked as the rate-limiting component of this reaction due to the oxygenic requirements and the hindering recruitment of tetrahydrobiopterin, an essential cofactor for TH (Daubner et al. 2011; Ayano 2016). TH is also inhibited by DA through a negative feedback loop that competes with tetrahydrobiopterin. Aromatic amino acid decarboxylase (AADC or DOPA decarboxylase) continues the reaction to act on L-DOPA to generate cytosolic DA. The latter is then actively transported by vesicular monoamine transporter 2 (VMAT2) to be packaged and aggregate within pre-synaptic vesicular compartments. Following a spike in action potential of DAnergic neurons, DA is then proportionately released from the these vesicles into the synaptic cleft to elicit its effect onto the numerous, widely distributed and conserved G-protein coupled DA receptors within the CNS and PNS (Elsworth and Roth 1997). The remaining DA within the synaptic cleft, following stimulation, can also be re-uptaken by the

dopamine transporter (DAT) to allow for further re-packaging within synaptic vesicles or for the degradation by monoamine oxidase (MAO) or extracellularly in glial cells (Meiser et al. 2013; Fig. 1.1). Noteworthy, neurons containing dopamine beta-hydroxylase and phenylethanolamine N-methyl transferase can convert DA to norepinephrine and epinephrin respectively, however their localization and function differ considerably from DAnergic neurons (Wong 2006).

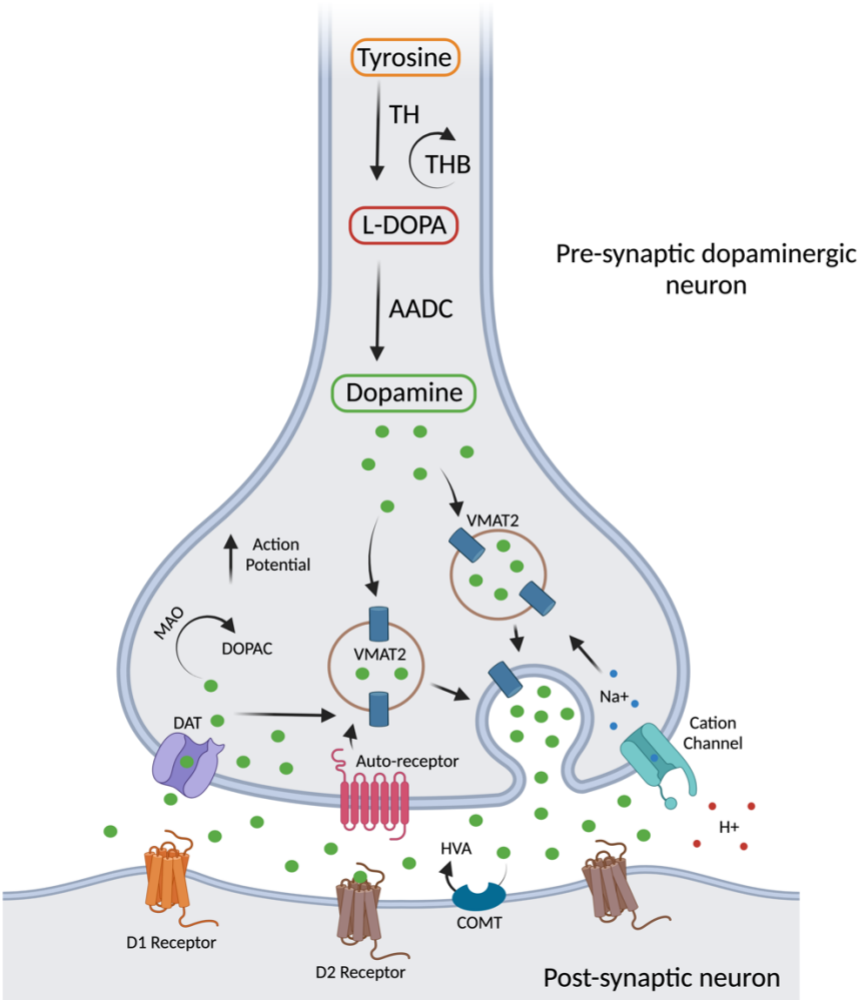

Figure 1.1. DA synthesis, release and metabolism in a DAnergic synaptic cleft. Tyrosine is first converted into L-DOPA via tyrosine hydroxylase (TH) which is then transformed into

dopamine (DA) by amino acid decarboxylase (AADC). Vesicular monoamine transporter 2 (VMAT2) packages cytosolic DA into vesicles to be released extracellularly from the pre-synaptic neuron following a spike in action potential. DA then binds to DA receptors D1 and D2 to transduce the signal to the post-synaptic neuron. DA can be re-uptaken by the dopamine transporter (DAT) or act on DA auto-receptors to control DA levels by subsequent metabolism through catechol-O methyl transferase (COMT) or monoamine oxidase (MAO). Feedback loops can also be activated to stimulate DA release following a change in pH mediated through cation channels.

1.2. Dopaminergic systems, functions and pathways

DAnergic systems are critical to a vast degree of primitive biological functions that range from movement to motivation, thus, any dysregulation of DA neurotransmission can lead to a plethora of debilitating psychiatric and neurodegenerative disorders (Reeves et al. 2002; Dunlop and Nemeroff 2007). Although encompassing less than 1% of all brain cells, midbrain DAnergic neurons are the primary source for DA output into the CNS and possess a profound impact on overall neurological homeostasis (Arias-Carrión et al. 2010). DAnergic neurons are widely distributed but organized into clusters, where these heterogeneous populations are abundant within the olfactory bulbs, substantia nigra, striatum, thalamus, ventral tegmentum area, nucleus accumbens and other mesencephalic, telencephalic and diencephalic nuclei (Chinta and Andersen 2005). Neurocircuitry studies have identified four distinct pathways that modulate various aspects of behavior and emotion.

The mesolimbic pathway originates in the ventral tegmental area (VTA) of the midbrain with extending fibrous DAnergic projections that terminate at the nucleus accumbens (NAc) of the ventral striatum, olfactory tubercle, pyriform cortex and the amygdala (Blaess et al. 2020).

Alternative endpoints comprising of thin axonal branching have been described in thalamic, habenular and hypothalamic nuclei (Adinoff 2004). Researchers suggest the predominant role of this pathway to be in the modulation of reward, motivation, stress and desire meaning that food, copulation and pleasurable activities all stimulate mesolimbic DA release (Gardner and Ashby 2000; Adinoff 2004). This circuit is also highly susceptible to stimulating substances that can facilitate the development of addiction. Studies have shown the NAc and VTA to be widely distributed with nicotinic (Collins et al. 2016), cannabinoid (Tsou et al. 1998), opioid (Margolis et al. 2014) and DAT receptors (targeted by psychostimulants that include cocaine and amphetamines; Brodie and Dunwiddie 1990). Given the cognitive implications associated with the mesolimbic tract, the vast majority of antipsychotic drugs used to alleviate schizophrenic episodes target DA receptors distributed among structures within this pathway (Adinoff 2004; Volkow and Morales 2015).

As the name suggests, *the mesocortical pathway* consists of DA fibers that connect the medial VTA region to the medial prefrontal, cingulate and perirhinal cortices, and to septo-hippocampal regions of the brain (Wise 2004). Closely associated with the mesolimbic system, this pathway is primarily associated with regulating cognition, motivation and goal-directed learning (Hauser et al. 2017). These circuits, however, do not always share similar function (Quessy et al. 2021). One study demonstrated this by optogenetically inhibiting the mesocortical and mesolimbic pathways to render the mice more susceptible to social defeat and depression or to be more resilient to these stresses respectively (Chaudhury et al. 2013). In humans, Hauser and colleagues were able to demonstrate further dissociative roles of the dorsomedial prefrontal cortex and NAc in the context of reward and effort prediction errors. They found the dorsomedial prefrontal cortex to predominantly encode for effort prediction errors and apathy estimation, but

not reward prediction errors, whereas the inverse was observed for the ventral striatum (Hauser et al. 2017). Nonetheless, dysfunction and dysregulation of DA transmission within this pathway has been shown to induce psychiatric symptoms reminiscence of schizophrenia and bipolar disorder, as well as, the cognitive impairments implicated in other DAnergic neurodegenerative diseases such as memory loss and depression commonly observed among Parkinson's patients (Ledonne and Mercuri 2017).

The tuberoinfundibular pathway resides along a hypothalamo-pituitary tract and is essential for the modulation of the neuroendocrine system. This pathway originates with DA synthesized in the arcuate nucleus of the hypothalamus where neurons send ascending projections to the median eminence of the pituitary gland while DA is also actively transported through hypothalamo-hypophysial portal vessels (Fitzgerald and G Dinan 2008). DA in this circuit behaves more similarly to a hormone than a neurotransmitter as it tonically suppresses the lactotrophic release and secretion of prolactin through binding to D2 receptors on the anterior pituitary lobe (E Moore and M Wuerthele 1979; Fitzgerald and G Dinan 2008). Prolactin possesses a large role in reproduction through regulating maternal lactation and care (Grattan 2015). In mice, studies have shown that during the nursing stage DAnergic neurons experience increases in membrane potential oscillatory speed and depolarization events which in turn decrease DA levels during high-prolactin states of lactation (Thörn Pérez et al. 2020). This hyperpolarized state rapidly returns to baseline of nulliparous cycling mice following the weaning stage demonstrating the plasticity and adaptivity of DAnergic signaling across one of many neural pathways (Hodson et al. 2012; Thörn Pérez et al. 2020).

The nigrostriatal pathway originates in the substantia nigra pars compacta (SNpc) of the midbrain and rostrally projects a series of neurons that connect to form the basal ganglionic loop. The basal ganglia is comprised of a group of basal subcortical nuclei that acts on cortical motor signals received through the thalamus to form the thalamocortical system (Lanciego et al. 2012). SNpc DAnergic efferents target the dorsal striatum, caudate nucleus and putamen where a hyperbranching network of unmyelinated DAnergic arbours and presynaptic terminals can be found. Given the proximity to the brain stem and structural identity of the regions involved in this pathway, DA release in this pathway is shown to regulate components of locomotion and sleep. Modulation of involuntary and voluntary movement is intricately balanced between indirect and direct signaling pathways within this system. The direct pathway is excitatory-dominant where the SNpc releases DA that binds to the D1 receptors of striatal medium spiny neurons (MSNs) to suppress GABAergic activity in the globus pallidus internal. This excites the motor cortex through glutamatergic signaling to result in movement. In contrast, the indirect pathway acts to inhibit motor activity. Once DA is bound to striatal MSN D2 receptors, these neurons send an inhibitory signal from the globus pallidus external to the subthalamic nucleus which excites the globus pallidus internal downstream. The global pallidus internal is GABA-dense where stimulation leads to a reduction of cortico-thalamic signal through increasing thalamic inhibition (Young and Sonne 2018). Notably, the MSNs described belong to distinct populations within the striatum as subpopulations only express D1, only D2 while a small group expresses both D1 and D2 receptors. Despite displaying unique properties in dendritic spine density and neurodegeneration in mice, the role of MSNs that possess both D1 and D2 receptors remains elusive in the context of direct and indirect control of movement (Gagnon et al. 2017). Given the implications in locomotion, DAnergic neurons residing in the SNpc are those highly affected in Parkinson's Disease (PD) and

other movement disorders. In PD, the reduction in SNpc DA output leads to an amplified cortico-thalamic inhibitory response and diminishes glutamate input to the cerebral cortex to result in the observed rigid and tremoring phenotypes (Sulzer et al. 2016).

1.3. Etiology and pathogenesis of Parkinson's disease

PD is the second most prevalent neurodegenerative disorder behind Alzheimer's and affects approximately 1.4% of the global population. Non-motor symptoms of cognitive (memory loss, anxiety, depression), sensory (impaired olfaction), autonomic (sexual dysfunction) and gastrointestinal defects (constipation) arise prior to the hallmarked motor impairments (Chaudhuri and Schapira 2009; Sveinbjornsdottir 2016). Motor symptoms manifest themselves following a 40-60% loss of DAnergic neurons and comprise of postural instability, bradykinesia, tremors and a rigid stature (Cheng et al. 2010). As mentioned previously in brief, the reduction in DA output from the SNpc in the nigrostriatal pathway results in thalamic over-inhibition within the basal ganglia to cause an imbalance of excitatory-inhibitory signaling to the motor cortex leading to impaired locomotion (Sulzer et al. 2016). One abnormality postulated to contribute to the pathogenesis of PD is the presence of intracytoplasmic inclusions, coined Lewy bodies, that reside within surviving DAnergic neurons. These structures are abundant in the presynaptic protein alpha-synuclein where genetic mutations have been linked to the onset of familial PD (Spillantini et al. 1997). In addition, the trafficking and distribution of these inclusions remain a topic of debate. Researchers have postulated varying hypotheses proposing that Lewy bodies spread in a prion-like fashion across many brain regions (pons, brain stem, midbrain and cortices; Visanji et al. 2013), whereas others suggest that retrograde transmission along the peripheral gastrointestinal tract and

gut-brain axis from the enteric DAnergic system initiates the progression of PD (Liu et al. 2017; Liddle 2018).

The development of PD has been attributed to both genetic and external risk factors. Of the latter lies age and sex, where incidence increases following the age of 65 and affects males:females at an estimated ratio of 3:2 respectively (Wooten et al. 2004). The mechanism behind the sex-difference remains elusive, however, it is hypothesized that estrogens may play a neuroprotective role in delaying the onset of PD in females (Haaxma et al., 2007). Exposure to neurotoxins and mitochondrial dysfunction are also prominent among patients. Interestingly, many genes linked to the onset of familial PD are also involved in mitochondrial maintenance and homeostasis (Winklhofer and Haass 2010; Pilsl and Winklhofer 2012). Familial PD only accounts for an approximated 15% of cases while the remaining are sporadic or idiopathic in nature. Thus, it is not far reached to hypothesize that a combinatory or synergistic effect between both genetic and external risk factors contribute to exacerbate the onset of PD in certain individuals.

To date there is no cure for PD, however, there are therapies focused around the adeno-associated viral delivery of neurotrophins (glial derived neurotrophic factor or *GDNF* is currently undergoing a phase 1 clinical trial) and levodopa (L-DOPA) that provide symptomatic relief to patients through ectopic supplementation for DA biosynthesis to occur (Manfredsson et al. 2020). Deep-brain stimulation of the subthalamic nuclei, globus pallidus internal and ventral posterolateral nucleus of the thalamus are also found to be effective, however, relief manifests gradually over the course of a longer period of time and may pose alternative health risks due to the invasiveness of the surgery (Pedrosa and Timmermann 2013).

1.4. Genetic risk factors of Parkinson's disease

Over recent decades considerable efforts have been made in search of genetic links or predispositions to familial PD. Primarily detected in human samples and recapitulated in rodent models, various mutagenic loci have been identified (*PINK1* "PTEN induced kinase 1" (Winklhofer and Haass 2010), *PRKN* "parkin" (Pickrell and Youle 2015), *LRRK2* "leucine-rich kinase 2" (Di Fonzo et al. 2006), *DJ-1* "Parkinson protein deglycase DJ-1" (Paterna et al. 2007) and *SNCA* "alpha-synuclein" (Chartier-Harlin et al. 2004)) that confer an increased susceptibility to the development of PD. The transmission and nature of mutation also varies as *PRKN*, *PINK1* and *DJ-1* are recessively inherited, while *SNCA* and *LRRK2* in contrast result from a mode of dominant inheritance. Additionally, early-onset PD can be complex and arise from monogenic or polygenic origins (Klein and Westenberger 2012). Researchers have since attributed the onset of familial PD to one of two hypotheses; the common disease common variant (CDCV) or the common disease rare variant (CDRV). CDCV is suggestive of a large frequency of polygenic contribution with low variant penetrance to contribute to the pathogenesis of disease while CDRV suggests few variants with high penetrance are the main contributors of PD susceptibility (Billingsley et al. 2018). However, the classification of PD between CDCV and CDRV likely varies depending on the individual's genetic predisposition and environmental exposures.

The first conclusive report of a genetic defect contributing to PD was *SNCA* where pleiomorphic mutations have since been described in many patients. Missense, duplication and triplication events readily promote Lewy body aggregation and the subsequent neuronal death through a variety of neurotoxic mechanisms that range from mitochondrial to synaptic dysfunction (Singleton et al. 2003; Chartier-Harlin et al. 2004; Gómez-Benito et al. 2020). The natural role of alpha-synuclein remains elusive but growing evidence suggests alpha-synuclein to influence

synaptic plasticity and neurotransmitter release (Burré et al. 2010; Yamada and Iwatsubo 2018). There remains controversy, however, surrounding its function in disease versus healthy states since neuroprotective properties have been described in cultured DAnergic neurons under mild exposure to oxidative stress while the same exposure was cytotoxic to cells possessing larger quantities of intracellular alpha-synuclein (Musgrove et al. 2011, 2013). Transgenic rodent models overexpressing WT and mutant (A53T and A30P variants) human *SNCA* have since been at the forefront to mimic synucleopathies for therapeutic testing as they consistently display the cardinal features of PD including reductions in striatal DA and distinct behavioral changes (Kirik et al. 2002; Lo Bianco et al. 2002; Decressac et al. 2012).

LRRK2 is a multi-domain and highly conserved gene that encodes for the protein dardarin. The function of *LRRK2* is not completely understood, however, it is proposed to drive an array of cellular functions that include the regulation of phosphorylation, cytoskeletal maintenance and neurite growth (Di Fonzo et al. 2005; Winklhofer and Haass 2010; Bartel et al. 2020). Mutations in *LRRK2* comprise the majority of all known heritable cases of PD. *LRRK2* mediated PD affects (or discriminates against) certain populations differently as the p.G2385R variant is associated with increased risk in Asian but not Caucasian populations (Billingsley et al. 2018). Researchers have accurately modeled human variants of *LRRK2* in animals, where the knock-in of mutation G2019S (predominant mutation described in humans) in rats resulted in DAnergic neuronal loss and axonal mispatterning via GTPase activity (Nguyen et al. 2020).

Many other genes affiliated with familial PD also possess a role in mitochondrial function, maintenance, and regulation such as *PINK1*, *PRKN* and *PARL*. These genes all work in concert within healthy mitochondria to control the fission and fusion dynamics of mitophagy and apoptosis in the removal of damaged mitochondria (Winklhofer and Haass 2010; Pilsl and Winklhofer 2012;

Pickrell and Youle 2015; Merhi et al. 2021). With the high metabolic requirements of DAnergic neurons, mutations in these genes disrupt cellular biogenesis and the response to oxidative stress which leads to the accumulation of reactive oxygen species, inhibition of mitochondrial respiration, superoxide radical formation and consequential cell death (Truban et al. 2017). In addition to the *PINK1/PRKN* cascade, *DJ-1* acts to regulate and mitigate damage to oxidative stress, where Paterna and colleagues (2007) demonstrated that the overexpression of *DJ-1* confers neuroprotection to DAnergic neurons. Mutations and deficiencies in *DJ-1* expression inversely increase neuronal susceptibility to oxidative injury (Paterna et al. 2007; Winklhofer and Haass 2010). Taken together, these and many other genetic links (to date mutations in fifteen genes have been shown to contribute to monogenic PD (Billingsley et al. 2018)) can only explain 15% of PD cases while the remaining are attributable to external factors such as exposure to neurotoxic compounds and pesticides, as elaborated on below.

1.5. *NR4A2* in Parkinson's disease

The development of the DAnergic system is intricately balanced by a number of transcription factors that include Pitx3, Lmx1, Otp and Shha (Ang 2006). Mutations affecting these genes have been shown to be deleterious to DAnergic health and can contribute to the pathogenesis of PD. This is the case for *nuclear receptor 4A2* (*NR4A2;* alternatively named *nuclear receptor related 1*, *NURR1*). *NR4A2* is an orphan nuclear receptor that guides midbrain DAnergic development by regulating *TH*, *DAT, VMAT2* and *AADC* gene expression (Chinta and Andersen 2005). At least four unique *NR4A2* single nucleotide polymorphic (SNP) variants have been shown to increase the concentration and abundance of Lewy body structures with patients displaying classic Parkinsonian symptoms and response to levodopa (Jankovic et al. 2005; Grimes et al.

2006). However, alike *LRRK2*, there appears to be demographic influence and variability across populations as the 704G7049 variant associated with PD progression reported in a study conducted in Texas (Xu et al. 2002) was not observed in French and Swedish cohorts (Levecque et al. 2004). Nonetheless, in mice and autopsied brains of human patients, reduced *NR4A2* protein and transcript levels have been detected in conjunction with reduced SNpc TH and increased synucleopathic presence (Jankovic et al. 2005). Jia and colleagues recently revealed a possible mechanism *in vitro* describing the interaction between *NR4A2* and *SNCA*. *SNCA* supressed *NR4A2* activity through increasing nuclear factor kappa-B (NF-kB) binding capacity and DNA damage that contributed to a negative feedback loop further promoting aggregate formation and neurodegeneration (Jia et al. 2020). Genetic knockout of *Nr4a2 in vivo* results in complete midbrain DA agenesis and mouse lethality, however, loss-of-function studies have been performed using heterozygous populations where slight reductions in striatal DA and hyperactivity were observed but movement turns hypokinetic in an age-dependent manner (Jiang et al. 2005). Single-cell transcriptomic data of DAnergic neurons following the conditional knockout of *Nr4a2* in adult mice provided additional insight to the complexity in *Nr4a2* function as the differential expression of many nuclear encoded mitochondrial genes involved in oxidative phosphorylation (*Ndufb2*, *Cox5a* and *CHCHd2*), reactive oxygen species (ROS) detoxification (*Sod1*) and ribosomal activity (*Lars2*, *Rpl13* and *Mrps12*) was observed in degenerative states suggesting *Nr4a2* to be essential in regulating mitochondrial homeostasis (Kadkhodaei et al. 2013).

1.6. Neurotoxic risk factors associated with Parkinson's disease

With the majority of PD cases not associated with inheritability, much research has been done to investigate non-genetic sources that contribute to mitochondrial dysfunction and DAnergic

cell death in aim to model sporadic pathologies. To date, exposure to numerous environmental pesticides and neurotoxins have been shown to increase the risk of DAnergic damage and result in the development of Parkinsonian symptoms. The most widely used chemicals to recapitulate PD-related phenotypes are 1-methyl-4-phenyl-1,2,3,6-tetrahydropyridine (MPTP), 1-methyl-4-phenylpyridinium (MPP+), 6-hydroxydopamine (6-OHDA), rotenone and N,N'-dimethyl-4,4'-bipyridinium dichloride (paraquat).

MPTP was first discovered mistakenly by drug users as a byproduct for 1-methyl-4-phenyl-4-propionoxy-piperidine (MPPP; a synthetic heroin analog to meperidine) in the 1980s. Unbeknownst to them, these individuals would intravenously inject MPTP leading to the progression of Parkinsonian symptoms in the subsequent weeks to months (Langston et al. 1983). MPTP is lipophilic and readily permeates the blood-brain barrier (BBB) to cumulate in the proximal glial cells (or astrocytes). Monoamine oxidase B (MAO-B) then acts to convert MPTP into its active neurotoxic metabolite MPP+. MPP+ enters DAnergic cells through DAT and inhibits complex I of the electron transport train (ETC) resulting in impaired ATP synthesis, mitochondrial respiration and increased superoxide radical formation (Sian et al. 1999; Przedborski et al. 2000). MPTP has since been extensively used to mimic PD pathologies (such as hypokinesis, reduced striatal (or brain) DA levels and DAnergic degeneration) in a variety of invertebrate and vertebrate models of PD that range from drosophila (Aryal and Lee 2019) to zebrafish (Bretaud et al. 2004; Kalyn et al. 2019) to rodents (Meredith and Rademacher 2011; Bové and Perier 2012) and to non-human primates (Tieu 2011). Despite being coined the "gold-standard" in chemo-ablative studies, one limitation of MPTP is the lack of consistent Lewy body formation where aggregates have been reported following chronic low-dose administration in mice and non-human primates but not in other more acute modeling (Forno et al. 1986; Fornai et al. 2005).

Rotenone had been widely adopted for use as an industrial piscicide, herbicide and insecticide (Nanda et al. 2009). Hydrophobic in nature, rotenone permeates the BBB, astrocytes and neuronal cellular membranes independent of DAT. Once integrated into the cell, rotenone inhibits complex I of the ETC and increases ROS while inhibiting proteosome activity (Betarbet et al. 2000; Greenamyre et al. 2003). Nuclear translocation has also been observed to activate NF-kB and DNA fragmentation to further exacerbate cytotoxic insult (Ott and D 2006; Cabezas et al. 2013). The use of rotenone administration in murine models has shown to be advantageous as it recapitulates the majority of PD related phenotypes including reliable Lewy body formation. Stereotaxic, intrabdominal and intramuscular injections have all shown to yield DAnergic degeneration and motor impairments (Cannon et al. 2009; Xiong et al. 2009). Noteworthy, α-synuclein aggregates have also been documented in the SNpc and many regions of the enteric nervous system following intragastric administration of rotenone in mice (Pan-Montojo et al. 2010). This finding supports the "dual-hit" hypothesis proposed by Braak and colleagues describing the trans-synaptic transmission of synucleopathies in PD along the gut-brain axis originating in the enteric system (Hawkes et al. 2009).

Paraquat had been the most predominantly used commercial herbicide in agriculture (Bromilow 2004). Epidemiological studies have revealed that extensive paraquat exposure contributes to the development of PD in farming populations (Dhillon et al. 2008). Structurally similar to MPP+, this divalent cation is transported into DAnergic neurons where it targets the mitochondrial ETC to generate oxidative stress (Rappold et al. 2011; Reczek et al. 2017). Unlike MPTP and MPP+ however, paraquat has a low affinity for complex I and damages mitochondria through impairing cellular redox cycling and the antioxidizing properties of glutathione and thioredoxin. Paraquat also promotes cytochrome-c release and downstream proapoptotic

mechanisms (Fei et al. 2008; Ren et al. 2009). In rodents, chronic injections recapitulate the PD-related symptoms of DAnergic neuronal loss and deafferentation in the SNpc, VTA and striatum while displaying impaired locomotion (McCormack et al. 2002; Thiruchelvam et al. 2003). These effects were amplified when co-administered with maneb (a fungicide), however, maneb alone fails to elicit DAnergic damage (Cicchetti et al. 2005; Wills et al. 2012). Exposure to paraquat orally also results in the enteric activation of idiopathic PD in transgenic mouse models (Naudet et al. 2017). Similarly to rotenone, paraquat administration results in the robust accumulation of Lewy bodies within the SNpc and striatal regions in mice (Betarbet et al. 2000; Manning-Bog et al. 2002) but this increase is also paralleled with the hyperphosphorylation of Tau, a protein involved in the pathogenesis of Alzheimer's disease (Wills et al. 2012).

As previously mentioned in brief, 6-OHDA is a synthetically hydroxylated DA compound that facilitates the easy penetrance of catecholaminergic neurons. Highly oxidizable and unable to cross the BBB, 6-OHDA is commonly co-administered intracerebrally with compounds to maintain molecular stability. 6-OHDA acts on a similar neurotoxic mechanism as MPTP, but 6-OHDA can also be taken up by norepinephrine neurons in addition to DAnergic. It is for this reason that MPTP is the most adopted neurotoxin despite 6-OHDA being isolated and shown to be effective in recapitulating PD-related symptoms first (Senoh and Witkop 1959; Senoh et al. 1959; Ungerstedt 1968). Because of this non-discriminate characteristic, studies commonly co-administer this 6-OHDA with epinephrine or DAnergic inhibitors to target select neuronal populations (Fulceri et al. 2006; Bové and Perier 2012). In addition to complex I suppression, 6-OHDA acts on complex IV while rapidly oxidizing to produce superoxide and hydroxyl radicals (Hwang 2013). 6-OHDA is widely used as a neurotoxic model for its predictable behavioral and degenerative phenotypes, as well as, the ability to easily generate an "early-stage" PD model

through partial lesions to the dorsal striatum in rodents (Amalric and Koob 1987). However, alike MPTP and MPP+, 6-OHDA fails to consistently yield Lewy body formation.

Table 1.1. Common chemicals used to model Parkinson's disease. Adapted from (Keow 2016).

Neurotoxin	Structure	Molecular Weight	Description
MPTP (1-methyl-4-phenyl-1,2,3,6-tetrahydropyridine)	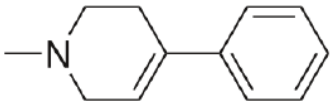	173.26g/mol	Neurotoxin derived as byproduct from MPPP synthesis
MPP+ (1-methyl-4-phenylpyridinium)	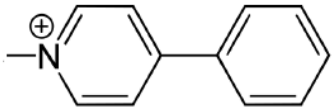	170.25g/mol	Active metabolite of MPTP
6-OHDA (6-hydroxydopamine)	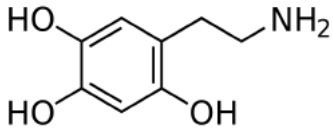	169.18g/mol	First identified neurotoxin that targets noradrenergic and DAnergic neurons
Rotenone	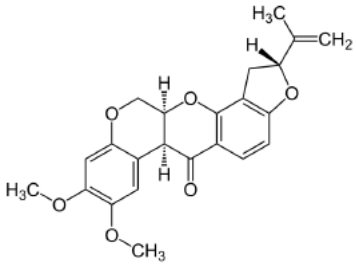	394.42g/mol	Industrial piscicide and insecticide linked to DAnergic damage and the development of PD
Paraquat (N,N'-dimethyl-4,4'-bipyridinium dichloride)	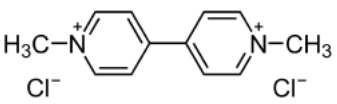	257.16g/mol	Industrial herbicide linked to DAnergic damage and the development of PD

1.7. Mitochondrial dynamics within healthy and Parkinsonian microenvironments

Mitochondria are dynamic organelles that intricately balance the bioenergetic requirements of the cell through one of two main mechanisms; glycolysis and oxidative phosphorylation. Highly energetic cells commonly rely on the latter and neurons fall into this category. Neurons are metabolically active to sustain membrane potentials, facilitate neurotransmission and maintain oscillatory patterns thus dysfunction in the mitochondrial network can lead to debilitating neurological consequences (Dauer and Przedborski 2003). One subset of neurons that are particularly susceptible to insult and oxidative stress are SNpc DAnergic neurons. As previously mentioned, these neurons project to a branching axonal lattice in the striatum that contains an approximated 1 to 2 million synapses in humans (Misgeld and Schwarz 2017) and 200 to 400 thousand in rats (Moss and Bolam 2008; Matsuda et al. 2009). This may explain why mitochondrial dysfunction is a prominent characteristic in all forms of monogenic, polygenic and idiopathic PD (mechanisms reviewed in Fig. 1.2).

1.7.1. Mitochondria in apoptosis and mitophagy

In addition to respiratory ATP production, mitochondria are multifunctional and critical to a number of processes that include ROS mitigation, Ca^{2+} handling and cell-fate determination (Contreras et al. 2010; Zorov et al. 2014). To determine fate, mitochondria play an active role in mediating apoptosis and mitophagy directed pathways of cell death in response to varying environmental cues (Youle and van der Bliek 2012)

In apoptosis, mitochondria regulate the proportion of anti- and proapoptotic signaling through Bcl-2 and Bax mechanisms of cytochrome-c release. Cytochrome-c is a protein localized to the intermembrane space (between the inner mitochondrial membrane and outer mitochondrial

membrane) and is released into the cytosol upon the recruitment and localization of proapoptotic Bax on the outer mitochondrial membrane. Bax binding triggers a signal for the formation of a complex containing Apoptotic peptidase activating factor 1 (Apaf-1; apoptosome-containing adaptor) and the initiator Caspase-9 to facilitate the activation of downstream effector caspases involved cell death, namely Caspase-3 (Baliga and Kumar 2003; Danial and Korsmeyer 2004). This pathway was demonstrated *in vitro* where recombinant Bax stimulated cytochrome-c release in cultured mitochondria (M. et al. 1998) and where the formation of the Apaf-1/Caspase-9 initiation complex is dependent on cytochrome-c (Li et al. 1997), as well as, *in vivo* where Caspase-9 deficient mice failed to form the apoptosomal complex and activate Caspase-3 (Kuida et al. 1998). Together, these studies solidify our mechanistic understanding and suggests that the proper functioning of all components involved is necessary to carry out apoptosomal formation and mitochondrial apoptosis.

Alternatively, mitophagy acts as a cellular fail safe to selectively remove damaged mitochondria through a process called autophagy (Ding and Yin 2012). Autophagy is evolutionary conserved and uses the lysosomal pathway to degrade intracytoplasmic components that range from organelles to toxic proteins or aggregates (Vijayakumar and Cho 2019). To sequester mitochondria, ubiquination of the outer mitochondrial membrane takes place to recruit the autophagosome complex that engulfs the dysfunctional organelle. The initiation of mitophagy is induced by intrinsic PINK1/Parkin signaling. Under conditions of stress, mitochondria undergo a conformational change or fission event which cleaves a larger mitochondria into fragmented bodies. Reduced membrane potential of these bodies leads to the accumulation of PINK1 on the outer mitochondrial membrane to subsequently recruit Parkin to translocate and ubiquinate various mitochondrial substrates for autophagosomal degradation (Ding and Yin 2012). One target of

Parkin mediated ubiquination is mitochondrial fusion proteins, Mitofusin (Mfn) 1 and 2, which further exacerbates mitochondrial isolation and impairs the rescue potential of the surrounding network to integrate the reduced bodies (Tanaka et al. 2010). The exact mechanism of PINK1 signaling to Parkin remains somewhat elusive where some researchers suggest that indirect phosphorylation of the kinesin anchoring substrate Miro in drosophila (Wang et al. 2011) is responsible, while others propose that it stems from the direct phosphorylation or anchoring of Parkin by PINK1 (Kim et al. 2008; Sha et al. 2010). Regardless, this pathway is reliant on both drivers as Parkin fails to bind to the outer mitochondrial membrane in the absence of PINK1 and in the absence of Parkin there is no phagosomal activation. Under healthy conditions, however, these events rarely occur as PINK1 is readily cleaved by proteases such as Parl prior to Parkin recruitment (Merhi et al. 2021).

1.7.2. Mechanisms of mitochondrial maintenance

As previously alluded to, mitochondria can undergo conformational changes in response to environmental cues or the metabolic demand of the cell. These changes alter between fission and fusion states. Fission can often be observed under glycolytic conditions of rapid proliferation and as a defense mechanism, whereas oxidative phosphorylation can predominantly be found within healthy, demanding and differentiated cells (Rossignol et al. 2004; J. and M. 2012; Westermann 2012; Seo et al. 2018).

Throughout fragmentation, the accessory (or adaptor) proteins: mitochondrial dynamics protein 49 and 51 (Mid49 and Mid51), mitochondrial fission factor (Mff) and mitochondrial fission protein 1 (Fis1) all signal to recruit dynamin related protein 1 (Drp1; Dnm1 in yeast) to the outer mitochondrial membrane (J. and M. 2012)). Drp1 is the most important component to this

mechanism where deficiencies result in elongated and hyperfused mitochondrial morphologies (Qian et al. 2012). Membrane constriction then occurs in concert with assembly of dynamin-2 (Dyn2), a protein necessary for the terminal scission event (Lee et al. 2016). Cleavage sites are determined through contact microdomains with the endoplasmic reticulum (ER; Aoyama-Ishiwatari and Hirabayashi 2021). The ER also releases pro-fission related proteins such as INF-2 that has been shown to "prepare" the mitochondria prior to Drp1 binding (Korobova et al. 2013).

In contrast, mitochondrial fusion is regulated by fusogens Mfn 1, Mfn2 and optic atrophy-1 (Opa1; Mgm1 in yeast). These proteins work together to combine nearby mitochondrial bodies through three steps; tethering, docking and fusing the two outer mitochondrial membranes through GTP hydrolysis (Hoppins and Nunnari 2009; Gao and Hu 2021). Mfn1 and Mfn2 form homo- and heterotypic complexes to facilitate outer mitochondrial membrane hybridization. In parallel, Opa1 and cardiolipin (CL) synergistically drive inner mitochondrial membrane integration and cristae remodelling between the merging mitochondria (Ban et al. 2017). Mutations in genes encoding *Mfn* or *Opa1* machineries have resulted in fragmented and spherical mitochondria, as well as, impaired cristae biogenesis (Chen et al. 2003; Meeusen et al. 2006).

Fusion is important for promoting the rescue of damaged mtDNA or mitochondrial compartments while fission is important to segregate defective segments to be subsequently tagged for mitophagy or apoptosis (Youle and van der Bliek 2012). mtDNA is 10 to 20 times more vulnerable to mutation than gDNA which renders the mitochondria more sensitive to oxidative damage. This creates a negative feedback loop where stress results in more mutations and more mutations increases stress susceptibility. Age amplifies this which may explain the commonality of mitochondrial dysfunction underlying PD and other neurodegenerative disorders. Many animal models have been used to recapitulate these effects *in vivo*, however, the zebrafish has rapidly

emerged as a promising model in this field due to its conserved genetics, neural circuitry and behavioral cues with higher order mammals.

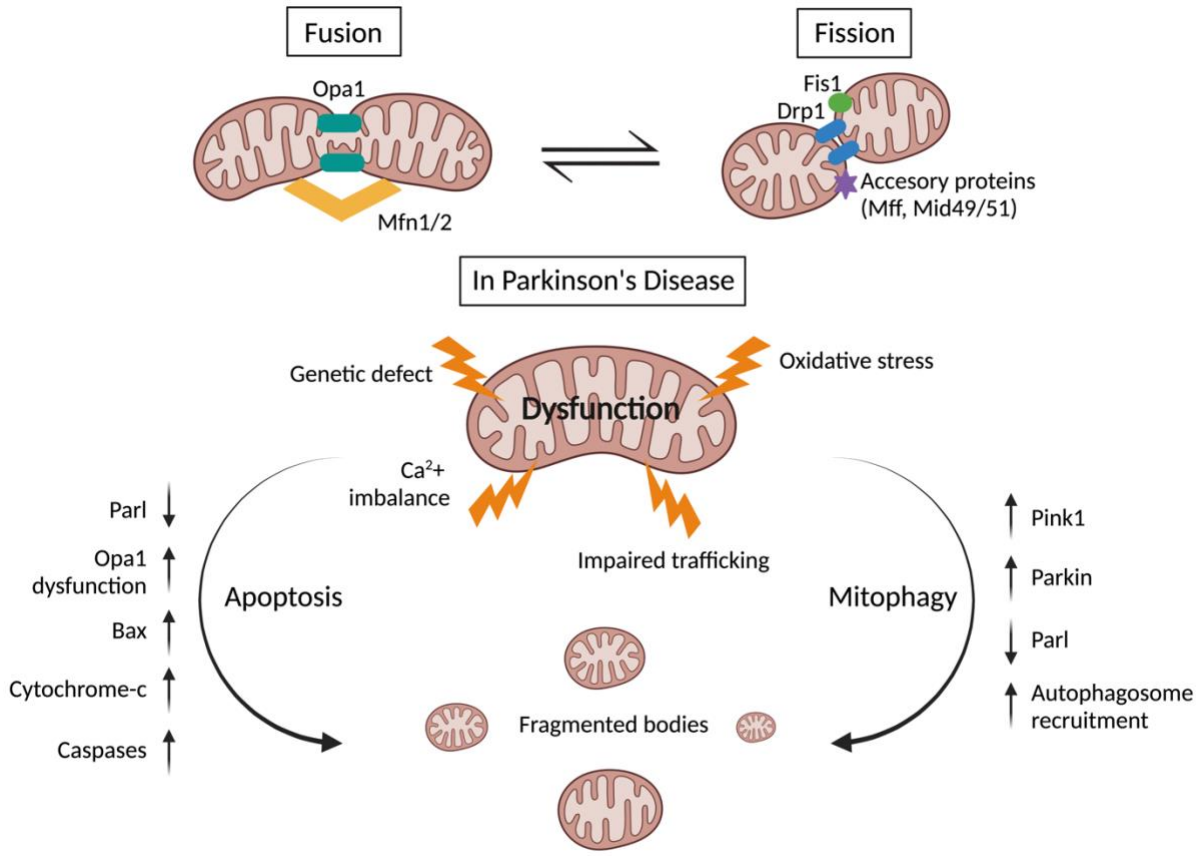

Figure 1.2. Mitochondrial dynamics in Parkinson's disease. Fusion is mediated by optic atrophy 1 (Opa1) located on the inner mitochondrial membrane and mitofusins 1/2 (Mfn1/2) located on the outer mitochondrial membrane. Fission is coordinated through multiple accessory proteins (Fis1, Mff, Mid49/51) binding to the outer mitochondrial membrane to recruit dynamin-related protein 1 (Drp1) to catalyze the cleavage event. In Parkinson's disease, mitochondrial dysfunction is a prominent feature that can result from genetic defects, oxidative stress, impaired

trafficking and calcium imbalances. Consequentially, damaged mitochondria begin fragmenting and activating either mitophagy or apoptosis cell death mechanisms.

1.8. Dopaminergic organization and distribution in the zebrafish brain

Different DAnergic populations in the brain are responsible for various cognitive, behavioral and physiological functions. In order to contrast the effects on DAnergic circuity in zebrafish with high order vertebrates, it is first important to review the anatomical distribution and projectome described in mammals to draw parallels. In mammals (characterized using rodent models) DAnergic clusters can be subdivided into mesencephalic, diencephalic and rhombencephalic nuclei. Within the mesencephalon, clusters A8, A9 and A10 belong to the retrorubral, substantia nigra and VTA respectively. Groups A11, A12, A13 and A14/15 represent DAnergic populations in the caudal diencephalon within the periventricular gray matter of thalamic and hypothalamic regions, arcuate nucleus, zona incerta and the rostral periventricular nucleus. Alternative clustering corresponds to the olfactory grouping A16 and amacrine cells described in the retina A17. Groups C1 to C3 and A1-7 belong to adrenergic and noradrenergic catecholaminergic identities respectively (Smeets and González 2000).

DAnergic classification in the zebrafish brain does not follow the classical A1-17 system since they lack distinct mesencephalic populations. Following the the description of DAnergic system development in zebrafish larvae, there have been conflicting assignments of DAnergic neurons to different clusters. Going forward in this thesis, groupings will be described in accordance with Sallinen et al. (2009), as opposed to those proposed by Rink and Wullimann , where the primary focus is on diencephalic subclassification (Rink and Wullimann 2002b). Correlating to the positioning in the adult brain, groupings include; 1: the olfactory bulbs, 2:

telencephalic nuclei, 3-4: anterior parvocellular preoptic nucleus, 5 (DC1): posterior parvocellular preoptic nucleus, 6 (DC1): thalamic nuclei, 7: periventricular pretectal nucleus, 8 (DC3): anterior paraventricular organ, 9 (DC5): intermediate paraventricular organ, 10: posterior paraventricular organ, 11 (DC2): periventricular nucleus of the posterior tuberculum, 12 (DC4): paraventricular organ and posterior tuberculum, 13 (DC6): posterior tuberculum and periventricular hypothalamus, 14: locus coerulus, 15-16: internal retinal formation and vagal lobe, and 17: area postrema and vagal lobe (Sallinen et al. 2009).

The DAnergic system in zebrafish is fully functional by 3dpf and originates within the posterior tubercular region of the ventral diencephalon where TH+ fibers are observable from 18 to 20hpf. Complex behaviors that include swimming and hunting are subsequently reported as early as 4dpf to 5dpf (Tay et al. 2011; Fig. 1.3A). Descending projections are first described from the posterior tuberculum to the locus coeruleus and spinal cord regions in the diencephalospinal tract and are followed by ascending efferents from the posterior tuberculum to the dorsal preoptic region, telencephalon (pallium and subpallium) and ventrally to the hypothalamus in the endohypothalamic tract. More recent projectome data showed the only diencephalic groups to project into the subpallium reside in the periventricular nucleus of the posterior tuberculum. This tract expresses DAnergic transcription factor *orthopedia* (*otp*) suggesting these neurons share identity with mammalian group A11 (Ryu et al. 2007; Tay et al. 2011). Additionally, efferents from the paraventricular organ and posterior tuberculum project to the hypothalamus and are proposed to confer similar function to the tuberoinfundibular pathway in mammals. The telencephalon possesses local DAnergic circuitry between pallial (dorsal, ventral, medial), subpallial and olfactory bulb subregions observed through retrograde tracing in combination with TH immunoreactivity (Rink and Wullimann 2002a; Schweitzer and Driever 2009). Using

genetically mosaic zebrafish, Tay et al. identified a group of endogenous subpallial DAnergic neurons that send descending projections to the ventral diencephalon by 4dpf (Tay et al. 2011; reviewed in Fig. 1.3B-C). Exposing this population of cells to neurotoxic insult resulted in impaired motor function comparable to hypokinetic and PD-related symptoms observed in mice and other vertebrate models (Sallinen et al. 2009; Tieu 2011). Based on DAnergic subpallial arborization and the behavioral effects of ablating DA output in this system, studies have since proposed this structure and tract to be the functional analog of the striatum (mammalian A9) and nigrostriatal pathway described in mammals and affected in PD respectively. The conserved nature of this pathway and many others contribute to the use of zebrafish as a robust model to study vertebrate neurocircuitry and a wide range of neurological diseases.

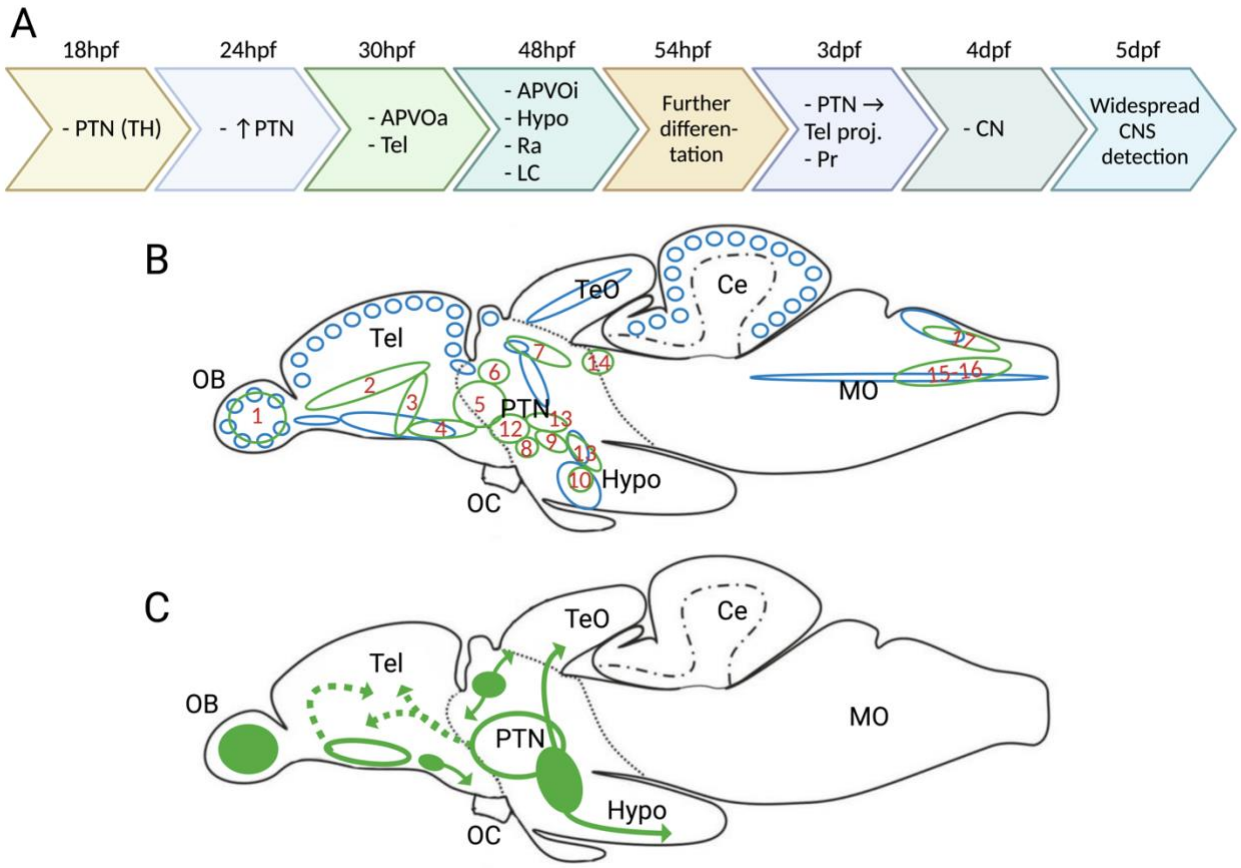

Figure 1.3. Zones of constitutive neurogenesis and DAnergic development, distribution and projectome in zebrafish. A) Tyrosine hydroxylase (TH) positive neurons are first detected at 18 hours post-fertilization (hpf) in the posterior tubercular nucleus (PTN) followed by the paraventricular organ (APOVa) and the telencephalon (Tel) at 30hpf. At 48hpf dopaminergic (DAnergic) neurons are observed within the hypothalamus (Hypo), raphe nuclei (Ra) and locus coerulus (LC). DAnergic projections from the PTN to the Tel can subsequently be observed at 3dpf in addition to populations within the pretectum (Pr). At 4dpf DAnergic neurons can be detected the caudate nucleus (CN) of the hypothalamus and by 5dpf all DAnergic neurons have and been identified. B) Zones of neurogenesis and constitutive proliferation in the adult zebrafish brain are represented in blue. DAnergic populations 1-17 are represented in green. C) DAnergic projections within the adult zebrafish brain. The dashed green line represents the functional analog

to the mammalian nigrostriatal pathway implicated in Parkinson's disease (PD). Abbreviations: OB: olfactory bulbs; Tel: telencephalon; PTN: posterior tubercular nucleus; OC: optic commissure; TeO: optic tectum; Ce: cerebellum; MO: medulla oblongata; Hypo: hypothalamus; CN: caudate nucleus; APOV: paraventricular organ; LC: locus coerulus; Pr: pretectum; Ra: raphe nuclei. Adapted from (Rink and Wullimann 2002a,b; Sallinen et al. 2009; Du et al. 2016).

1.9. Zebrafish as a model for neurological disease

Zebrafish are a teleostean species that have several advantages over other vertebrate models. They produce optically transparent embryos that develop rapidly *ex utero*, are small in size and possess high fecundity rates (females can produce up to 300 eggs per week). These properties make zebrafish very amendable to high-throughput pharmacological screens, live-imaging throughout development and gene-editing thanks to embryological access at the 1-cell stage. The accelerated and synchronous development also results in zebrafish reaching sexual maturity by 90dpf. These short generational times and the ability to perform phenotypic and behavioral analyses as early as 1- and 3dpf, respectively, combine to make this an attractive model for loss- or gain-of-function studies (Gilbert 2000; D'Costa and Shepherd 2009).

Despite drastic anatomical differences between species, the zebrafish genome is 71% similar to humans and contains 87% of disease related orthologs (Sassen and Köster 2015). The molecular toolbox of zebrafish contributes to the feasibility in generating transgenic and mutant models of various neurological diseases. Researchers have injected human amyloid-$\beta_{1\text{-}42}$ and phosphorylated Tau to study Alzheimer's related plaques and taupathies (Best and Alderton 2008a). Other studies have also identified and generated neurogenetic models for Swedish amyloid precursor protein to mimic specific pathologies in hereditary Alzheimer's (Saleem and Kannan

2018). Zebrafish have been adopted to study the monogenic PolyQ disorder Huntington's as well where Schiffer and colleagues generated zebrafish that possess varying N-terminal fragment sizes of polyQ repeats on the huntingtin (Htt) gene. These mutations resulted in increased mortality, inclusion body formation and abnormalities as seen with disease progression in mammals (Schiffer et al. 2007). These are just two examples as zebrafish have since been used to model a wide range of neurological and neurodevelopment disorders that include amyotrophic lateral sclerosis (Ramesh et al. 2014), epilepsy (Rodríguez-Ortiz and Martínez-Torres 2021), autism (Kozol et al. 2015), schizophrenia (De Rienzo et al. 2011) and PD elaborated on below.

1.10. Zebrafish as a model for Parkinson's disease

1.10.1. Genetic models of Parkinson's disease using zebrafish

As mentioned, 87% of genes associated with human disease are expressed within the zebrafish genome. Many genes associated with the progression of familial PD fall into this category including *dj-1*, *lrrk2*, *parkin*, *pink1* and *parl* (Prabhudesai et al. 2016; Brown et al. 2021; Merhi et al. 2021).

Targeting these genes in loss-of-function studies has been well adopted using zebrafish through morpholino KD or gene-editing KO methodologies. The genetic KD of *lrrk2* caused developmental defects, β-synuclein aggregation and the loss of TH+ neurons that was later replicated in a KO model (Prabhudesai et al. 2016; Suzzi et al. 2021). Reducing *dj-1* expression through morpholino administration did not induce neuronal death but made the zebrafish more susceptible to oxidative stress (Bretaud et al. 2007). However, a KO model was later generated where *dj-1* mutants developed normally but experienced reduced TH levels in an age-progressing

manner similarly to what is observed among PD patients (Edson et al. 2019). *Pink1* and *parkin* morphants and mutants displayed impaired mitochondrial function, increased DAnergic mispatterning, increased inflammation, decreased neurogenesis and perturbed behavior (Anichtchik et al. 2008; Flinn et al. 2009, 2013; Xi et al. 2011a; Brown et al. 2021). Recently, the loss of *parla* was shown to be deleterious to DAnergic health similarly to what was observed in *pink1* and *parkin* mutants, however, *parla* null zebrafish display additional impairments in sensory olfaction (Noble et al. 2012; Merhi et al. 2021).

One limitation of zebrafish as a model for familial PD may be the lack of α-synuclein. Zebrafish do however possess β- and γ-synuclein isoforms that confer DAnergic degeneration and hypokinesis following KD that can be rescued by introducing exogenous human α-synuclein (Milanese et al. 2012). Another study addressed the lack of α-synuclein by microinjecting large quantities of this protein into developing embryos that resulted in vast aggregate formation and synucleopathic apoptosis (Prabhudesai et al. 2012).

Targeting DAnergic transcription factors, such as *nr4a2*, in zebrafish also provides a great opportunity to investigate the lethality observed in homozygous mice mutants (Zetterström et al. 1997). Individual *nr4a2b* and *nr4a2a* KDs using varying concentrations of morpholinos have been explored in larvae resulting in reduced *th* and *dat* transcript levels, as well as, perturbed locomotion (Filippi et al. 2007; Luo et al. 2008). These studies, however commonly overlook the impact in adulthood, compensatory mechanisms between paralogues, the effects on other neural systems (GABAergic or serotonergic signaling and neurotrophic factors) and the functional implications in escape and motivated behaviors, thus warranting the establishment of a KO model.

1.10.2. Neurotoxic models of Parkinson's disease using zebrafish

Alike mammalian models, MPTP, MPP+, rotenone, paraquat and 6-OHDA have all been used to induce harmful effects to DAnergic neurons and mimic sporadic PD in larval and adult zebrafish (Vaz et al. 2018; Kalyn et al. 2019; Robea et al. 2020; Doyle and Croll 2022; reviewed in Fig. 1.4).

The most widely used, MPTP and MPP+ exposures elicit widespread TH and green fluorescent protein (GFP) loss (on a reporter line that labels *vmat2* expressing neurons) in the posterior tubercular, hypothalamic and diencephalic regions of the brain (Wen et al. 2008; Dukes et al. 2016). However, similar to acute treatments in mammals, MPTP and MPP+ fail to generate Lewy body inclusions despite elevated γ_1- and γ_2-synuclein levels (Sarath Babu et al. 2016). Pre- or co-treatment with MAO-B inhibitors (L-deprenyl) can mitigate both DAnergic and behavioral defects (Sallinen et al. 2009).

Besides injecting into or lesioning the brain region of interest, 6-OHDA may permeate the BBB more readily in zebrafish than mammals demonstrated through reports of reduced DA levels and hypokinesis following intramuscular injections (Anichtchik et al. 2004). Once in the brain, 6-OHDA targets a similar mechanism as MPTP and MPP+ to perturb ETC function and promote cell death without aggregate formation in the surviving DAnergic neurons (Feng et al. 2014; Vijayanathan et al. 2017). In addition, zebrafish exposed to 6-OHDA also experienced reductions in swimming speed and distances traveled. Pharmacological screens have revealed a number of compounds that confer neuroprotection when zebrafish are pre-treated prior to 6-OHDA administration. These include antioxidants such as vitamin E and microglial inhibitor minocycline however there lacks evidence of clinical effectiveness despite promise (Feng and Chen 2014; Cankaya et al. 2019).

Similar to mammalian models, rotenone use in zebrafish has yielded conflicting reports regarding DAnergic and behavioral insult. One study reported that only high doses were shown to be lethal in adult and larvae where no effects were observed following treatment of lower doses (Bretaud et al. 2004). Subsequently in a chronic model using the same lower dose, Wang and colleagues observed severely perturbed motor function, decreased TH, mitochondrial dysregulation and cognitive defects (Wang et al. 2017b). Rotenone, however, fails to generate Lewy bodies as observed in mammals but it can be concluded that it remains harmful to DAnergic health across species.

Likewise, there are variable results reported following treatment with paraquat. Bretaud and colleagues (2004) did not find any deleterious effects on DAnergic neurons or motor function in adult or larval zebrafish. Whereas a more recent study found that chronic injections of paraquat generated freezing bouts and reduced *dat* expression but failed to recapitulate all PD pathologies as they surprisingly found elevated DA protein levels (Bortolotto et al. 2014). All behavioral effects, including aggressiveness that was later evaluated, are minimized by antioxidizing chemicals such as sodium selenite (Müller et al. 2018).

The contradictory findings and large discrepancies in reproducibility amongst chemo-ablative zebrafish models in the literature may be attributed to the wide range of doses and treatment regimens used that are compared between studies without proper account for all experimental parameters. Several parameters include injection or immersion technique, quantity of fish per plate or well, light cycling, animal size and lethal concentration (LC) 50 dosing. To bridge the gap, a study exposing zebrafish under the same treatment conditions is needed. The ability for zebrafish to repopulate neuronal clusters in adulthood also serves as an opportunity to

gain mechanistic insights into the regeneration of specific cell types, in this case for DAnergic neurons.

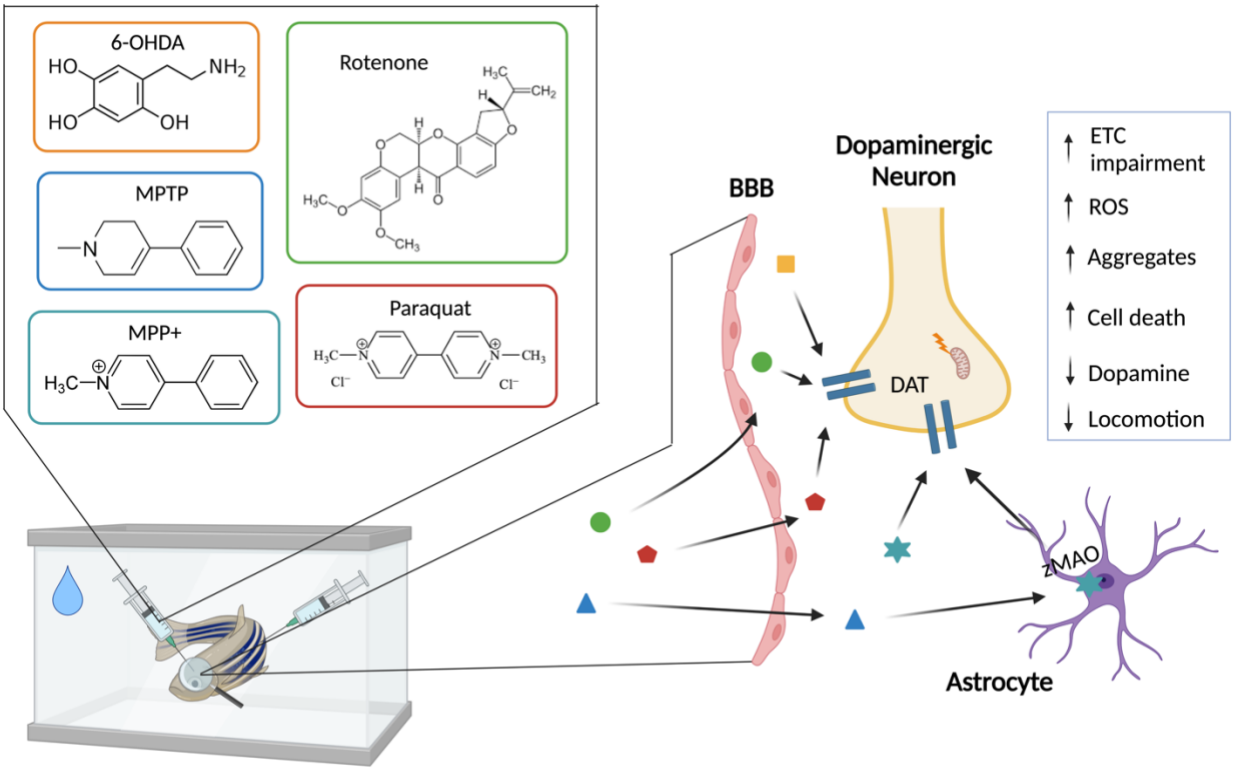

Figure 1.4. Mechanism of entry into dopaminergic neurons for Parkinson's disease-inducing neurotoxins. 6-Hydroxydopamine (6-OHDA), rotenone, 1-methyl-4-phenyl-1,2,3,6-tetrahydropyridine (MPTP), paraquat and 1-methyl-4-phenylpyridium (MPP+) all selectively target dopaminergic (DAnergic) neurons to elicit cytotoxic insult. Methods of administration using zebrafish rely on tank immersion, cerebroventricular microinjections, intracerebroventricular microinjections and intrabdominal injections. Most neurotoxins rely on the dopamine transporter (DAT) to enter the DAnergic neurons. Once inside, all neurotoxins induce oxidative stress damage leading to the subsequent neuronal death. MPTP, however, must first be metabolized by

monoamine oxidase B (MAO; zMAO in zebrafish) in proximal astrocytes to be converted into the active metabolite MPP+.

1.11. Adult neurogenesis and regeneration in zebrafish and other species

Once a controversial topic, it is now well known that the production of new neurons continues throughout the life most invertebrate and vertebrate species. Neural stem cells (NSCs) are generated in various zones around the brain to re-innervate existing neural networks in the multi-step process of proliferation, fate specification and differentiation, migration, maturation and integration (Liu and Song 2016). Adult neurogenesis has since been studied to gain therapeutic insights on cell replacement therapies and for various neurodegenerative disorders including PD (Sailor et al. 2006).

The capacity for neurons to regenerate, however, varies greatly in rate and physiology across the animal kingdom. Previous studies have demonstrated the functional recuperation of newly formed hippocampal granule neurons to be 0.02% per day in mature non-human primates (Jabès et al. 2010), 0.2% per day in rats (Cameron and Mckay 2001) and 0.1-0.7% per day in birds (Gahr et al. 2002). Regeneration is restricted to various niches in the adult brain and different species also possess differing numbers of niches. In mammals and birds, only two have been described (subventricular zone and subgranular zone of the dentate gyrus) (Ming and Song 2011), four in certain reptiles (cerebellum, olfactory bulbs, ventral and dorsal telencephalon) (Kaslin et al. 2008) and sixteen in the zebrafish (Grandel et al. 2006).

The zones of constitutive proliferation in the zebrafish brain reside along the rostral-caudal axis and include the olfactory bulbs, ventral and dorsal telencephalon, protic diencephalon, ventral thalamus, habenula, pretectal nucleus, dorsal thalamus, posterior tuberculum, hypothalamus, tectal

and torus longitudinalis mesencephalon, mesencephalic lamina, facial and vagal lobes of the medulla oblongata, rhombencephalon and the region extending through the valvular and copus cerebelli (Zupanc et al. 2005; Grandel et al. 2006; Ghaddar et al. 2021; reviewed in Fig. 1.3B). CNS regeneration in zebrafish is not exclusive to the brain as a NSC population within the spinal cord is also reported to generate motor neurons following mechanical injury (Reimer et al. 2009). Moreover, reactive gliosis and neuro-inflammatory processes are only transiently activated throughout regeneration to promote NSC proliferation without the consequence of scarring commonly observed in mammals (Ghaddar et al. 2021). Pertaining to DAnergic health, a recent study found DAnergic neurons to regenerate in the olfactory bulbs following chemogenetic ablation using the nitroreductase and metronidazole system, however the migratory paths of newly formed progenitors in this system or following chemical or mechanical injuries are not completely understood (Godoy et al. 2020). The morphogenic candidates hypothesized to be behind this cell specific regeneration are those activated throughout embryogenesis such as Hedghehog (Indian, Desert and Sonic) and Notch (1-4) signaling proteins. Sonic hedgehog (Shh) has been reported to drive midbrain DAnergic development and mesodermal dorsal-ventral polarity in vertebrates (Roussa and Krieglstein 2004; Carballo et al. 2018), whereas Notch1 promotes NSC proliferation, preserves progenitor pools while also being negatively impacted by synucleopathies observed in PD (Crews et al. 2008; Wang et al. 2009). The spatiotemporal involvement of Notch1 and Shh throughout the regeneration of DAnergic neurons, however, warrants further investigation, but the neurogenic potential of zebrafish serves advantageous to study these phenomena *in vivo*.

1.12. CRISPR-Cas9 gene-editing application in zebrafish

Loss-of-function and genome manipulating studies have always provided vast quantities of information, however, they came at a cost. Previous methodologies including zinc finger nucleases (ZFNs) and transcription activator-like effector nucleases (TALENs) are both laborious and time-consuming. Doudna and Charpentier revolutionized this field with the isolation of the clustered regularly interspaced palindromic repeat (CRISPR)-Cas9 nuclease system that has since been widely adopted in clinical, research and agricultural settings.

First identified in 1993 by Mojica and colleagues, the type II CRISPR-Cas9 system is native to archaea and bacteria as an adaptive immune response against invading viruses and phages (Mojica et al. 1993, 2005). This mechanism relies on CRISPR RNAs (crRNAs) and *trans*-activating crRNAs to assemble and guide the CRISPR-associated 9 (Cas9) nickase to a complimentary 20 nucleotide (nt) sequence, adjacent to a short 2-5nt PAM motif, that will induce a double-strand break (DSB) within HNH or RuvC domains (Jinek et al. 2012; Ran et al. 2013). The DSB generated can be repaired through two mechanisms; non-homologous end joining and high-fidelity directed repair, which will result in perturbed transcription through insertion or deletion mutations (indels) and abolished gene function or in the introduction of a repair template respectively (Mali et al. 2013; reviewed in Fig. 1.5). Since recognizing the application for genome engineering in mouse and human cell-lines *in vitro*, researchers raced to prove the effectiveness of germ-line editing eukaryotic organisms *in vivo*. The first demonstration of this was performed on zebrafish by Hwang and colleagues who reported the successful mutagenesis of endogenous *gsk3b* and *drd3* expression (Hwang et al. 2013). Zebrafish was an appealing model for CRISPR experimentation because unlike mammals, fecundity is elevated and their transparent *ex utero* embryogenesis facilitates the zebrafish's amenability to gene-editing application (Best and

Alderton 2008b). CRISPR-Cas systems have since been optimized and applied to a plethora of functions that range from multiplex editing at various loci (McCarty et al. 2020) to Sars-Cov2 diagnostics (Broughton et al. 2020) and to generating accurate models of human disease (Birling et al. 2017).

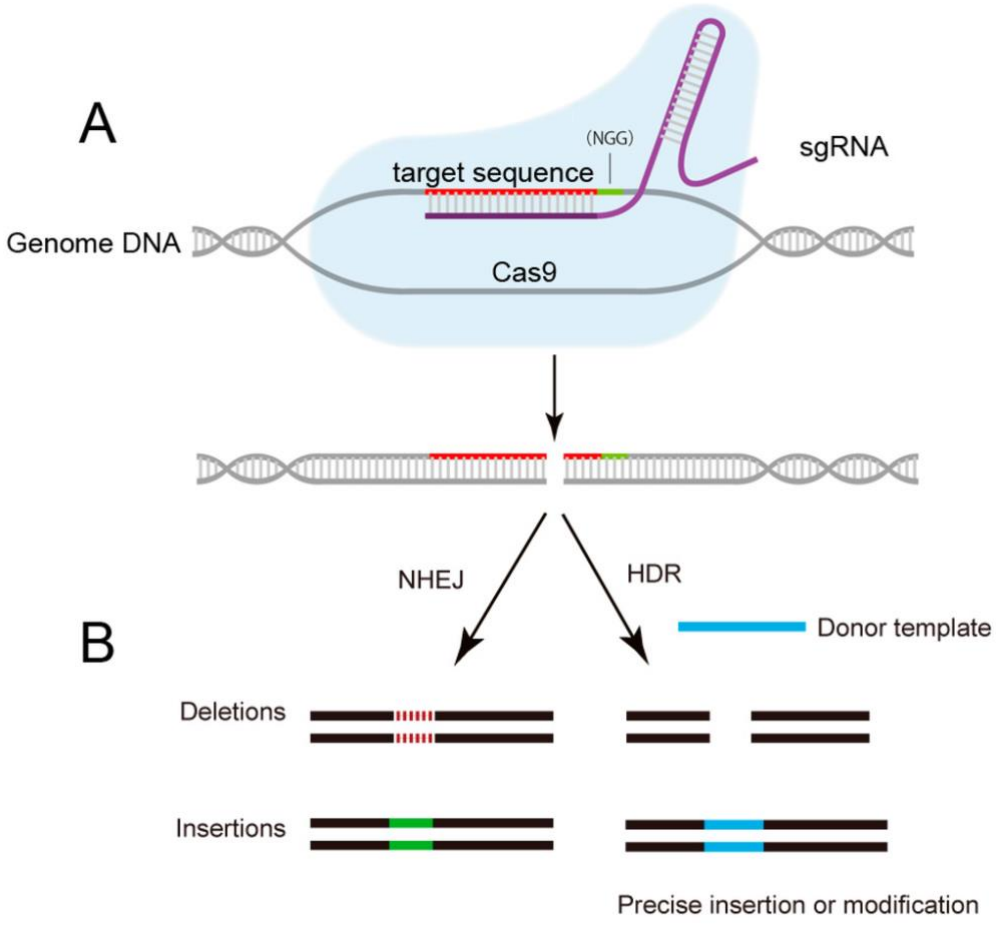

Figure 1.5. Schematic representation of CRISPR-Cas9 mediated gene-editing. A) The sgRNA (purple) guides the Cas9 enzyme (light blue) to the targeted cleavage site to induce a double-

stranded break (DSB) 3-4 base pairs (bp) upstream of the protospacer-adjacent motif (PAM; green) sequence. B) Homology-directed repair (HDR) or hon-homologous end joining (NHEJ) repair mechanisms are then activated to result in the precise edit of a target sequence or in the introduction of insertion or deletion (indel) mutations respectively. The system has since been modified to introduce four sgRNAs (two targeting the 5' untranslated region (UTR) and two targeting the 3' UTR) to completely excise the gene of interest. Retrieved from (Lin et al. 2015).

1.13. Statement of purpose

Numerous studies have shown the capacity for various neurotoxins to induce sporadic PD, however, this has been done to varying degrees of ablation and uncomplimentary effects in certain cases. These disparities are especially apparent in the literature surrounding chemical exposures using zebrafish. To address this, my first aim will use zebrafish larvae to identify the optimal compound between MPTP, MPP+, 6-OHDA, rotenone and paraquat that selectively targets diencephalic DAnergic neurons without inducing morphological defects.

The model of neurodegeneration generated will help us to then perform a screen of various phytochemicals to protect against oxidative stress mediated damage. The analysis of biomarkers associated with fission and DA synthesis will form a profile for the mitochondrial and DAnergic impact in addition to monitoring swimming activities to observe any preserved motor function. This will be useful for looking into alternative, dietary means of DAnergic neuroprotection prior to the onset of Parkinsonian symptoms.

Following the optimization of a model using zebrafish larvae, we aim to also generate a reliable sensorimotor deprived neurotoxic model of PD using adults. We will implement a novel delivery technique to introduce a compound into the cerebroventricular fluid surrounding the

zebrafish brain in means to induce rapid DAnergic cell death. The impact on fission-fusion dynamics will also be evaluated in Tg(*dat:tom20 MLS:mCherry*) transgenic zebrafish, in parallel to gene expression for mitophagy and apoptotic biomarkers to differentiate the mechanism of mitochondrial clearance and subsequent cell death.

Once the establishment of efficient larval and adult models of environmentally-induced PD has been completed, we seek to investigate genetic links to PD and DA-associated diseases through a loss-of-function study targeting DAnergic transcription factor *nr4a2* paralogs, *nr4a2a* and *nr4a2b*. This will be carried out using CRISPR-Cas9 genome editing to excise the gene of interest for subsequent behavioral, immunohistochemical, regenerative and transcriptomic analysis. Previous studies on *nr4a2* in zebrafish have been focused on *tyrosine hydroxlase (th*) and general DAnergic characterization, thus the investigation into other biomarkers of DA health and neurological homeostasis will help depict if these mutants are suitable models for PD and other diseases linked to DA deficiencies.

CHAPTER 2: COMPREHENSIVE ANALYSIS OF NEUROTOXIN-INDUCED ANALYSIS ABLATION OF DOPAMINERGIC NEURONS IN ZEBRAFISH LARVAE

2.1. Abstract

Neurotoxin exposure of zebrafish larvae has been used to mimic a Parkinson's disease (PD) phenotype and to facilitate high-throughput drug screening. However, the vulnerability of zebrafish to various neurotoxins was shown to be variable. Here, we provide a direct comparison of ablative effectiveness in order to identify the optimal neurotoxin-mediated dopaminergic (DAnergic) neuronal death in larval zebrafish. Transgenic zebrafish, Tg(*dat*:eGFP), were exposed to different concentrations of the neurotoxins MPTP, MPP^+, paraquat, 6-OHDA, and rotenone for four days, starting at three days post-fertilization. The LC50 of each respective neurotoxin concentration was determined. Confocal live imaging on Tg(*dat*:eGFP) showed that MPTP, MPP^+, and rotenone caused comparable DAnergic cell loss in the ventral diencephalon (vDC) region while, paraquat and 6-OHDA caused fewer losses of DAnergic cells. These results were further supported by respective gene expression analyses of *dat, th,* and *p53*. Importantly, the loss of DAnergic cells from exposure to MPTP, MPP^+, and rotenone impacted larval locomotor function. MPTP induced the largest motor deficit, but this was accompanied by the most severe morphological impairment. We conclude that, of the tested neurotoxins, MPP^+ recapitulates a substantial degree of DAnergic ablation and slight locomotor perturbations without systemic defects indicative of a Parkinsonian phenotype.

2.2. Introduction

Parkinson's Disease (PD) is a progressive and debilitating neurodegenerative disease in which clinical hallmarks comprise motor and cognitive impairments. Pathologically, motor symptoms in humans arise due to the progressive and irreversible loss of dopaminergic (DAnergic) neurons within the substantia nigra (Jankovic 2008). Although the etiology of PD remains ambiguous, it is likely due to the cumulative result of genetic and environmental insult. Familial PD has been linked to mutations in genes, however, this can only explain 15–30% of cases while the majority of cases are sporadic (Klein and Westenberger 2012). It is believed that exposure to environmental toxins is widely associated with idiopathic PD (Dexter and Jenner 2013)

Animal models contribute to our knowledge of PD progression and help explore possible therapeutics. Chemo-ablative models using neurotoxic compounds such as 1-methyl-4-phenyl-1,2,3,6-tetrahydropyridine (MPTP), 1-methyl-4-phenyl-pyridinium (MPP^+), 6-hydroxydopamine (6-OHDA), rotenone, and paraquat have been used to study the molecular mechanisms of DAnergic neurodegeneration in mammals (Przedborski et al. 2004a; Meredith and Rademacher 2011; Blesa et al. 2012; Bhurtel et al. 2019). The zebrafish (*Danio rerio*) has proven to be a robust in vivo vertebrate animal model for the studies of various neurodegenerative diseases (Bretaud et al. 2004; Best and Alderton 2008b) and high-throughput drug screening (Stewart et al. 2014)due to their large clutch size and transparent ex utero embryogenesis. With ~87% of their genome similar to humans, zebrafish also display a variety of conserved molecular and pathological pathways (Holzschuh et al. 2001a; Du et al. 2016). In particular, a proportion of the DAnergic system in zebrafish (primarily in the ventral diencephalic region) is postulated to be functionally homologous to that of the nigrostriatal pathway in mammals (Sallinen et al. 2009). Dopaminergic projections in zebrafish are fully formed by 3–4 days post-fertilization (dpf) (Fleming et al. 2013; Du et al. 2016)compared to

E12.5 observed in mice (Sillitoe and Vogel 2008), E20 in rats (Santana et al. 1992), and by embryonic day 73 in macaques (Lidow 1995). The rapid neurodevelopment and optical transparency throughout embryogenesis in zebrafish allow for facilitated study of DAnergic-related diseases such as PD.

MPTP is the most widely used neurotoxin to induce DAnergic neuronal loss and PD-associated locomotor phenotypes in many animal models (Meredith and Rademacher 2011; Tieu 2011; Hare et al. 2013). MPTP is lipophilic and it is metabolized by astrocytes (glia) into its active toxic form, MPP^+, by monoamine oxidase B (MAO-B). MPP^+ enters DAnergic neurons through the dopamine transporter (*dat*) where it can act on complex I of the electron transport chain (ETC), resulting in the inhibition of ATP synthesis, mitochondrial respiration, and in the promotion of superoxide radical production (Przedborski et al. 2004a; Hare et al. 2013)

Paraquat is the most predominantly used commercial herbicide (Bromilow 2004; Richardson et al. 2005). Recent epidemiological studies have outlined the increased risk of developing PD following extensive exposure to paraquat (Dhillon et al. 2008). This divalent cation undergoes redox cycling and its presence results in enhanced oxidative-stress within DAnergic mitochondria (Rappold et al. 2011). However, exposure to paraquat has been shown to yield inconsistent reports in the literature. This is particularly evident in zebrafish studies, where some have outlined a severe neurodegenerative impact of paraquat on dopamine and serotonin protein levels (Nellore and P 2015; Wang et al. 2017a), while others observed no obvious phenotypes (Bretaud et al. 2004). This variable effect extends to behavioral symptoms following treatment, where some groups observed significant motor impairment (Bortolotto et al. 2014), while others report no fluctuations in any swimming activity parameter (Bretaud et al. 2004). These results may be the consequence of varying treatment regimens. Paraquat-induced Parkinsonian-related phenotypes in vivo warrant further investigation.

6-OHDA is a synthetically hydroxylated dopamine compound that is taken up into catecholaminergic neurons through dopamine or norepinephrine transporters (Reader and Dewar 1999; Dauer and Przedborski 2003). 6-OHDA exposure is commonly co-administered with a norepinephrine transporter inhibitor to increase the specificity of neurotoxicity to DAnergic neurons (Fulceri et al. 2006; Bové and Perier 2012) Although 6-OHDA has been shown to be effective in inducing DAnergic neuronal loss in a wide variety of mammals from mice, cats, dogs, monkeys, and rats (Blesa et al. 2012), few studies have shown the sensitivity of zebrafish to 6-OHDA.

Likewise, rotenone is commonly used as an industrial insecticide and as piscicide, a compound used to eradicate fish (Nanda et al. 2009). Rotenone's hydrophobic nature allows for the easy penetrance of astrocyte and neuronal cellular membranes (Ott and D 2006; de Juan Romero et al. 2010). The mechanism of action of rotenone is similar to MPTP, through the impairment of complex I of the ETC. Additionally, through nuclear translocation, rotenone leads to the activation of NF-κB and the subsequent DNA fragmentation to result in cellular damage (Sinha et al. 2016). The toxic nature of rotenone to fish makes it difficult to determine an optimal dose that results in efficient DAnergic ablation with low mortality. Rotenone exposure studies in zebrafish have yielded conflicting results (Bretaud et al. 2004; Martel et al. 2015)

To date, the susceptibility of zebrafish to neurotoxic drugs remains contradictory. This may be due to varying concentrations, duration of exposure, and initial time of treatment which typically occurs at 24 h post-fertilization (hpf), before the full DAnergic neuronal system and blood–brain barrier (BBB) have developed (Fleming et al. 2013). In addition, behavioral assays and methods of determining DAnergic neuronal loss vary greatly between studies. Most studies primarily utilize TH as a marker for detecting DAnergic cells in either *in situ* hybridization or

whole mount immunostaining approaches. The use of a transgenic model, Tg(*dat*:*eGFP*) (Xi et al. 2011b) that expresses enhanced green fluorescent protein (eGFP) under the control of the dopamine transporter (*dat*) cis-regulatory element in zebrafish, allows for live visualization of DAnergic neurons. In this study, we provide a comprehensive comparison of PD-associated neurotoxins and determine the optimal concentration required to induce maximal decrease of DAnergic neurons along with PD-like locomotor phenotypes.

2.3. Materials and Methods

2.3.1. Zebrafish care and husbandry

Transgenic zebrafish of the Tg(*dat*:*eGFP*) line (Xi et al. 2011b) were used in this study. Zebrafish were maintained at 28.5 °C under a 14-h light/10-h dark cycle. Embryos were collected by natural spawning and raised in E3 embryo media (13 mM NaCl, 0.5 mM KCL, 0.02 mM Na_2HPO_4, 0.04 mM KH_2PO_4, 1.3 mM $CaCl_2$, 1.0 mM $MgSO_4$, and 4.2 mM $NaHCO_3$). Embryos were screened using fluorescence microscopy and $eGFP^+$ larvae were sorted accordingly. We expressed the embryonic stages in days post-fertilization (dpf). The University of Ottawa Animal Care Committee approved all animal care procedures, which were conducted under the Animal Care and Veterinary Service guidance in accordance with the recommendations of the Canadian Council for Animal Care following ethical code BL-2081.

2.3.2. Environmental toxin preparation and exposure

At 3 dpf, 20 larvae were sorted and placed into each well of a 6-well plate in a solution volume of 3 mL. De-chorionated larvae were treated at 3 dpf until 7 dpf. Room temperature (~23 °C) was chosen for exposures due to an increase of rotenone-associated neurotoxicity observed at 28.5 °C (Keow 2016) and to ensure all treatment groups are exposed to the same conditions. Five different concentrations were chosen to determine an accurate sub-lethal dosage. The exposure gradient followed an increasing half log series. Solutions were changed daily and replaced with freshly prepared ones. Toxins were discarded in accordance to current safety protocols. All larvae were co-treated with 0.2 M phenylthiourea (PTU), a pigmentation inhibitor, to facilitate confocal live imaging. Previous studies have shown that PTU does not impair *th* or *dat* expression throughout embryonic and larval neurodevelopment (Holzschuh et al. 2001a)

1-methyl-4-phenyl-1,2,3,6-tetrahydropyridine hydrochloride (MPTP; Sigma) was reconstituted in distilled water to a stock concentration of 500 mM. MPTP was further diluted to the working concentrations of 0.25 mM, 0.5 mM, 1.0 mM, 1.5 mM, and 2.5 mM. MPP^+ iodide (Sigma) was re-constituted in distilled water to a stock concentration of 4.86 mM. MPP^+ was further diluted to the working concentrations of 0.025 mM, 0.05 mM, 0.075 mM, 0.1 mM, and 0.5 mM. Methyl viologen dichloride hydrate (Paraquat; Sigma) was reconstituted with sterile distilled water at a concentration of 100 mM, then diluted into 25 mM, 10 mM, 5 mM, 3 mM, and 1 mM working dosages. 6-Hydroxydopamine hydro-chloride (6-OHDA; Sigma) was dissolved in and co-administered with 1% ascorbic acid to prevent precipitation and preserve molecular stability at a concentration of 100µm. The solution was further diluted to the working concentrations of 30µM, 10µM, 3µM, and 1µM. Controls for 6-OHDA were exposed to a 0.01% ascorbic acid solution. Rotenone (Sigma) was prepared in 100% dimethyl sulfoxide DMSO at a concentration of 100 mM,

then serially diluted up to 1,000,000-fold in 10% water-diluted DMSO to working concentrations of 5 nM, 10 nM, 25 nM, 50 nM, and 100 nM. Rotenone controls were exposed to a 0.01% DMSO solution. All treatments were conducted in the dark as MPP^+, 6-OHDA, and rotenone are photosensitive.

2.3.3. Live confocal imaging

At 7 dpf, treated zebrafish larvae were transferred from their respective exposure media to fish water, anaesthetized with 3× tricaine, and live-mounted dorsal side up on slides using a 1% low-melting point agarose solution. Larvae were continuously re-hydrated while mounted using system water to ensure survival. Imaging was conducted using the Nikon A1 confocal microscope with a 25× water immersion objective. Larvae were scanned using the laser at a wavelength of 488 nm to excite eGFP. Images were obtained in a 2–3 µm interval Z-stack that was processed and compiled to produce a three-dimensional image. The total cell numbers for clusters 8, 12, and 13 were determined in 3-D to avoid repeated counts of the same cell and by three independent researchers in a blinded fashion to remove bias. Maximum intensity projection images used for the study were produced using the NIS-Elements software (Nikon).

2.3.4. RNA isolation and qRT-PCR

RNA was extracted from five pools of 10 pestle-homogenized whole larvae using TRIzol (InVitrogen). Extractions were done according to the manufacturer's protocol. RNA integrity and purity was determined using gel electrophoresis and the NanoDrop 1000 Spectrophotometer (ThermoFisher). Samples with clear 18S, 28S bands and an absorbance ratio of 1.8–2.1 were used

for cDNA synthesis. RNA was reverse-transcribed using the iScript™ cDNA Synthesis Kit (Bio-Rad) in accordance with the manufacturer's protocol. qRT-PCR reactions were composed of 5 µL SsoFast™ EvaGreen® Supermix (Bio-Rad), 0.4 µL reverse primer, 0.4 µL forward primer, 0.2 µL nuclease-free water and 4 µL cDNA. Reactions were done in triplicates using the Bio-Rad CFX96 instrument. Normalized quantification of the number of *th1*, *dat*, and *p53* transcripts was achieved through the comparative Cq method using three reference genes*; tyrosine 3-monooxygenase/tryptophan 5-monooxygenase activation protein, zeta polypeptide* (*ywhaz*), *ribosomal protein l13a* (*rpl13a*), and *elongation factor 1 alpha* (*ef1a*). Oligonucleotide primers are listed in Table 2.1.

Table 2.1. List of primers designed for qRT-PCR.

Primer	Forward Sequence (5′–3′)	Reverse Sequence (5′–3′)	Reference
dat	AGACATCTGGGAAGGTGGTG	ACCTGAGCATCATACAGGCG	(Barreto-Valer et al. 2012)
th1	GACGGAAGATGATCGGAGACA	CCGCCATGTTCCGATTTCT	(Chen et al. 2016)
p53	ATATCCTGGCGAACATTTGG	ACGTCCACCACCACCATTTGAAC	
ywhaz	TCTGCAATGATGTGTTGGAGC	TCAATGGTTGCTTTCTTGTCGTC	
rpl13a	TCTGGAGGACTGTAAGAGGTATGC	AGACGCACAATCTTGAGAGCAG	(Tang et al. 2007)
ef1a	CTGGAGGCCAGCTCAAACAT	ATCAAGAAGAGTAGTACCGCTAGCATTAC	

2.3.5. Swimming activity

Following neurotoxin treatment, 7 dpf larval zebrafish from each treatment group (6-OHDA, Paraquat, Rotenone, MPP^+, and MPTP) were removed from their exposure media and monitored for their swimming activity. Individual larvae were transferred to E3 embryo media, placed in a 6-well plate, and allowed to acclimate in ambient light for 15 min prior to recording. The activity was recorded using the Zebralab software and the Zebrabox tracking system (ViewPoint Life Science). The tracking system consists of infrared illumination, LED lights, and a mounted camera for swimming recording under dark and light conditions. The parameters of larval swimming activity were total distance travelled and the average velocity for 5 min trials. Sample sizes of 18–25 were chosen to delineate the effects of each compound from natural variability in locomotion exhibited by larvae. Touch stimuli response was conducted by gently touching the posterior portion of the tail of 20–30 larvae from each respective group and was qualitatively assessed as normal or reduced (slow response or absence of response).

2.3.6. Statistical analysis

Statistical analysis was done using the software GraphPad Prism v.7. Swimming activity was evaluated on sample sizes ranging from 18–25 individuals, $eGFP^+$ cell counts were quantified from 10–15 zebrafish, and gene expression data were collected from three pools of 10 embryos. Data are shown as the mean ± the standard error of the mean. The total distance and average velocity were analyzed using a one-way ANOVA followed by Dunnett's multiple comparison test. vDC cell loss was analyzed using a two-way ANOVA followed by Tukey's multiple comparison test. Gene expression data were calculated using a multiple t-test comparison with significance determined using the Holm–Sidak method. Statistical significance was determined when *p*-value < 0.05 and was indicated as * $p < 0.05$, ** $p < 0.01$, *** $p < 0.001$.

2.4. Results

Given the ambiguity in alternative neurotoxin-mediated studies, the current study aimed at providing direct comparisons on the in vivo effects of PD-inducing neurotoxins to identify the optimal candidate for DAnergic neuron ablation and motor phenotypes. All treatments were conducted starting at 3 dpf to prevent the inhibition of neurogenesis and because there is, at this time, near complete DAnergic differentiation and BBB development (Du et al. 2016). The varying concentrations used were to determine the optimal dose for each compound that would result in greater than 50% survival and could be used in subsequent analyses. Following the establishment of each LC_{50} concentration, DAnergic neuronal death was quantified through in vivo imaging of $eGFP^+$ cells in various clusters of the vDC. These regions were chosen due to the proposed homology of this area to the nigrostriatal pathway depicted in higher vertebrate species (Holzschuh et al. 2001a; Sallinen et al. 2009). In parallel, larval zebrafish exposed to each compound were

examined for locomotor perturbances. Conducted under the same exposure regimen, these data will identify the most efficient of the neurotoxins to induce DAnergic ablation and motor impairment with any potential off target morphological malformations. This will serve as a platform for high-throughput pharmacological screening aimed at alleviating cellular, locomotor or morphological insults.

2.4.1. Effective LC_{50} dose for PD phenotypic induction (survival curve/median lethal concentration)

Following an MPTP exposure (0.25 mM, 0.5 mM, 1.0 mM, 1.5 mM, and 2.5 mM), the identified LC_{50} dose to carry out further DAnergic analyses was 0.25 mM (Fig. 2.1A). Concentrations of 2.5 mM and 1.5 mM resulted in complete mortality at 3-days post treatment (dpt) and 4 dpt respectively. In contrast, concentrations of 1.0 mM and 1.5 mM resulted in severe malformations and were shown to be completely lethal at 5 dpt. The selected concentration of 0.25 mM resulted in >50% survival, however, it is noted the mortality increased 2.5-fold from 4 dpt to 5 dpt.

Upon exposure to MPP^+, larvae treated with concentrations exceeding 0.05 mM showed 100% lethality by 7 dpf, whereas larvae treated with 0.05 mM displayed over 50% survival (Fig. 1B) without severe morphological defects (Fig. 2.2).

The herbicide paraquat was analyzed for its cytotoxic effects on DAnergic neurons due to its properties as an oxidizing agent. Exposure to 25 mM paraquat was shown to be lethal by 3 dpt, whereas, at 5 mM and 10 mM 100% lethality was observed by 4 dpt. Consequently, a concentration of 1 mM was used to examine a DAnergic loss phenotypic. This concentration contrasted with a

previous report by (Bretaud et al. 2004), where exposure to 3 mM for two days resulted in complete mortality by 5 dpt (Fig. 2.1C).

6-OHDA was administered at concentrations that ranged from 1 μM to 100 μM. A concentration of 100 μM resulted in 100% mortality at 1 dpt, whereas 30 μM was shown to be completely lethal by 5 dpt. Larvae exposed to concentrations of 1 μM, 3 μM, and 10 μM displayed >75% survival (Fig. 2.1D).

Previous studies have utilized concentrations of rotenone ranging from 10 nM to 1 μM under various treatment regimens (Barreto-Valer et al. 2012; Martel et al. 2015; Vaz et al. 2018). Here, we tested a range from 5 nM to 100 nM from 3 dpf to 7 dpf. The LC_{50} dose was observed to be 50 nM (Fig. 2.1E). All further experimentation with rotenone was carried out using this dose.

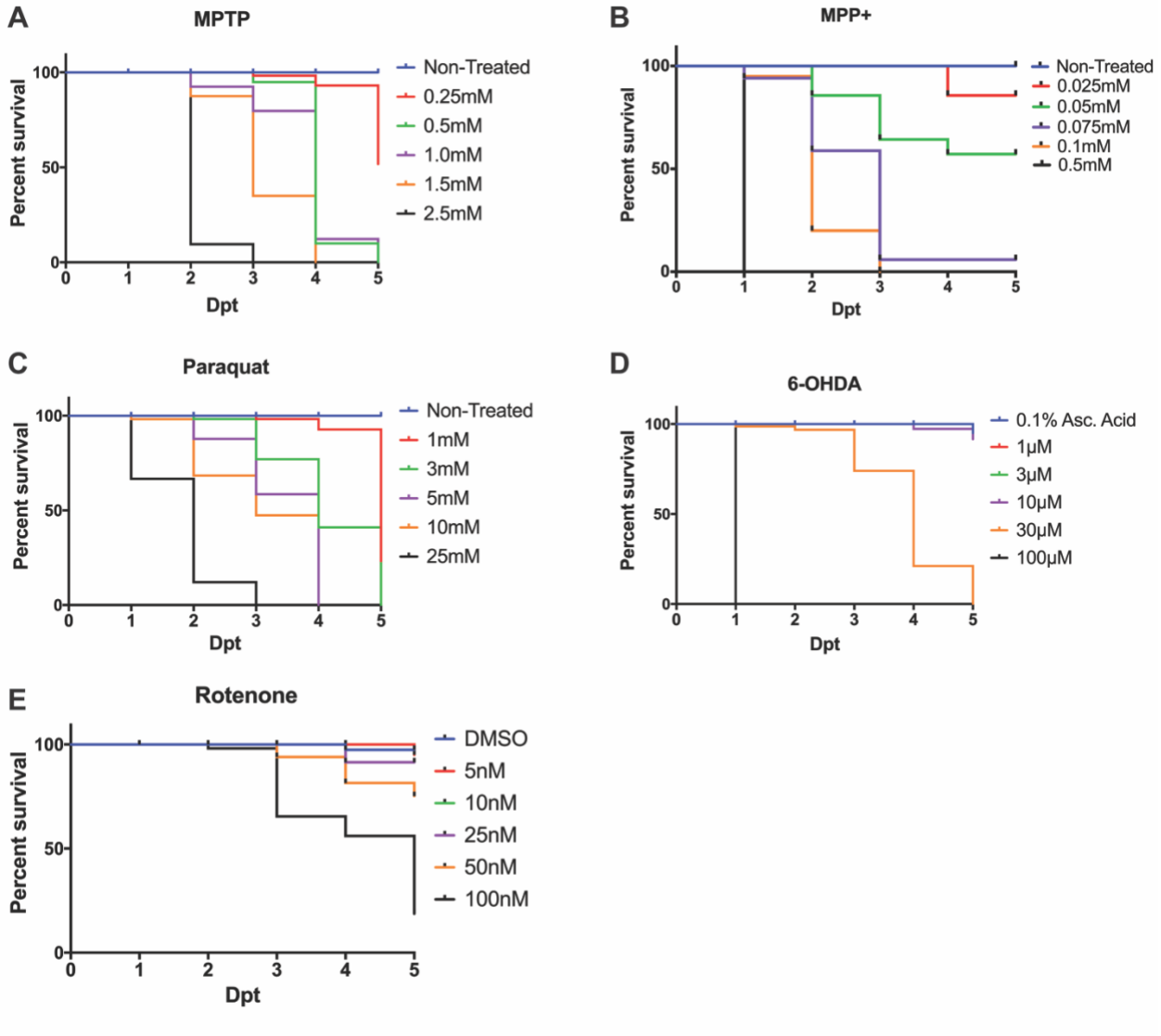

Figure 2.1. Zebrafish larvae survival following neurotoxin exposure. 3 dpf embryos were exposed to varying concentrations of A) MPTP, B) MPP^{+}, C) paraquat, D) 6-OHDA, and E) rotenone to determine the LC50 or sub-lethal dose. Lethality was quantified every 24 hpt until the zebrafish reached 7 dpf.

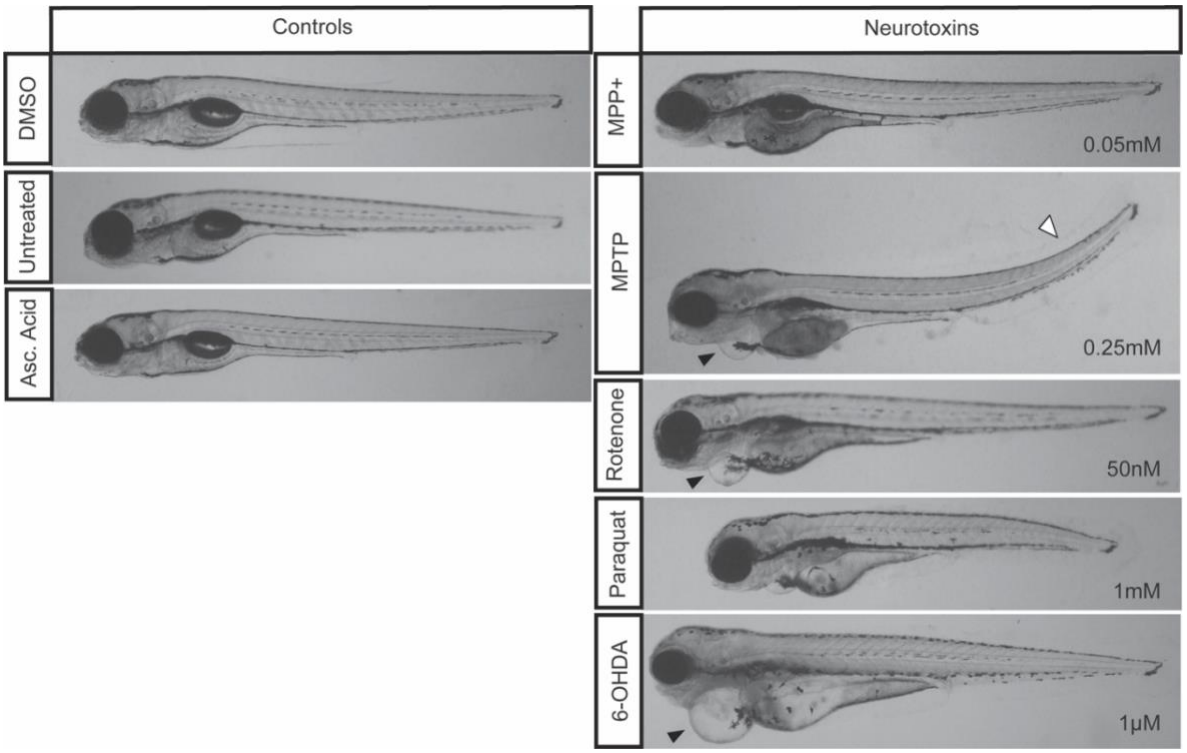

Figure 2.2. Zebrafish morphology following neurotoxic exposures. Larvae were exposed to 0.05 mM MPP^+, 0.25 mM MPTP, 50 nM rotenone, 1 mM paraquat, and 1μM 6-OHDA starting at 3 dpf and imaged at 7 dpf. Control larvae were exposed to 0.1% DMSO, 0.1% ascorbic acid, or left untreated. Cardiac defects are depicted by a black arrowhead and a tail curvature is depicted by a white arrowhead. Refer to Table 2 for the frequency of each morphological malformation.

Table 2.2. Summary of LC_{50} neurotoxic effects of MPTP, MPP^+, paraquat, 6-OHDA, and rotenone.

Drug	LC_{50} Concentration	Locomotion	Global vDC DAnergic Loss (%)	Morphological Defects	Other Effects
MPTP	0.25 mM	Severe	39%	Cardiac and tail curvature (9/20)	Unresponsive to touch
MPP^+	0.05 mM	Moderate	35%	None of significance	Unresponsive to touch
Paraquat	1 mM	None	16%	Stunted development (3/20)	None of significance
6-OHDA	1 µM	None	18%	Cardiac defect (2/20)	None of significance
Rotenone	50 nM	Moderate	36%	Cardiac defect (4/20)	None of significance

2.4.2. DAnergic neuronal loss in the ventral diencephalon (vDC)

To determine the degree of DAnergic neuronal decrease in the vDC, we treated 3 dpf larvae for four days with MPTP, MPP^+, 6-OHDA, and paraquat at their respective LC_{50} concentrations. Following exposure to 0.25 mM MPTP, larvae displayed a 39% decrease in the total number of eGFP positive neurons in clusters 8, 12, and 13 of the vDC. We observed a 56% and 35% decrease in clusters 8 and 13, respectively, in MPTP-treated animals compared to controls, while there was no significant difference in cluster 12 (Fig. 2.3B–D). Larvae exposed to 0.05 mM MPP^+ exhibited similar decreases in clusters 8 and 13 with 41% and 35% reduction, respectively, while cluster 12 remained unaffected. DAnergic cells expressing eGFP were shown to decrease by 36% globally between these vDC clusters (Fig. 2.3E–G).

In larvae treated with 1 µM 6-OHDA, there was a 19% decrease in the number of DAnergic neurons within the vDC. Interestingly, when looking at the changes within individual clusters, decreases did not reach statistical significance although there was a clear trend (Fig. 2.3H–J).

Exposure of fish to paraquat resulted in a 18% decrease in global ventral diencephalic DAnergic neurons, however, changes in individual clusters did not reach statistical significance (Fig. 2.3K–M).

Exposure to 50 nM rotenone was shown to significantly impact all three DAnergic clusters. Reductions of 49%, 35%, and 33% were observed following rotenone treatment in clusters 8, 12, and 13, respectively. The combined DAnergic loss cumulated to 38% within the vDC (Fig. 2.3N–P).

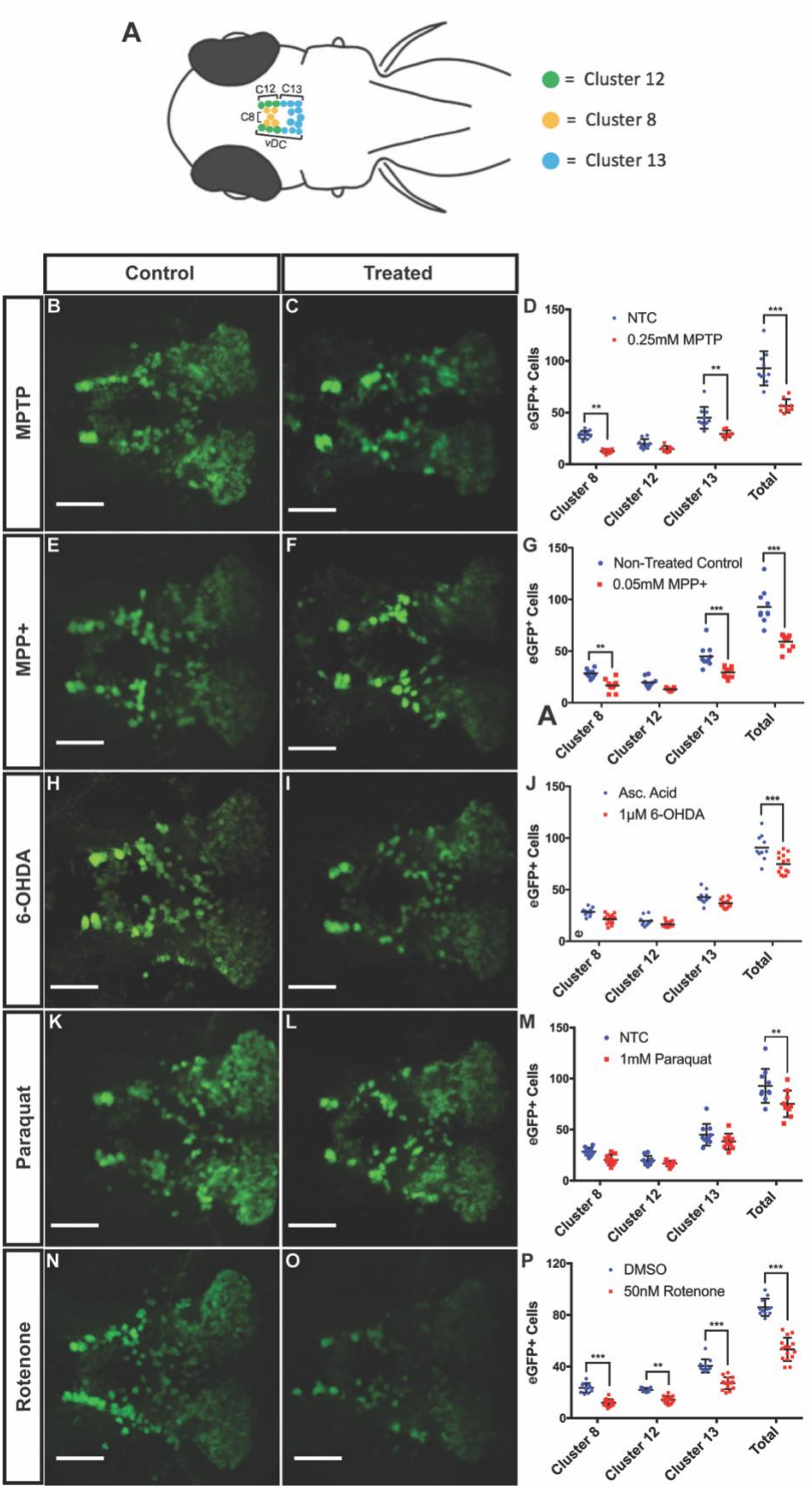
A
C12
C13
C8
vDC
= Cluster 12
= Cluster 8
= Cluster 13
Control
Treated
MPTP
MPP+
6-OHDA
Paraquat
Rotenone
B
C
D
E
F
G
H
I
J
K
L
M
N
O
P
NTC
0.25mM MPTP
Non-Treated Control
0.05mM MPP+
Asc. Acid
1μM 6-OHDA
1mM Paraquat
DMSO
50nM Rotenone
eGFP+ Cells
Cluster 8
Cluster 12
Cluster 13
Total

Figure 2.3. Effects of neurotoxins on ventral diencephalic (vDC) DAnergic clusters of 7 dpf Tg(*dat:eGFP*) zebrafish. A) Schematic representation of eGFP neuronal clusters 8, 12, and 13 within the vDC. Cluster 8 in yellow, cluster 12 in green, and cluster 13 in blue. Dorsal view with anterior to the left. B-P) Quantification $eGFP^+$ cells within the vDC through confocal fluorescent live imaging following exposure to 0.25 mM MPTP, 0.05 mM MPP^+, 1 µM 6-OHDA, 1 mM paraquat, and 50 nM rotenone (n = 9–15). All images were acquired using a maximum projection of 2µm z-stacks, scale bar = 100µm. Bars represent the Mean ± the SEM. * ($p < 0.05$), ** ($p < 0.01$), *** ($p < 0.001$).

2.4.3. Gene expression

We analyzed expression of genes such as *tyrosine hydroxylase 1* (gene: *th1;* protein: TH*)* and *dopamine transporter* (gene: *dat;* protein: DAT*)* to see if they correlated with the observed decreases in DAnergic cell numbers. In addition, we investigated whether neurotoxin exposure would trigger neuronal apoptosis through the *p53* pathway by looking at its mRNA expression. MPTP-treated larvae exhibited a 60% and 31% in *th1* and *dat* expression relative to the non-treated control, whereas, *p53* expression was shown to increase by 35% (Fig. 2.4A). Following MPP^+ exposure, there were 36% and 55% decreases in the expression of *th1* and *dat* respectively in treated compared to control fish. There was also a 39% increase in *p53* expression in MPP^+ treated fish (Fig. 2.4B). Paraquat exposure resulted in a 41% and 37% decrease in *th1* and *dat* expression respectively. However, there was no change in the expression of *p53* (Fig. 2.4C). 6-OHDA exposure resulted in a 55% decrease only in *th1* while *dat* and *p53* expression was unaffected (Fig. 2.4D). Finally, rotenone was shown to significantly impact *th1* expression resulting in a 41% reduction, whereas the

expression of *dat* and *p53* were observed to be slightly upregulated, although changes did not reach statistical significance (Fig. 2.4E).

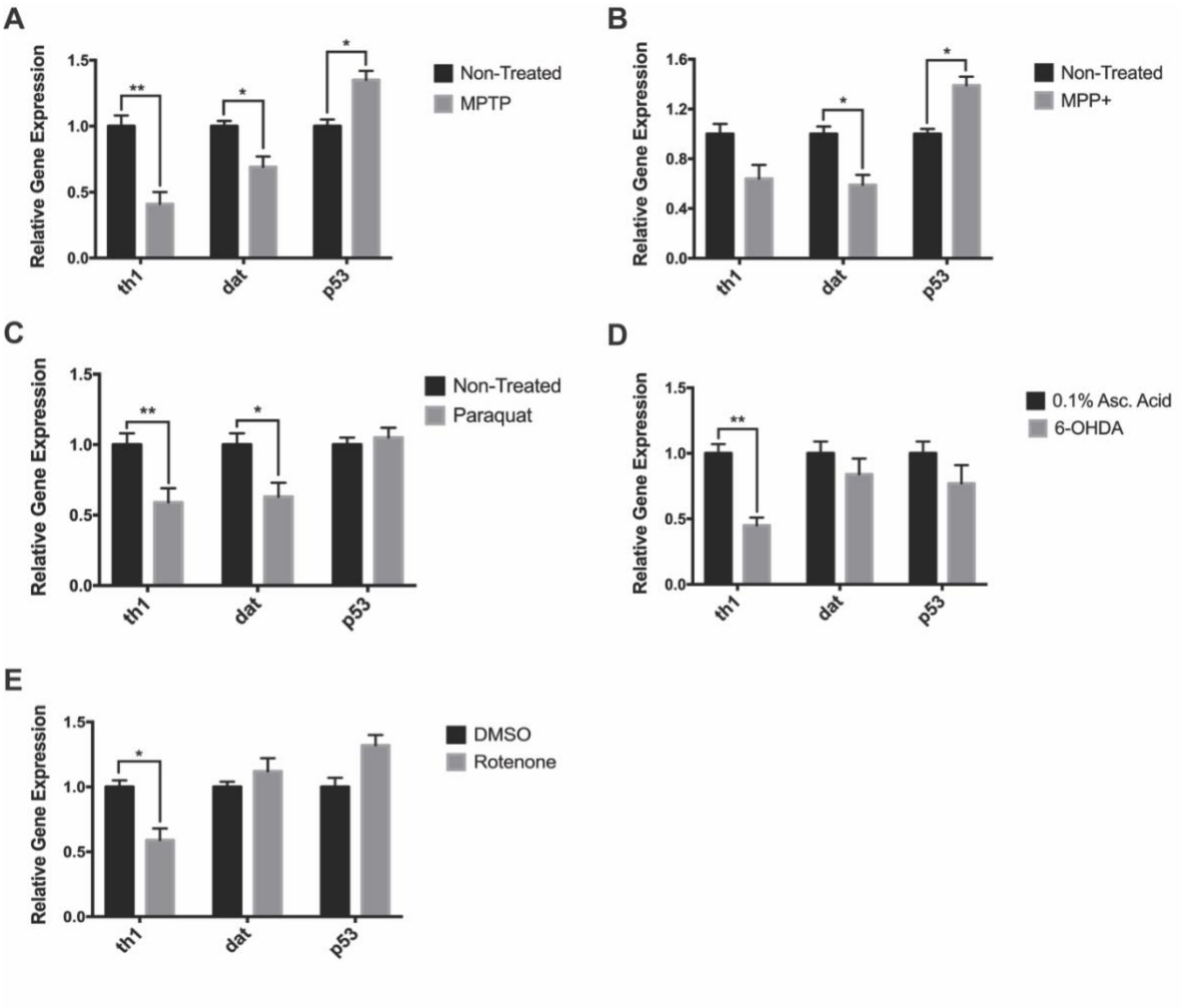

Figure 2.4. Impact of neurotoxin exposure on dopaminergic- and apoptosis-linked gene expression. A-E) Relative expression of *dat*, *th1*, and *p53* of 7 dpf zebrafish following exposure to MPTP, MPP^+, paraquat, 6-OHDA, and rotenone (n = 3 pools of 10 larvae). Bars represent the Mean ± the SEM. * ($p < 0.05$) and ** ($p < 0.01$).

2.4.4. Effects on locomotion

To further investigate whether the decrease in DAnergic neurons within the vDC affects behavior, we analyzed the zebrafish locomotor activity. The most important reductions in both total distance and velocity were obtained for MPTP-treated larvae (80% and 85% reductions, respectively, Fig. 2.5A,B). A milder impact on locomotion was obtained with the active metabolite MPP^+, with only slight 24% reductions in both total distance and velocity.

Both paraquat and 6-OHDA had no significant impact on locomotion. In contrast, rotenone elicited an effect only on total distance with a 46% reduction, while the average velocity was unaffected.

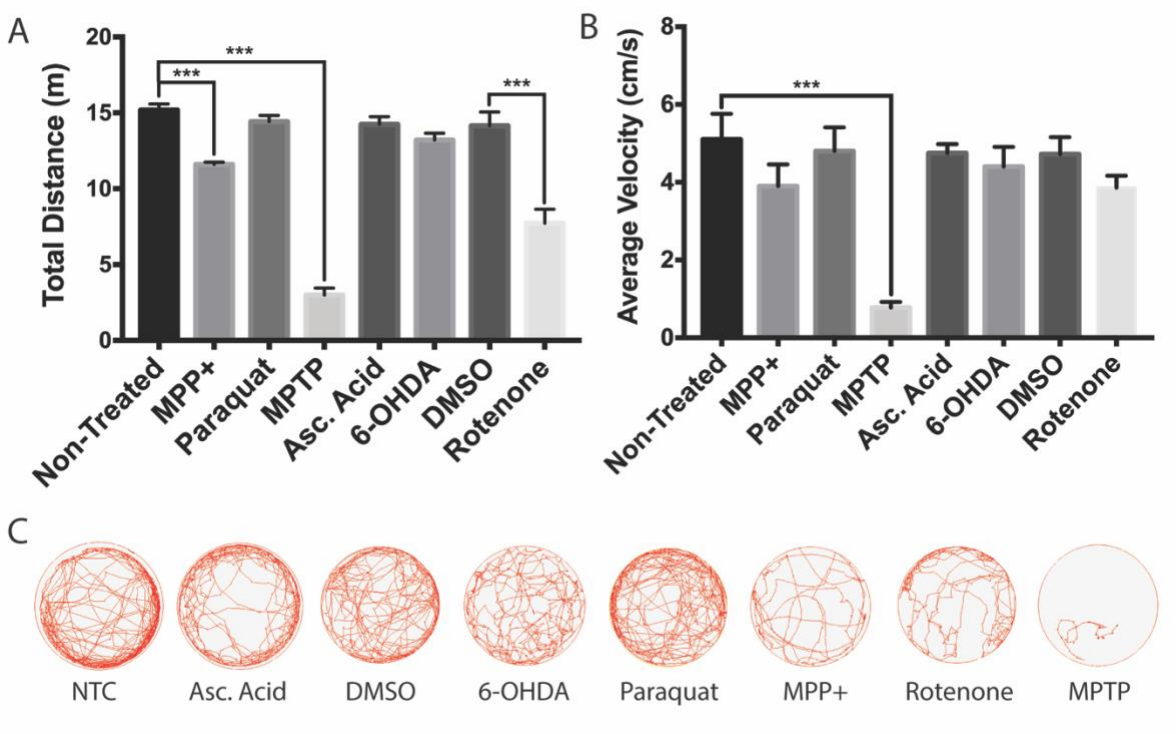

Figure 2.5. Swimming activity of zebrafish larvae following neurotoxin exposure. All zebrafish were transferred to acclimate to a 6-well plate for 15 mins prior to behavioral

analyses. A-B) Effects of MPTP, MPP^+, 6-OHDA, paraquat, and rotenone on total swim distance and average swimming velocity (n = 20–25 larvae). C) Overhead path images of a representative larvae for each exposure group. Bars represent the Mean ± the SEM. *** (p < 0.001).

2.5. Discussion

With the majority of Parkinsonian pathologies being sporadic, there lies considerable interest in the role of environmental neurotoxin exposure as a contributor of PD. While there have been studies that tested the effects of MPTP, MPP^+ (Sallinen et al. 2009), 6-OHDA (Feng et al. 2014), paraquat, and rotenone (Bretaud et al. 2004; Keow 2016) in larval zebrafish, there have been mixed and contradictory results for each drug. The majority of these studies begin treatment at 24 hpf and continue until 4 dpf or 7 dpf making it difficult to discern whether the observed reductions in DAnergic neurons result from cell death, impairment of DAnergic differentiation, or delayed neurogenesis. In this study, we conducted a direct comparative analysis between MPTP, MPP^+, rotenone, 6-OHDA, and paraquat using the same treatment regimen to extrapolate the optimal compound that induces a decrease in DAnergic cells and a locomotor impairing phenotype. In addition, these data will emphasize the neurotoxin-mediated contribution to the onset of PD-related symptoms on zebrafish larvae.

2.5.1. MPTP and MPP^+

The impact of MPTP on locomotion has been well characterized using in vivo models ranging from rodents (Meredith and Rademacher 2011), to amphibians (Barbeau et al. 1985), and medaka

(Matsui et al. 2009). Similarly, in zebrafish, larval exposure to MPTP has been shown to induce DA neurodegeneration within the vDC that translates into a motor phenotype (Sallinen et al. 2009). Following our treatment regimen, starting at 3 dpf to ensure a functional BBB and advanced DAnergic development, our results displayed significant locomotor dysfunction correlating with a 39% decrease in DAnergic neurons. When contrasting the effects with MPP^+, MPP^+ treated zebrafish showed a similar degree of DAnergic neuronal ablation, but did not display the same motor defects. MPTP requires metabolism MAO-B in the vDC to exert its neurotoxic effect, as well as the LC_{50} dose administered being 5-fold greater than MPP^+. However, in zebrafish, the expression of MAO-B within the vDC appears to be low based on spatial distribution, thus limiting MPTP conversion to its active toxic form in this region of the brain (Sallinen et al. 2009). Therefore, the perturbance in motor function shown in the current study may be a result of the constant systemic exposure to a large dose of MPTP. Furthermore, exposure to 0.25 mM of MPTP resulted in the most severe and frequent morphological defects (Fig. 2.2).

Previous studies have shown that MPP^+ exposure starting at 1 dpf continuing (Fleming et al. 2013) for three days resulted in a decrease in DA neurons only within the diencephalon (Lam et al. 2005; Sallinen et al. 2009). In addition, the decrease in DAnergic neurons was correlated with a decrease in total distance travelled (Sallinen et al. 2009), mean velocity and percent of time moving (Farrell et al. 2011). Our treatment regimen, starting at 3 dpf still resulted in a 36% loss in the number of DAnergic neurons. Larvae exposed to this concentration of MPP^+ were observed to be morphologically indistinguishable from controls. Consistent with previous data, the loss of DAnergic neurons was also correlated with a decrease in total distance travelled and mean velocity. However, the decrease in distance traveled and mean velocity observed were modest compared to those obtained with MPTP. This could be due to effects of MPTP secondary metabolites, as also

evidenced by the malformations observed that include the development of slight cardiac edemas and upwards tail curvatures (Fig. 2.2).

2.5.2. Paraquat

Although paraquat is structurally similar to MPP^+, there remains ambiguity in paraquat's mechanism of action. It is only recently that this mechanism has been linked to genetics where one study identified three candidate genes (POR, ATP7A, and SLC45A4) whose products are required for reactive oxygen species (ROS)-mediated cell death (Reczek et al. 2017). Paraquat has been shown to cross the BBB in rats to induce dopaminergic toxicity (Shimizu et al. 2001), but in the current study paraquat failed to elicit the same degree of DAnergic reductions within the vDC compared to MPTP and MPP^+. Paraquat did, however, cause a significant reduction in total eGFP expression in DAnergic cells, as well as a downregulation of *th1* and *dat* transcript levels. Moreover, paraquat had only mild effects, if any, on locomotion. Some reports document a near 3-fold difference in total distance (Nellore and P 2015), while others did not see the same deficit (Bretaud et al. 2004). Contrarily to Bretaud et al. we found notable morphological defects in zebrafish treated with paraquat alone. We did not observe effects that were specific to any particular organ, but rather a reduction in the overall size of treated larvae (Fig. 2.2).

2.5.3. 6-OHDA

Consistent with previous reports (Feng et al. 2014), zebrafish exposed to 1µM 6-OHDA showed a significant decrease of the number of DAnergic neurons in the vDC. However, this 18% reduction in DAnergic neurons did not translate into any impairment of locomotor activity.

Notably, although relatively scarce, larvae exposed to 1µM were shown to develop severe cardiac malformations. These results contradict those of the study conducted by Feng et al., where they observed moderate and severe motor defects in zebrafish treated with 100 µM and 250 µM 6-OHDA respectively (Feng et al. 2014). This effect may be a consequence of the treatment regimen adopted in that study where larvae were exposed to 6-OHDA once from 24 hpf to 5 dpf prior to the establishment of a functional DAnergic system. Furthermore, despite larval survival at higher concentrations (3 µM and 10 µM), we found that the effect of these doses on vDC DAnergic numbers to be indistinguishable from those obtained with 1µM. Nonetheless, the reduction in $eGFP^{+}$ neurons when contrasted to MPTP, MPP^{+}, and rotenone may be a consequence of the proposed neuroprotective effects of ascorbic acid (Riederer et al. 1989; Casarejos et al. 2002).

2.5.4. Rotenone

Rotenone-induced neurotoxicity has been well documented to contribute to motor deficits in various in vivo models ranging from mice (Bhurtel et al. 2019), rats (Swarnkar et al. 2010), and *Drosophila* (Coulom and Birman 2004). In addition, rotenone exposure has been shown to induce Lewy body inclusions and neurodegeneration in mice and rats (Betarbet et al. 2000; Dauer and Przedborski 2003; Liu et al. 2015). However, rotenone exposure in zebrafish has yielded conflicting results. An initial study demonstrated that rotenone exposure of 5 µg/L and 10 µ/L starting at 24 hpf did not result in a loss of DAnergic neurons or to PD-like locomotor dysfunction (Bretaud et al. 2004). In contrast, another study showed that exposure of larvae for six days starting at 24 hpf resulted in a significant decrease in the number of cells and severe mispatterning within the vDC and the olfactory bulbs (Martel et al. 2015). Despite the decrease in DAnergic neurons, there was no major locomotor impairment. Furthermore, morphological defects associated with

rotenone exposure in the study of Bretaud et al. only demonstrated a synergistic effect following co-treatment with paraquat. Here, we were able to show that exposure of larval zebrafish to 50 nM rotenone for four days starting at 3 dpf was sufficient to induce a loss of DAnergic neurons within the vDC and a mild locomotion defect. Moreover, we also observed zebrafish exposed to rotenone developing cardiac malformations (edema; Fig. 2.2, arrowhead). Unexpectedly, we also observed a slight upregulation of *dat* following rotenone exposure. This increase may be part of a compensatory mechanism to promote the reuptake of dopamine within surviving neurons.

2.5.5. Comparison of effectiveness between tested neurotoxins

Here we exposed larval zebrafish to respective neurotoxins starting at 3 dpf a time at which the DAnergic system is well established. This allowed us to test the effects of neurotoxic compounds on the survival of DAnergic neurons (Kastenhuber et al. 2010). Using a consistent immersion treatment regiment, we were able to assess the effectiveness of neurotoxic compounds on inducing DAnergic neuronal loss and locomotor behavior. In line with previously reported studies in mammalian models (Blesa et al. 2012), MPTP exposure resulted in the largest loss of DAnergic neurons. The large loss of DAnergic neurons also coincided with severe locomotion defects such as reduced total distance travelled and average velocity. Meanwhile, MPP^+ elicited a similar degree of DAnergic ablation. However, it only perturbed motor function through total distance travel and not average velocity. Noteworthy between the two neurotoxins, fish exposed to MPTP suffered detrimental cardiac and developmental abnormalities, whereas, fish treated with MPP^+ were indistinguishable from the non-treated controls suggesting the increased efficiency of MPP^+ for DAnergic ablation without systemic defects in contrast to MPTP. Like MPP^+, rotenone was shown to be effective in DAnergic ablation, while only disrupting total distance traveled,

although the systemic exposure of rotenone was observed to result in apparent cardiac edemas. The effectiveness of MPTP and rotenone could be attributed to their lipophilic structure allowing for the ease of permeating the BBB (Przedborski et al. 2004b; Tieu 2011; Hare et al. 2013). This molecular nature of MPTP and rotenone is beneficial regarding our treatment regimen that uses an immersion approach. This approach relies on BBB diffusion following gill, gut, and skin absorption, and circulatory transport to the brain (Fleming et al. 2013). Moreover, 6-OHDA uptake is not specific to DAnergic neurons; the use of a norepinephrine transporter inhibitor to block noradrenergic neuron uptake could increase the specificity of neurotoxicity to DAnergic neurons in future zebrafish studies. Paraquat was the least efficient neurotoxic compound to induce DAnergic neuronal loss and locomotor defects in zebrafish. A detailed mode of action of paraquat-induced cell death remains to be defined. However, our result further supports the notion that paraquat alone may not be able to generate substantial oxidative stress to induce cell damage without increasing the exposure to a concentration that will result in significant mortality. Overall, our data suggest that under the current exposure conditions and concentrations, MPP^+ is the most effective neurotoxin. Being the active metabolite of MPTP, MPP^+ provides a more direct route to induce substantial DAnergic neuronal loss that translates to a locomotor phenotype without the systemic toxicity observed from MPTP exposure.

2.6. Conclusions

Despite MPTP and rotenone's efficiency in DAnergic ablation and motor perturbation, MPP^+ remains as the optimal compound for PD-related recapitulation. Given the ongoing issue of experimental reproducibility, the results of this comprehensive comparison will contribute to alleviate this problem and to shed light onto the extensive neurotoxin contribution to the pathology

of PD. Following this exposure regimen, using MPP^+ will provide a most effective and consistent phenotype for Parkinsonian insult that will contribute to the facilitation of therapeutic screening for cellular and motor symptoms.

CHAPTER 3: NEUROPROTECTIVE SCREENING OF NATURAL PHENOLICS IN AN MPTP-INDUCED MODEL OF PARKINSON'S DISEASE USING ZEBRAFISH

3.1. Abstract

Mitochondrial dysfunction and oxidative stress are a prominent features that underlie both genetic and non-genetic cases of Parkinson's disease (PD). Without a definitive cure for PD and with current therapies being associated to the development of undesirable side effects, the scope of preventative measures have shifted (or reverted back) to investigating naturally occurring phytochemicals that possess antioxidizing properties to mitigate against the accumulation of reactive oxygen species (ROS) commonly observed in disease pathologies. DAnergic neurons are particularly metabolically demanding and susceptible to bioenergetic imbalances, thus we sought to examine the neuroprotective effects of ascorbic acid (AA), ferulic acid (FA) and vanillic acid (VA) on DAnergic survivability against MPTP exposures. MPTP is a neurotoxin known to target mitochondrial complex I of DAnergic neurons leading to the formation of superoxide radicals and cell death. By analyzing motility and the expression levels of genes associated with dopamine production and mitochondrial fission in an MPTP model of neurodegeneration, we found AA to mitigate more transcriptional damage than motor, whereas VA did not prevent any impaired gene expression but slightly rescued locomotion. Overall, we found FA to be the most effective natural phenol to protect against MPTP-induced Parkinsonism.

3.2. Introduction

Parkinson's disease (PD) is a debilitating disease that currently affects 1.4% of the global population (Muangpaisan et al. 2011). PD is onset by the gradual and age-associated loss of dopaminergic (DAnergic) neurons that populate the substantia nigra pars compacta and supply the striatum with dopamine (DA) (Dauer and Przedborski 2003). The resulting decrease in DA generates the cardinal symptoms of PD that include bradykinesia, tremors, instability, in addition, to sensory and cognitive impairments that commonly precede motor perturbance (de Lau and Breteler 2006; Sulzer et al. 2016). PD is extremely complex in its origins as 15% of cases result from familial inheritance, while the remaining 85% are sporadic (Cheng et al. 2010). Despite the discrepancy between the pathogenic prevalence of sporadic and genetic PD, mitochondrial dysfunction and oxidative stress are prominent features that underlie all forms of PD. This susceptibility can largely be attributed to the high metabolic demand and oxygenic requirements of the brain and more specifically of midbrain DAnergic neurons (Magistretti and Allaman 1999; Plaitakis and Shashidharan 2000). Many animal models have since been generated to mimic disease pathologies and help elucidate various aspects of disease for both familial and sporadic PD. Of which, several transgenic mouse lines have been made that express the same mutation involved in human PD that recapitulate age-associated Parkinsonian symptoms for certain variants that include *LRRK2-R1441G* (Li et al. 2009), *PINK1-G309D* (Gispert et al. 2009) and *LRRK2-G2019S* (Garcia-Miralles et al. 2015). Conversely to model sporadic PD, 1-methyl-4-phenyl-1,2,3,6-tetrahydropyridine (MPTP) has been the most commonly adopted neurotoxin to selectively degenerate DAnergic neurons.

The impact of MPTP on the nigrostriatal tract of humans was discovered in the 1980s by drug users who mistakenly injected MPTP instead of the meperidine analog 1-methyl-4-phenyl-4-

propionoxy-piperidine (MPPP) (Langston et al. 1983). Innocuous MPTP can permeate the blood-brain-barrier where it is metabolized by astrocytic monoamine oxidase-B (MAO-B) into toxic MPP+ to be taken into DAnergic neurons by the dopamine transporter (DAT). Once in the cytosol, MPTP inhibits mitochondrial complex I to disrupt mitochondrial function leading to the activation of mitophagy or apoptotic cell death mechanisms (Przedborski et al. 2004a; Kizil and Brand 2011; Sarath Babu et al. 2016). Since, MPTP has been shown to induce vast DAnergic ablation that consistently translates into PD-related phenotypes using a number of rodent (Meredith and Rademacher 2011; Bhurtel et al. 2019), non-human primate (Park et al. 2019), aquatic (Kalyn et al. 2019) and invertebrate (Aryal and Lee 2019) models alike. The widespread use of MPTP has also pioneered the way for mitochondrial targeted therapeutics that alleviate the suffering of PD.

Currently there is no cure for PD, however, several advances have been made that provide symptomic relief to patients. These treatment primarily consist of MAO-B antagonists (selegiline), DA agonists (pergolide), viral delivery of glial delivered neurotrophic factor (GDNF) or on levodopa supplementation that can all also pose alternative health risks. Risks most commonly arise regarding dosing, however, side effects manifest themselves in a wide range of symptoms that include hallucinations, anxiety, pain, euphoria, insomnia and confusion (Cummings 1991; Pedrosa and Timmermann 2013; Manfredsson et al. 2020). Moreover, many treatments are only available after substantial DA loss detected in mid- to later-onset patients. Thus, the search for preventative measures prior to diagnosis continues to look into natural or dietary sources for pretreatments or supplementation. Of which, phytochemicals with strong antioxidizing properties are highly sought after given the prevalence of mitochondrial dysfunction among both forms of PD.

One metabolite that has been shown to mitigate oxidative stress damage in both in vitro and in vivo systems is ascorbic acid (AA; the reduced form vitamin C). Endogenous AA is synthesized in the liver of most mammals except for a few species that include humans that rely on exogenous supplementation. Despite widespread distribution throughout the body, AA accumulates to high concentrations (2-10mM) in the brain and relies on sodium vitamin C and glucose transporters to cross the blood-brain-barrier (Nualart et al. 2014). The dietary dependance is what popularized AA in the 1930s for alleviating the clinical manifestations of scurvy. Several studies have since come forward demonstrating AA's activity in mediating a large number of cellular processes that include ROS detoxification (Arrigoni and De Tullio 2002), cholesterol metabolism (Ginter 1975), hippocampal synaptic plasticity (Fraga et al. 2020) and as a cofactor for enzymatic redox cycling (Krishnan et al. 2009). In a neurological context, recent work using zebrafish has highlighted AA's ability to relieve butachlor-, deltamethrin-, lead- and neomycin-induced neurotoxicity through the observation of reduced morphological abnormalities, hatching defects, mortality and normalized levels of expression for genetic markers indicative of oxidative stress such as *superoxide dismutase* (*sod*) and *catalase* (*cat*) (Wu et al. 2015; Xiang et al. 2018; Paduraru et al. 2021).

Another natural phenol known to possess antioxidizing properties is ferulic acid (FA). FA is one of the primary active components of traditional Chinese medicines and has been documented to influence many cellular processes as well. Some processes include but are not limited to free-radical scavenging (Ogiwara et al. 2002), lipid metabolism (Son et al. 2010), inflammation (Cheng et al. 2008) and anti-cancer signaling pathways (Kawabata et al. 2000). In recent years, the scope of FA treatment has broadened to investigate the effects in neuroprotection where FA was shown

to protect rodent neurons and PC-12 cell cultures against hypoxia and ischemia-induced cytotoxicity (Koh 2013; Ren et al. 2017).

Similarly, the use of plant derived vanillic acid (VA) has recently come forth with therapeutic effects that attenuate the impacts of oxidative stress in a number of models and processes. VA is produced as a byproduct from the conversion of ferulic acid into vanillin and has been shown to modulate healthy in disease states of cardiac (Kumar et al. 2011), neurological (Khoshnam et al. 2018), metabolic (Salau et al. 2020) and inflammatory (Stanely Mainzen Prince et al. 2011) function.

The use of zebrafish has recently taken the spotlight in pharmacological screening due to their high fecundity, transparent ex utero embryogenesis and rapid development into adulthood (Rubinstein 2003; Kari et al. 2007). From early larval stages, zebrafish can exhibit complex behaviors that appeal to studies that investigate the acute or chronic effects of bioactive compounds in ecotoxicological research. Comparing genetic studies with humans has also gained more traction due to 71% homology between genomes that comprises of 87% of disease-related genes (Howe et al. 2013). This conserved nature extends into signaling pathways as a nigrostriatal counterpart has been described in zebrafish. DAnergic projections in this circuit are two-fold that project from the posterior tuberculum through to the pallium, as well as, local projections from the subpallium that terminate in the dorsal pallium (Rink and Wullimann 2002a,b; Tay et al. 2011). These properties have rendered zebrafish optimal to investigate the comparative effects of various biomolecules on DAnergic health, insult and survivability.

Several studies have demonstrated the implications of each phytoconstituent in the context of PD and neurotoxicity, however, there remains controversy in the optimal neuroprotectant to prevent DAnergic loss. In this study, we bridge this gap by contrasting the neuroprotective effects

of AA, FA or VA in an MPTP-induced DAnergic degenerative model using Tg(*dat:eGFP*) zebrafish larvae. We analyzed the differential expression of *tyrosine hydroxylase 1* (*th1;* essential to DA biosynthesis) and *mitochondrial fission protein 1* (*fis1;* essential in mitochondrial fission-fusion dynamics) in addition to various swimming parameters. FA elicited the largest protective effect on all proxies examined for DA, mitochondria and locomotion. AA only alleviated MPTP-induced insult to gene expression, however, motor function remained perturbed. Conversely, VA did not prevent the deleterious effects on *th1* and *fis1* expression, however, VA did slightly ameliorate locomotor phenotypes. The data obtained from this research elucidated FA as the most promising candidate for future therapeutic investigation.

3.3. Materials and Methods

3.3.1. Zebrafish care and husbandry

All experiments were approved by the University of Ottawa and conducted according to the Canadian Council Animal Care and the Animal Care and Veterinary Service (ACVS) guidelines. Tg(*dat:eGFP*) adult zebrafish were bred to generate the larvae used within this study. Housing conditions included a temperature of 28.5 ^{O}C, 14-hour dark/10-hour light cycles, recirculating tank water and appropriate E3 media for embryos (13mM NaCl, 0.5mM KCl, 0.02mM Na2HPO4, 0.04mM KH2PO4, 1.3mM CaCl2, 1.0mM MgSO4, and 4.2mM NaHCO3).

3.3.1. Neurotoxic and antioxidant exposures

Zebrafish larvae were exposed to neuroprotectants and MPTP in 6-well plates that were kept at room temperature (~23^{O}C) for the length of the treatment. Pretreatment exposures took

place from 1dpf to 3dpf and followed by exposure to 0.25mM MPTP from 3dpf until analysis. All exposure mediums were refreshed daily.

To determine the optimal dose ensuring increased survivability relative to the MPTP-treated control, larvae were first exposed to a gradient of four concentrations of AA, FA and VA under the treatment regimen detailed above. The working concentrations for AA, VA and FA that were used for the experiments performed within this study were 50µM, 250µM and 100µM respectively.

3.3.3. RNA extraction, cDNA synthesis and qRT-PCR

In accordance to the manufacture's protocol of TRIzol (InVitrogen), RNA was extracted from three biological replicates, each containing 7 whole larvae collected at 6 dpf. To ensure RNA quality, the samples were run on an bleached agarose gel to visualize 18S and 28S bands. Sample concentration and purity was also quantified using the NanoDrop 1000 spectrophotometer (ThermoFisher) where only samples with (1.8-2.1) 260/280nm absorption ratios were carried out for further experimentation. RNA samples were reverse-transcribed to synthesize cDNA using the iScript™ cDNA Synthesis Kit (Bio-Rad). 5 µL SsoFastTM EvaGreen® Supermix (Bio-Rad), 0.4 µL forward primer, 0.4 µL reverse primer, 0.2 µL nuclease-free water, and 4 µL cDNA were used in the reaction mix. The Bio-Rad CFX96 instrument and Maestro software were used to run the reactions. Normalized quantification of the number of *th1* and *fis1* transcripts was achieved through the comparative Cq method using three technical replicates and two reference genes: *beta-actin* (*β-act*) and *elongation factor 1 alpha* (*ef1a*). The oligonucleotide primers' sequences are listed in Table 3.1.

Table 3.1. List of primers designed for qRT-PCR.

Primer	Forward Sequence (5'-3')	Reverse Sequence (5'-3')	Reference
b-actin	CGAGCTGTCTTCCCATCCA	TCACCAACGTAGCTGTCTTTCTG	(Tang et al. 2007)
ef1a	CTGGAGGCCAGCTCAAACAT	ATCAAGAAGAGTAGTACCGCTAGCATTAC	
th1	GACGGAAGATGATCGGAGACA	CCGCCATGTTCCGATTTCT	(Chen et al. 2016)
fis1	CCCTGAACCTTCCAGTGTTT	GTCTCTGGAAACGGGTCCTT	

3.3.4. Locomotion

To assess swimming activities following exposure, 20 larval zebrafish from each treatment group (non-treated control (NTC), MPTP, AA, VA, FA) were removed from their media and placed in 24-well plates to be analyzed at 6dpf. The larvae acclimated to the ambient light for 10 minutes before recording began. The Zebralab software and the Zebrabox tracking system (ViewPoint Life Science) were used to record the motility of the larvae over 10 minutes. The tracking system consists of infrared illumination, LED lights, and a mounted camera to facilitate recording in both light and dark conditions. The parameters collected for the behavioral assessment included total distance traveled and inactivity duration.

3.3.5. Statistical analysis

GraphPad Prism v.7 (software was used to perform all statistical analyses. One-way ANOVA followed by Dunnett's multiple comparison test was used to analyze the distance of moving larvae and average velocity. a multiple t-test comparison was used to calculate gene expression data, and the Holm–Sidak method determined significance. Statistical significance was

determined when p-value < 0.05 and was indicated as * p < 0.05, ** p < 0.01, *** p < 0.001, ****p < 0001.

3.3. Results

3.3.1. Optimal dose screening for ascorbic acid, ferulic acid and vanillic acid in a MPTP-induced PD model

The use of transgenic animals has provided us with robust means to perform precise measurements. We adopted the use of Tg(*dat:eGFP*) zebrafish for this reason as it efficiently labels all neurons that expression the *dopamine transporter* (*dat*) with *enhanced green fluorescent protein* (*eGFP*). Larvae were bred and pretreated with a gradient of AA, FA and VA concentrations to find the optimal dose ensuring increased survivability relative to the MPTP-treated positive control (Fig. 3.1). MPTP was selected despite MPP+ demonstrating the most reliable effects in Kalyn and colleagues (2019) because we wanted to investigate the full protective capacity of each compound on the most deleterious model to DAnergic health, locomotion and development (Kalyn et al. 2019). Pretreatment began at 1-day post-fertilization (dpf) and continued to 3dpf upon switching to MPTP-refreshed media. The working concentrations for AA, VA and FA that were used in subsequent experimentation were 50 μM, 250 μM and 100 μM respectively.

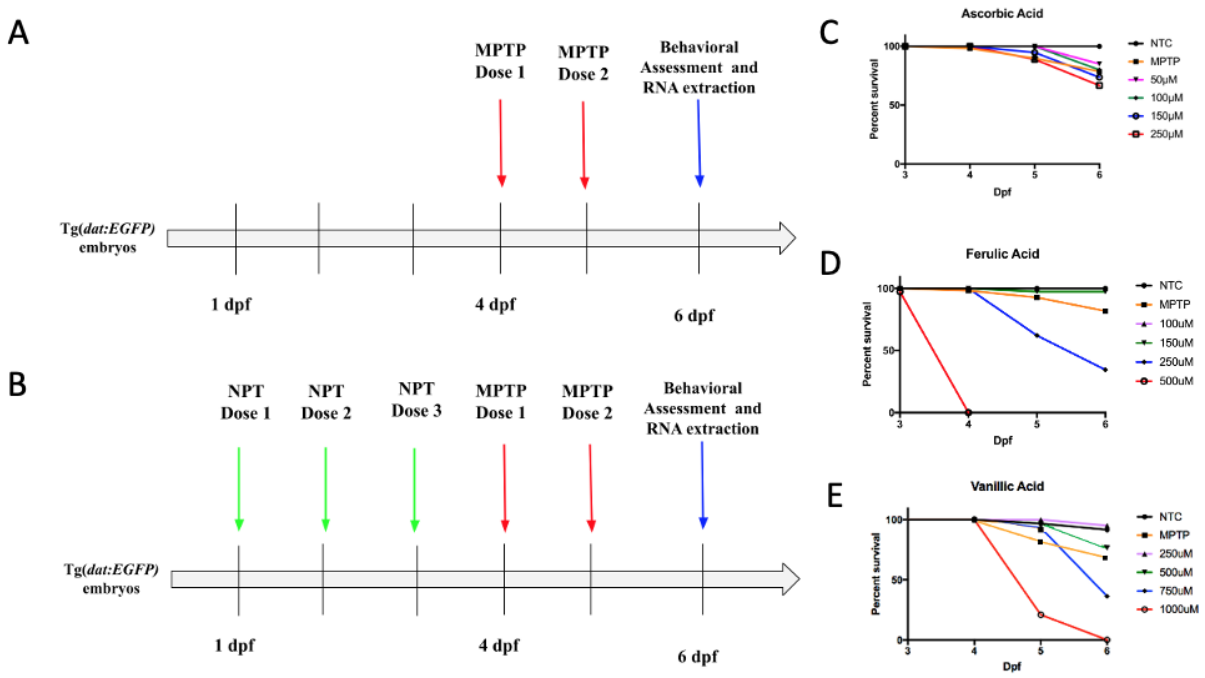

Figure 3.1. Experimental design and survivability of larvae zebrafish to varying phenolic concentrations. A-B) Positive control and neuroprotective treatment regimen. C-E) Concentration gradient survival curves for ascorbic, ferulic and vanillic acid.

3.3.2. Preventative effects of AA, FA and VA on locomotion

Impaired locomotion is a hallmark feature of PD and a central target of symptomic relief. To delineate the largest preventative effects of AA, FA and VA on motor performance, we examined total distance swam and freezing bout durations as proxies for functional recuperation in an MPTP-induced model of PD. Relative to the positive control, FA and AA pretreated larvae displayed the largest improvement in both parameters. For FA, the larvae froze ~52% less and swam on average 1.83 further than the MPTP-treated group. Larvae pretreated with VA were observed to freeze ~25% less, however, this group travelled 2.64 times larger distance than the MPTP-control. AA yielded the lesser preventative effect on locomotion where no significance or

dramatic change in distance from MPTP-treatment was observed and only a ~17% increase in mobility was observed (Fig. 3.2.).

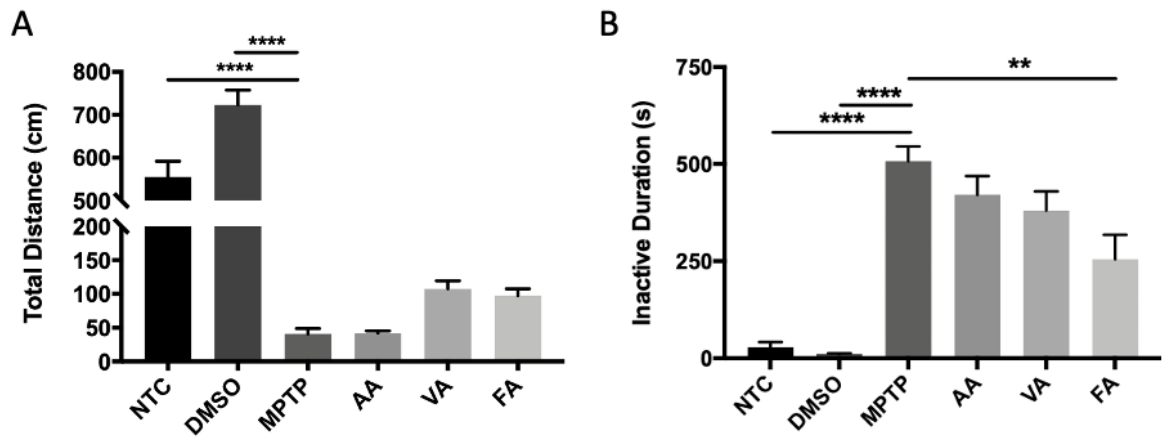

Figure 3.2. Neuroprotective effect of phenolics on locomotion following MPTP exposure. A) Total distance and B) inactivity duration quantified for non-treated controls (NTC), DMSO controls, MPTP, ascorbic acid, vanillic acid and ferulic acid exposure groups. (*n*=20). Bars represent the Mean ± the SEM. **($p<0.01$).and ****($p<0.0001$).

3.3.3. DAnergic and mitochondrial gene expression changes following pretreatment with AA, FA and VA

DAnergic neurons are highly metabolic cells that rely on oxidative phosphorylation for energy. Because of this, DAnergic are particularly susceptible to any flux in oxidative metabolism, thus perturbed mitochondrial function can be consequential to DAnergic health and behavior. To examine the neuroprotective effects on mitochondria and DA homeostasis, we examined the differential expression of genes associated with mitochondrial fission (*mitochondrial fission protein 1*; *fis1*) and the biosynthesis of DA (*tyrosine hydroxylase 1*; *th1*). First to confirm the

experimental model, MPTP-treated larvae exhibited a 57% decrease and 71% increase in the expression of *th1* and *fis1* relative to the non-treated control (NTC), respectively. FA pretreated larvae showed an 18% decrease and 1% increase in *th1* and *fis1* relative to the NTC. AA yielded similar results regarding *th1*, however, a slight decrease in *fis1* was observed compared to the NTC. VA was observed to possess the least protective effects on gene expression where a *th1* was reduced by 51% and *fis1* increased by 34% in contrast to the NTC. However, statistical significance has not yet been reached (Fig. 3.3.).

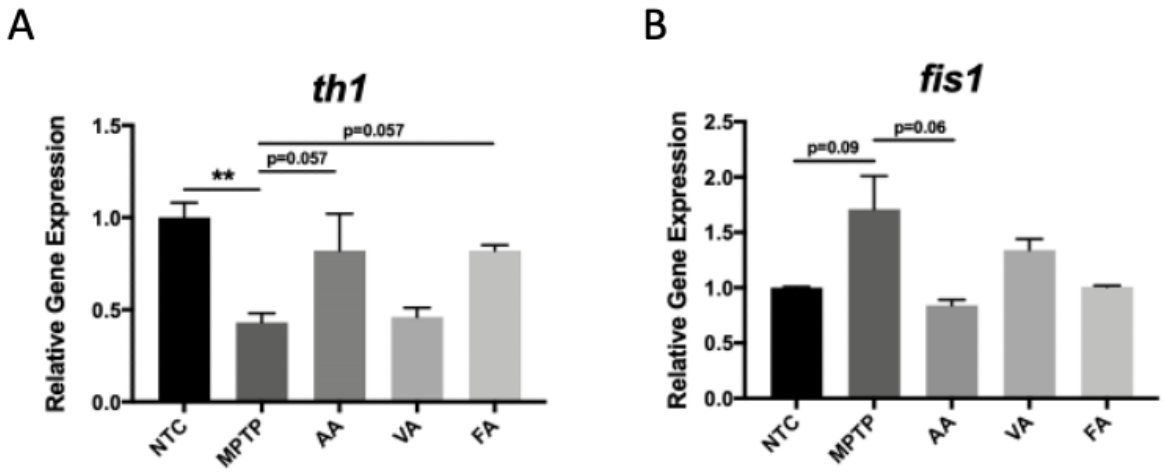

Figure 3.3. Protective impact on mitochondrial fission and DAnergic gene expression. A) Relative gene expression of *th1* and B) *fis1* analyzed between NTC, MPTP, ascorbic acid, vanillic acid and ferulic acid. (*n*= 2 pools of 7 larvae). Bars represent the Mean ± the SEM. **($p<0.01$).

3.4. Discussion

3.4.1. Ascorbic acid

AA has been shown to be a potent antioxidant involved in DAnergic homeostasis for decades. Under pathological conditions, the recycling capacities of AA become significantly impaired which acts to further amplify disease states. Several early studies implemented pre- and co-treatments of AA using mice and human derived cell lined to protect against MPTP- and levodopa-induced neurotoxicity respectively (Sershen et al. 1985; Pardo et al. 1993). AA was not only shown to protect against neurotoxicity, but to also promote the gene expression of DOPA and TH in vitro (Seitz et al. 1998). These studies highlighted the capacity of AA to alleviate ROS damage and to stimulate the components essential for DA, but failed to demonstrate the functional implications of neuroprotection as well as the impact on mitochondrial dynamics. A cohort study performed on elderly PD patients also documented increases in absorption of levodopa for those with poor bioavailability when co-administered dietary AA (Nagayama et al. 2004), however, no documentation of prior supplementation to protect or prevent was suggested or implied. In our study we showed the functional translation of AA pretreatment using an MPTP-induced PD model of larval zebrafish. Our results first complimented the foundational gene expression work of Seitz and colleagues through observed increases in *th1* expression relative to the MPTP-treated control and near levels of the NTC. The pretreatment of AA also protected against MPTP-induced mitochondrial fragmentation that is mediated through *fis1* activity (Yu et al. 2019; Kalyn and Ekker 2021). Surprisingly, the protective effects observed at the genetic level had no functional translation in locomotion. Future directions may investigate co-treatment with agents to maintain

molecular stability to prevent oxidization or to promote AA recycling through increasing the reduction rate of dehydroascorbic acid back into AA (Covarrubias-Pinto et al. 2015).

3.4.2. Ferulic acid

The therapeutic effects of FA on neurobiology had first been well investigated in the context of Alzheimer's disease (Cho et al. 2005; Huang et al. 2011; Kikugawa et al. 2016). However, in the past decade more attention has shifted to explore mechanisms of neuroprotection in neurotoxin-induced models of PD but fail to do so using zebrafish. Here we demonstrate the first protective effects of FA pretreatment on DAnergic and mitochondrial homeostatic gene expression, as well as, motor performance following MPTP exposures using zebrafish larvae. In 6-OHDA lesioned mice, FA preserved mitochondrial dynamics through suppressing *Drp* expression involved fission and maintaining *Mfn2* expression involved in fusion. The free radical scavenging and antioxidizing effects also resulted in comparable *Th* mRNA levels to the sham control (Anis et al. 2020). Despite no recorded effects on behavior following 6-OHDA lesioning, we found FA pretreatment to be similarly efficacious in mitigating the MPTP-induced downregulation of *th1* and *fis1* gene expression in zebrafish. Our results on locomotion were corroborated by mouse studies that found FA to ameliorate the behavioral consequence of MPTP detected through rotarod and swimming assays. Interestingly, these protective effects were abolished in *nuclear factor E2-related factor 2* (*Nrf2*)-null mice suggesting that the MAPK activation of the Nrf2 pathway involved in antioxidation is responsible for FA's counteracting MPTP-induced oxidative stress (Li et al. 2020). This pathway was previously explored in a complementary neuroprotective study using the bioflavonoid pinustrobin in zebrafish larvae where Li and colleagues report restored TH+ immunoreactivity and swimming activity following

prolonged Nrf2 and PI3K/ATK activation relative to MPTP-treated controls. Given the shared activation of Nrf2 following FA and pinustrobin pretreatments in an MPTP-induced PD model using zebrafish, we can postulate that Nrf2 signaling is the driving force behind the observed neuroprotective effects on locomotion, in addition to gene expression.

3.4.3. Vanillic acid

Mitochondrial dysfunction plays an important role in the pathogenesis of various neurodegenerative disorders that include PD. Recent studies have begun to explore different phytochemicals that can reduce oxidative stress damage and VA has become increasingly popular due to its free scavenging properties. In SH-SY5Y cells, VA augmented mitochondrial biogenesis while also increasing the expression of genes associated with the synthesis and differentiation of DAnergic neurons (TH, *nuclear receptor subfamily 4 group A member 2* (*NR4A2*), and *solute carrier family 6 member 3* (*SLC6A3*)). Conversely, VA was shown to negatively impact the transcript levels of genes associated with onset PD such as *LRRK2* (Ay 2022). These effects contrast those observed in our MPTP-induced model of neurodegeneration. We found that VA failed to improve mitochondrial fission states through increase *fis1* expression, while also exhibiting decreased DA production through reduced *th1* mRNA levels. Interestingly, we observed VA to produce the largest protective effect on distance swam which may be attributed to increased DA uptake in the presence of reduced *th1* expression. VA neuroprotection had previously been unexplored in the context of MPTP, however, a similar outcome was observed in a rotenone-induced model of neurotoxicity using rats. Sharma and colleagues (2021) showed that co-treatment of VA with rotenone showed improvements in locomotion and behavior at low-doses without altering DA levels in the brain relative to the positive control (Sharma et al. 2021). Higher

doses did, however, improve the therapeutic effect of VA. With MPTP and rotenone possessing similar mechanisms of oxidative stress and cytotoxicity, it may be promising to explore the local administration of higher doses intracerebrally or intraabdominally to enhance VA neuroprotection.

3.5. Conclusion

In summary, these data provide the first comprehensive comparison of the antioxidizing effects for AA, FA and VA in an MPTP-induced model of PD using larval zebrafish. We found varying degrees of neuroprotection at the level of gene expression and locomotion. AA and FA elicited the largest preventative effect on *th1* and *fis1* gene expression against MPTP-induced neurotoxicity, however, larvae pretreated with AA swam the least of the three phenolic groups. Surprisingly the inverse was observed for VA that maintained some degree of locomotion, but gene expression did not differ from the positive controls. Overall, it can be concluded that FA confers the largest protective effects on DAnergic, mitochondrial and motor networks that may serve as a base for PD-related therapies.

CHAPTER 4: CEREBROVENTRICULAR MICROINJECTIONS OF MPTP ON ADULT ZEBRAFISH INDUCES DOPAMINERGIC NEURONAL DEATH, MITOCHONDRIAL FRAGMENTATION AND SENSORIMOTOR IMPAIRMENTS

4.1. Abstract

Mitochondria are dynamic organelles that mediate the energetic supply to cells and mitigate oxidative stress through the intricate balance of fission and fusion. Mitochondrial dysfunction is a prominent feature within Parkinson Disease (PD) aetiologies. To date, there have been conflicting studies of neurotoxin impact on dopaminergic (DAnergic) cell death, mitochondrial function and behavioral impairment using adult zebrafish. Here, we performed cerebroventricular microinjections of MPTP on adult transgenic zebrafish that resulted in significant reductions in DAnergic neurons within the telencephalon and olfactory bulbs of Tg(*dat:eGFP*) fish. Visualization of mCherry and mitochondrial gene expression analysis in Tg(*dat:tom20 MLS:mCherry*) fish reveal that MPTP induces mitochondrial fragmentation in DAnergic neurons and the activation of the pink1/parkin pathway involved mitophagy. Moreover, the loss of DAnergic neurons translated into a transient locomotor and olfactory phenotype. Taken together, these data can contribute to a better understanding of the mitochondrial impact on DAnergic survivability.

4.2. Introduction

Idiopathic in nature, Parkinson disease (PD) is the 2nd most prevalent neurodegenerative disease in the world where symptoms comprise of motor, sensory and cognitive impairments (de Lau and Breteler 2006; Muangpaisan et al. 2011). The pathology of PD has been characterized as a progressive loss of dopaminergic (DAnergic) neurons within the substantia nigra of the human midbrain (Dauer and Przedborski 2003; de Lau and Breteler 2006; Muangpaisan et al. 2011). Motor and sensory symptoms develop following 40-60% loss of these neurons (Cheng et al. 2010).

PD is believed to be a cumulative result of genetic and environmental insult. Researchers have elucidated mutations in various genes (*PINK1* (Hatano et al. 2004), *Parkin* (Kitada et al. 1998; Dawson and Dawson 2010), *LRRK2* (Funayama et al. 2002; Zimprich et al. 2004) and *DJ-*1(Bonifati et al. 2003)) that increase an individual's susceptibility to developing PD. However, this can only explain 5-10% of cases, while the majority are sporadically induced through external factors such as; age, gender, neurotoxic exposure and mitochondrial dysfunction (Dexter and Jenner 2013).

Chemo-ablative models for PD commonly consist of the administration or exposure to 1-methyl-4-phenyl-1,2,3,6-tetrahydropyridine (MPTP)(Meredith and Rademacher 2011; Tieu 2011; Hare et al. 2013). Being lipophilic, MPTP readily permeates the blood-brain-barrier and is metabolized into its active toxic form MPP+ through monoamine oxidase-B (MAO-B) in proximal astrocytes (Przedborski et al. 2004b; Hare et al. 2013). MPP+ enters DAnergic neurons through the dopamine transporter (Dat) protein to exert its cytotoxicity through the inhibition of complex I activity in the electron transport chain (ETC) of mitochondria (Przedborski et al. 2004b). MPTP has been extensively used in PD studies in a variety of models ranging from mice, rats, primates and zebrafish (Van Kampen et al. 2000; Meredith and Rademacher 2011; Bové and Perier 2012).

Previous studies in zebrafish have been carried out using at embryonic or larval stages in development. These studies have demonstrated the effect of MPTP on locomotion, morphology, DAnergic survivability and have identified various neuroprotective compounds (Lam et al. 2005; Sallinen et al. 2009; Díaz-Casado et al. 2016; Kalyn et al. 2019; Zhao et al. 2020). However, studies pertaining to MPTP exposure in adult zebrafish address the behavioral phenotype but commonly disregard or report inconsistencies surrounding the impact on sensory perception, DAnergic neurons and their mitochondria (Anichtchik et al. 2004; Bretaud et al. 2004).

Many studies have adopted the use of mammalian models to study PD, however, the use of zebrafish has rapidly emerged and proven to be considerably beneficial. Zebrafish possess transparent *ex utero* embryogenesis allowing for in-depth developmental imaging, as well as, large clutch sizes following breeding to facilitate high-throughput drug screening (Stewart et al. 2014). This model also displays many conserved pathologies and molecular pathways due to their genome being ~87% homologous to humans (Du et al. 2016). Pertinent to PD, zebrafish possess a functional analogue to the DAnergic nigrostriatal system described in humans (Holzschuh et al. 2001a; Sallinen et al. 2009).

Given the accessibility of zebrafish embryos into adulthood, this model is widely used for pharmacological studies. Conventional drug delivery methods comprise of direct immersion, intraperitoneal (IP) injections and intramuscular (IM) injections, however, there are significant pitfalls to each. In this study, we optimized a drug delivery method through cerebroventricular microinjections (CVMI) to administer MPTP to adult zebrafish. MPTP is shown to selectively ablate DAnergic populations through mitophagy mediated cell death demonstrated through increased mitochondrial fragmentation, as observed in adult Tg(*dat:tom20 MLS:mCherry*) zebrafish. This effect was complimented with gene expression analyses of mitochondrial

regulatory genes. Moreover, this decrease in DAnergic neurons translates into transient sensorimotor perturbing phenotypes.

4.3. Materials and methods

4.3.1. Zebrafish care and husbandry

The transgenic zebrafish lines used for this study are Tg(*dat:eGFP*) and Tg(*dat:tom20 MLS:mCherry*) (Xi et al. 2011b; Noble et al. 2015). Embryos were collected by natural spawning to be raised in E3 embryo media (13 mM NaCl, 0.5 mM KCL, 0.02 mM Na2HPO4, 0.04 mM KH2PO4, 1.3 mM CaCl2, 1 mM MgSO4 and 4.2 mM NaHCO3). Zebrafish were sorted by fluorescent intensity detected at 4dpf and raised into adulthood for experimentation. All procedures were approved by the University of Ottawa Animal care committee and conducted under the Animal Care and Veterinary Service guidance in accordance with the Canadian council for Animal care following protocol number BL-2081.

4.3.2. MPTP preparation and cerebroventricular microinjections in adult zebrafish

MPTP (MPTP; $C_{12}H_{15}N \cdot HCl$, Product: M0896, CAS: 23007-85-4, Sigma, Oakville, ON, Canada) was reconstituted in distilled water to a stock concentration of 500 mM and diluted to the working concentrations of 10 mM, 25 mM, 35 mM and 100 mM.

Adult Tg(*dat:eGFP*) and Tg(*dat:tom20 MLS:mCherry*) zebrafish (~10-month-old) were anaesthetized with Tricaine. In accordance with the procedure outlined in Kizil et al., a small incision of 200um was then generated with a 30-gauge syringe (BD Ultra-fine II, BD Biosciences) in the cranium above the anterior portion of the optic tectum without damaging the brain. The

prepared MPTP was loaded into a thin glass capillary microinjecting needle (Sutter Instrument) to inject the contents through the incision into the cerebroventricular fluid surrounding the brain. Microinjections were performed using the IM-300 vacuum pump microinjector station (Narishige) at a pressure range of 55-65 psi. Phenol Red (Sigma) was co-administered to ensure proper distribution throughout the CVF.

4.3.3. Immunohistochemistry on zebrafish cryosections

Zebrafish heads were collected and fixed in a 4% paraformaldehyde (PFA) solution dissolved in 1X phosphate buffered saline (PBS) overnight at 4^{o}C. Brain-dissections were conducted in 1X PBS and washed thrice in PBS-T followed by equilibration in 30% sucrose/PBS overnight at 4^{o}C. The brains were flash frozen in Tissue-tek OCT (VWR) for coronal cryosectioning. Section thickness performed range from 16-20μm and were stored at -20^{o}C.

Sections were thawed for 30mins prior to respective antigen retrieval. Sections were placed in 0.05% sodium citrate in 1X PBS-T for 15 mins at 85^{o}C then cooled at RT for 15mins. Slides were then washed with 1X PBS twice prior to rehydration in 1X PBS-T for 10mins. Blocking was then performed, and the slides were incubated with primary antibodies diluted in 1% FBS in PBS-T overnight at 4^{o}C. Primary antibodies used were; polyclonal rabbit anti-GFP (A11122, Invitrogen) and polyclonal rabbit anti-DsRed (632496, Clontech). Slides were washed and incubated with the secondary antibodies for 2hrs at RT in a dark chamber. Secondary antibodies used were; goat anti-rabbit Alexa 488 conjugate (A11008, Invitrogen) and goat anti-rabbit Alexa 594 conjugate (A11012, Invitrogen). Slides were then washed in 1X PBS-T prior to mounting with DAPI-infused Vectashield mounting media (Lynx Biosciences). Images for eGFP+ quantification were captured with the Olympus FV1000 Confocal microscope using a 20X air immersion

objective and images for mCherry+ quantification were captured using a Zeiss LSM 880 Confocal microscope using a 63X oil immersion objective. Mitochondria were ranked according to their morphology. Fused refers to uniformly linked mitochondria surrounding the nucleus. Partial refers to mitochondrial fragmentations observed in less than 50% of the mitochondria within the field of view. Fragmented refers mitochondria that appear scattered (>50%), truncated and less dense surrounding the nucleus. Counts were performed using ImageJ software and were performed by two to three independent researchers in a blinded approach to remove personal bias.

4.3.4. Whole brain qRT-PCR

RNA was extracted from homogenized adult whole zebrafish brains using TRIzol in accordance to the manufacturer's protocol (InVitrogen). The purity and integrity of RNA was determined using the NanoDrop 1000 spectrophotometer (ThermoFisher) and through gel electrophoresis. Samples only with absorbance of 1.8-2.1 and clear 18S and 28S bands were used for cDNA synthesis. The reverse-transcription was performed using the iScript cDNA Synthesis Kit following the supplier's protocol. qRT-PCR reactions were done in triplicates composed of 5 µL SsoFast™ EvaGreen® Supermix (Bio-Rad), 0.4 µL forward primer, 0.4 µL reverse primer, 0.2 µL nuclease-free water and 4 µL cDNA. All readings were analyzed using the Bio-Rad CFX96 instrument. Relative quantification for *th1*, *dat*, *p53*, *pink1*, *parkin*, *mao-b*, *fis1*, *mfn1*, *opa1*, *parla*, *sox2* and *nestin* transcripts was obtained through the comparative Cq method using the following reference genes; *ribosomal protein l13a* (*rpl13a*), *elongation factor 1 alpha* (*ef1a*) and *tyrosine 3-monooxygenase/tryptophan 5-monooxygenase activation protein, zeta polypeptide* (*ywhaz*). Oligonucleotide primer sequences are listed in Table 1.

Table 4.1. List of primers designed for qRT-PCR.

Primer	Forward Sequence (5'-3')	Reverse Sequence (5'-3')	Reference
ywhaz	TCTGCAATGATGTGTTGGAGC	TCAATGGTTGCTTTCTTGTCGTC	(Tang et al. 2007)
rpl13a	TCTGGAGGACTGTAAGAGGTATGC	AGACGCACAATCTTGAGAGCAG	
ef1a	CTGGAGGCCAGCTCAAACAT	ATCAAGAAGAGTAGTACCGCTAGCATTAC	
dat	AGACATCTGGGAAGGTGGTG	ACCTGAGCATCATACAGGCG	(Barreto-Valer et al. 2012)
th1	GACGGAAGATGATCGGAGACA	CCGCCATGTTCCGATTTCT	(Chen et al. 2016)
p53	ATATCCTGGCGAACATTTGG	ACGTCCACCACCACCATTTGAAC	
sox2	GACAGCTACGCGCATATGAA	AGCCGTTCATGTAGGTCTGC	
nestin	ATGCTGGAGAAACATGCCATTGCAG	AGGGTGTTTACTTGGGCCTGAAGA	
fis1	CCCTGAACCTTCCAGTGTTT	GTCTCTGGAAACGGGTCCTT	
opa1	GCTTGAGCGCTTGGAAAAGGAA	TGGCAGGTGATCTTGAGTGTTGT	
mfn1	CTGGGTCCCGTCAACGCCAA	ACTGAACCACCGCTGGGGCT	
pink1	GGCAATGAAGATGATGTGGAAC	GGTCGGCAGGACATCAGGA	
mao-b	CGTACATTGGACCAACTCAAAA	CCTCCAGAGGTTGTTGTAGTCC	(Sarath Babu et al. 2016)
parkin	GCGAGTGTGTCTGAGCTGAA	CACACTGGAACACCAGCACT	

4.3.5. Locomotion analysis

Following treatment and recovery, adult zebrafish were monitored for swimming activity. Fish were placed individually in static tanks and allowed to acclimate in the ambient light for 15 min prior to the trials. Recordings were taken using the ZebraCube tracking system (ViewPoint

Life Science) and analyzed with Zebralab software. The swimming parameters examined in this study consist of total distance traveled, average swimming velocity and freezing bout duration over the course of 7 min trials. Sample sizes of 10 were selected to delineate the effects of individual swimming variability. Additionally, the same fish were analyzed from the last injection and the recovery period.

4.3.6. Olfactory analysis

Following treatment and recovery, adult zebrafish were placed in a customized static tank that is comprised of a midline division to result in a neutral zone, left and right arm (Hussain et al. 2013). Fish were allowed 15 min for tank acclimation in the ambient ZebraCube lighting. Following acclimation, cadaverine (Sigma Aldrich) was added to the arm the fish was in at that time-point referred to as the stimulus arm. Trials of 3 min were conducted to limit cadaverine diffusion into the non-stimulus arm or neutral zone. Data was captured using the ZebraCube tracking system and interpreted with the Zebralab software.

4.3.7. Statistical analysis

All statistical analysis was performed using the software GraphPad Prism v7.0. Swimming parameters were examined for n=10 adult zebrafish from each treatment group, while the olfactory evasion assay evaluated n=5. Both data sets were analyzed using multiple t-test comparison with significance determined using the Holm-Sidak method. Gene expression analysis was collected from whole brains from n=3 of each treatment group. Similarly, significance was quantified using multiple t-test and Holm-Sidak analysis. eGFP+ and mCherry+ cells, with n=6 and n=4 respectively, were analyzed using a 2-way ANOVA with multiple comparisons. eGFP+ multiple

comparisons were performed using the Sidak method, while mCherry+ multiple comparisons used the Holm-Sidak method. Statistical significance was determined using a 95% confidence interval where $p<0.05$. *($p<0.05$), **($p<0.01$), ***($p<0.001$) and ****($p<0.0001$).

4.4. Results

4.4.1. CVMI optimization and the LC_{50} dose for MPTP

CVMI, based on the protocol of Kizil and colleagues (Kizil and Brand 2011), was performed on 10-month old adult Tg(*dat:eGFP*) and Tg(*dat:tom20 MLS:mCherry*) zebrafish. A range of MPTP concentrations was administered to 8 fish in each group to determine the sublethal dose. The range comprised of 10mM, 25mM, 35mM and 100mM concentrations of MPTP. Injections were performed daily for 4 consecutive days. Mortality rates were quantified following each injection point. A concentration of 100mM was shown to be completely lethal following the last injection, whereas 35mM resulted in 50% survival. Both 10mM and 25mM did not result in any observed death, thus 25mM was determined to be the working dose for the experiments performed in this study.

4.4.2. Effect of MPTP on DAnergic neurons

One common discrepancy in PD literature is the correlation between tyrosine hydroxylase (TH) and DAnergic neurons. Although a widely accepted proxy, TH is involved in the biosynthesis of epinephrine in addition to dopamine. Here we performed injections on Tg(*dat:eGFP*) zebrafish to analyze eGFP signal, providing a more direct assessment of DAnergic degeneration as *dat* expression is localized specifically to DAnergic neurons.

MPTP was shown to impact DAnergic neurons in three prominent regions within the zebrafish brain; the olfactory bulbs (OB; Fig. 4.1B-C), telencephalon (Fig. 4.1E-F) and periventricular pretectal nucleus (PPv; Fig. 4.1G-H). The more immediate effects of MPTP were observed in the olfactory bulbs with 2% and 38% reductions in eGFP+ cells following the first and second injections, respectively. In the olfactory bulbs, this loss continued with each injection as MPTP-injected zebrafish resulted in losses of 32% and 47% following the third and fourth injections (Fig. 4.1I). Likewise, MPTP-injected fish displayed reductions up to 41% in the telencephalon following the same injection regimen (Fig. 4.1J). These effects were less severe within the PPv where a 25% loss of eGFP+ cells was observed following the final injection (Data not shown).

To consolidate these findings at the genetic level, global brain transcripts for *dat* and *th1* were quantified using qRT-PCR. We found that both *dat* and *th1* expression levels decreased by 40% and 20% respectively in MPTP-injected zebrafish (Fig. 4.1K). Interestingly, we found 71% and 35% increases in *sox2* and *nestin* gene expression following the fourth injection point suggesting immediate regenerative activation following DAnergic chemo-ablation (Fig. 4.1K). To investigate potential pathways involved, we analyzed *shha* (*sonic hedgehog a*) expression, as *shha* has been identified as a key regulator of DAnergic embryonic neurogenesis in zebrafish and other vertebrates (Hynes et al. 1995; Wullimann and Umeasalugo 2020). We found a 29% increase in *shha* expression in MPTP-injected zebrafish; however, this increase did not reach statistical significance (Fig. 4.1K). Our findings demonstrate the CVMI delivery of MPTP to induce considerable DAnergic cell death and that there is a rapid neurogenic signaling response following the last injection.

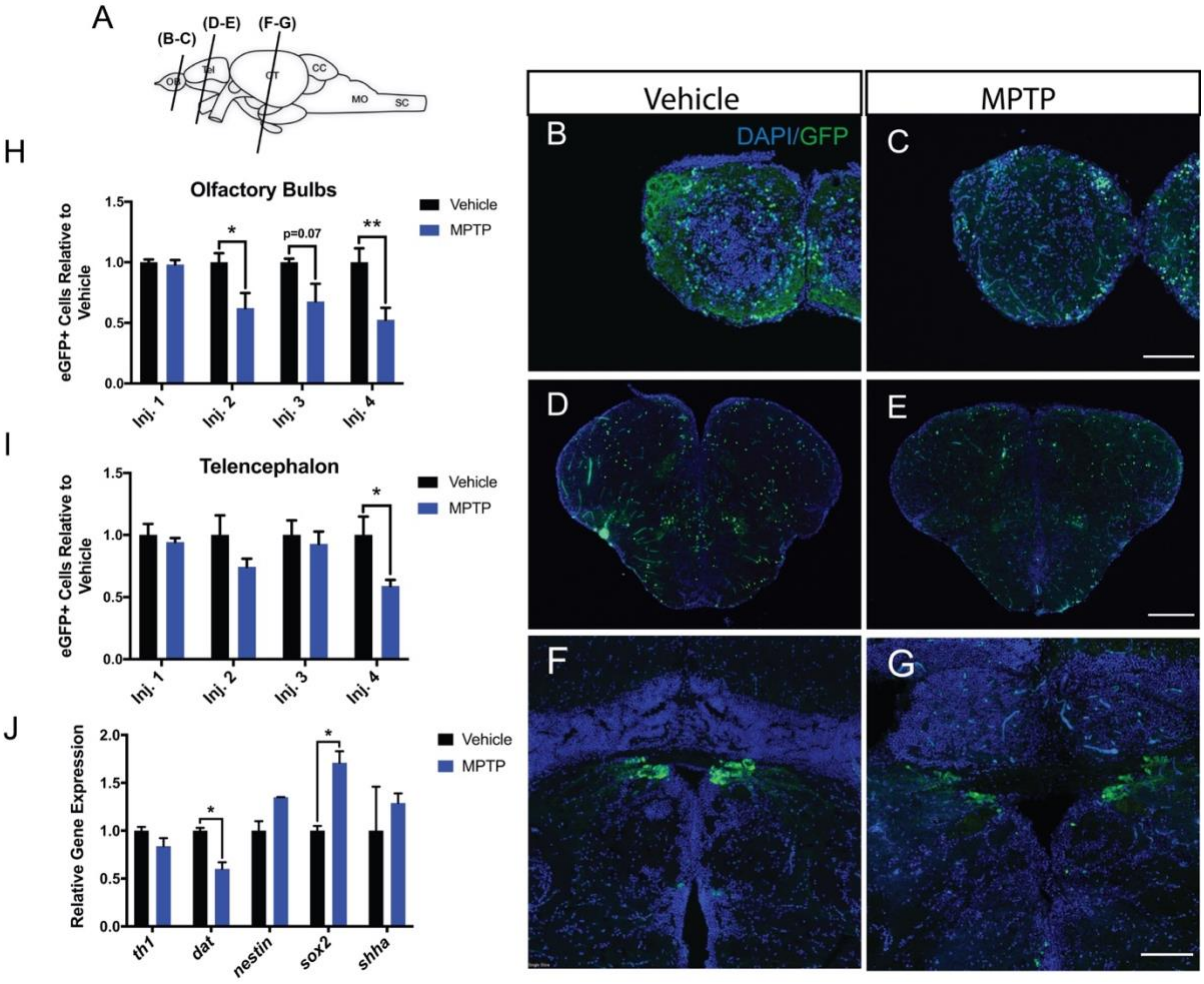

Figure 4.1. Impact of MPTP on various brain regions of adult Tg(*dat:eGFP*) zebrafish. A) MPTP dose-response. B) Schematic representation of the zebrafish brain with the planes of section indicated. Immunohistochemical labeling of eGFP (green) and DAPI (blue) to observe DAnergic neurons in the olfactory bulbs C-D), telencephalon E-F), and periventricular pretectal nucleus (PPv) G-H). I-J) Quantification of eGFP+ cells within the olfactory bulbs and telencephalon respectively. (*n* = 6). K) Whole brain qRT-PCR analysis for DAnergic, and regeneration-related genes; *th1*, *dat*, *sox2*, *nestin* and *shha.* (*n* = 3 whole brains from each respective group). Bars represent the Mean ± the SEM. *($p<0.05$), **($p<0.01$). (Scale bars =

100μm and 200μm for the OB/PPv and telencephalon respectively). OB, olfactory bulbs; Tel, telencephalon; OT, optic tectum.

4.4.3. Effect of MPTP on DAnergic mitochondria

To assess the effects of MPTP on DAnergic mitochondrial morphology, we performed injections in Tg(*dat:tom20 MLS:mCherry*) zebrafish that label the mitochondria of DAnergic neurons with mCherry (Noble et al. 2015). Following the last injection, cryosections were stained with dsRed, an antibody that recognizes mCherry, to visualize any potential disequilibrium between fission and fusion. The OBs were selected for assessment due to their involvement in both sensory and motor function. We observed a significant increase in fragmented mitochondria of the MPTP-injected zebrafish relative to the PBS control (Fig. 4.2B-C). Thus, 65% of all mitochondria analyzed in the MPTP-injected fish were fragmented, compared to only 8% in controls. Inversely, 4% of mitochondrial displayed a fused morphology in the MPTP-treated fish, compared to 39% in controls (Fig. 4.2D).

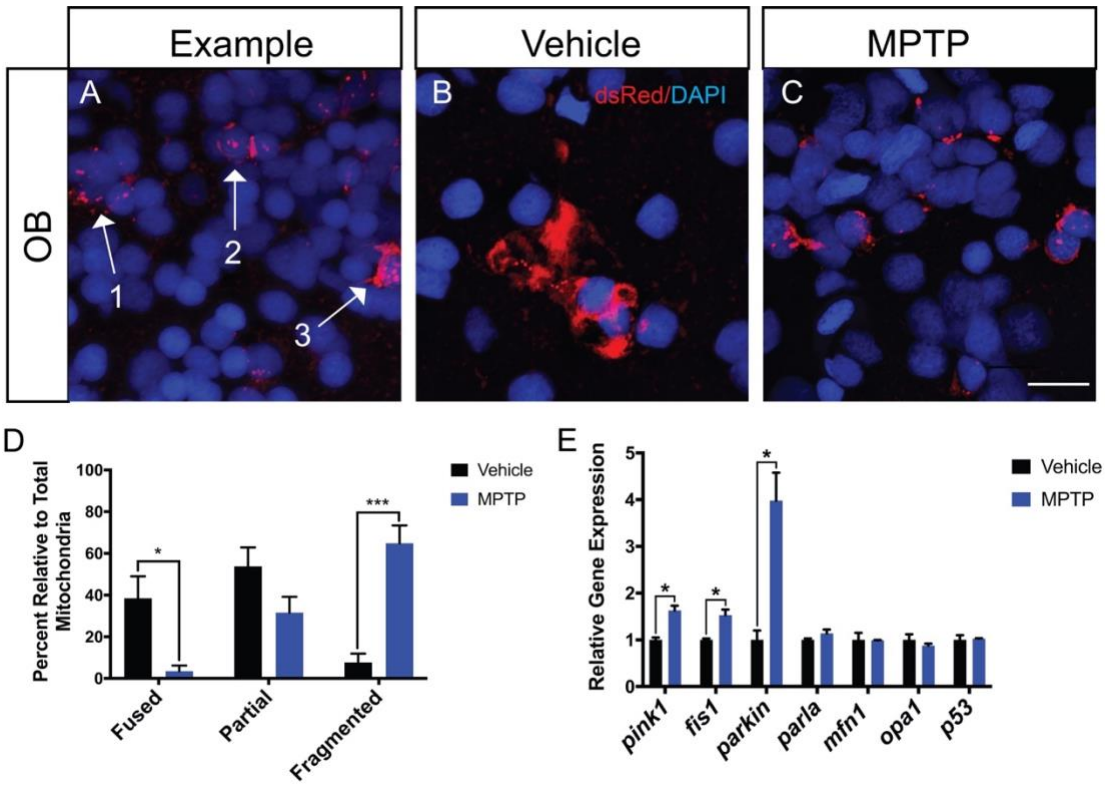

Figure 4.2. Effect of MPTP on mitochondrial fission-fusion dynamics in Tg(*dat:tom20 MLS:mCherry*) adult zebrafish. A) Representative image depicting fragmented mitochondria (Arrow 1), partially fragmented mitochondria (Arrow 2) and fused mitochondria (Arrow 3). B-C) Immunohistochemical labeling marked mCherry+ for mitochondrial visualization and nuclei with DAPI+ on coronal olfactory bulb cryosections from vehicle and MPTP injected zebrafish. D) Proportion of fused, partially fragmented and fragmented mitochondria. (*n*=4*)*. E) Whole brain qRT-PCR analysis for mitochondrial and apoptotic genes; *mao-b*, *pink1*, *fis1*, *parkin*, *parla*, *mfn1*, *opa1* and *p53*. (*n* = 3 whole brains from each respective group). Scale bar = 10μm. Bars represent the Mean ± the SEM. *(p<0.05), **(p<0.01), ***(p<0.001).

To further support these findings, we analyzed genes associated with mitochondrial maintenance, structure and function. Most notable are increases observed in genes involved in mitophagy, where *pink1* is increased by 63% and *parkin* mRNA levels reach approximately 4-times of those levels seen in controls. Consistent with the fragmented phenotype observed through IHC, *fis1* (*mitochondrial fission 1*) transcript levels were significantly increased by 53%, whereas *mfn1* (*mitofusion 1*) expression remained unaffected (Fig. 4.2E). Moreover, we analyzed *opa1* (*optic dominant atrophy 1*) as it is involved in regulating mitochondrial cytochrome-c release and found expression to remain unchanged. The apoptotic marker *p53* was also analyzed and revealed that there was no effect of MPTP on this mechanism of cell death. Together these data suggest MPTP induces cell death in DAnergic neurons via a mitophagy directed mechanism with mitochondrial fragmentation.

4.4.4. Effect of MPTP on zebrafish behavior

To determine if the observed neurotoxicity translates into a locomotor or sensory phenotypes, zebrafish activities were monitored following every injection point and after a two-week recovery period. The same individuals were analyzed throughout the experiment to delineate the effects of MPTP from individual variability within the population.

The locomotion parameters that were examined included the total distance traveled, average velocity and freezing bout (inactivity) duration. MPTP-injected zebrafish elicited 46.7% and 47% reductions in total distance and average velocity relative to the controls following the fourth injection (Fig. 4.3B-C). Inversely, freezing activity increased gradually with each injection and a 51% increase was observed following the fourth injection (Fig. 4.4A). Notably, all swimming patterns returned to normal following a 2-week recovery.

Due to the substantial loss of DAnergic neurons within the olfactory region, we sought to determine if this translates into any functional impairment of the olfactory response. To address this, we performed a repulsive stimulus test where cadaverine is administered to the arm of the apparatus the zebrafish is residing in. From quantifying the ratio of time spent in the stimulus arm, we found that cadaverine did not provoke a rapid repulsion response in MPTP-injected fish as observed in the controls. Control zebrafish spent 8% of the total time in the stimulus arm, whereas MPTP-injected zebrafish spent 19%, more than double the amount of the time in that arm (Fig. 4.4A). Similarly to swimming activities, these effects were shown to return to normal 2-weeks post injection. Together these data suggest that DAnergic ablation via CVMI impairs the olfactory response and perturbs motor function.

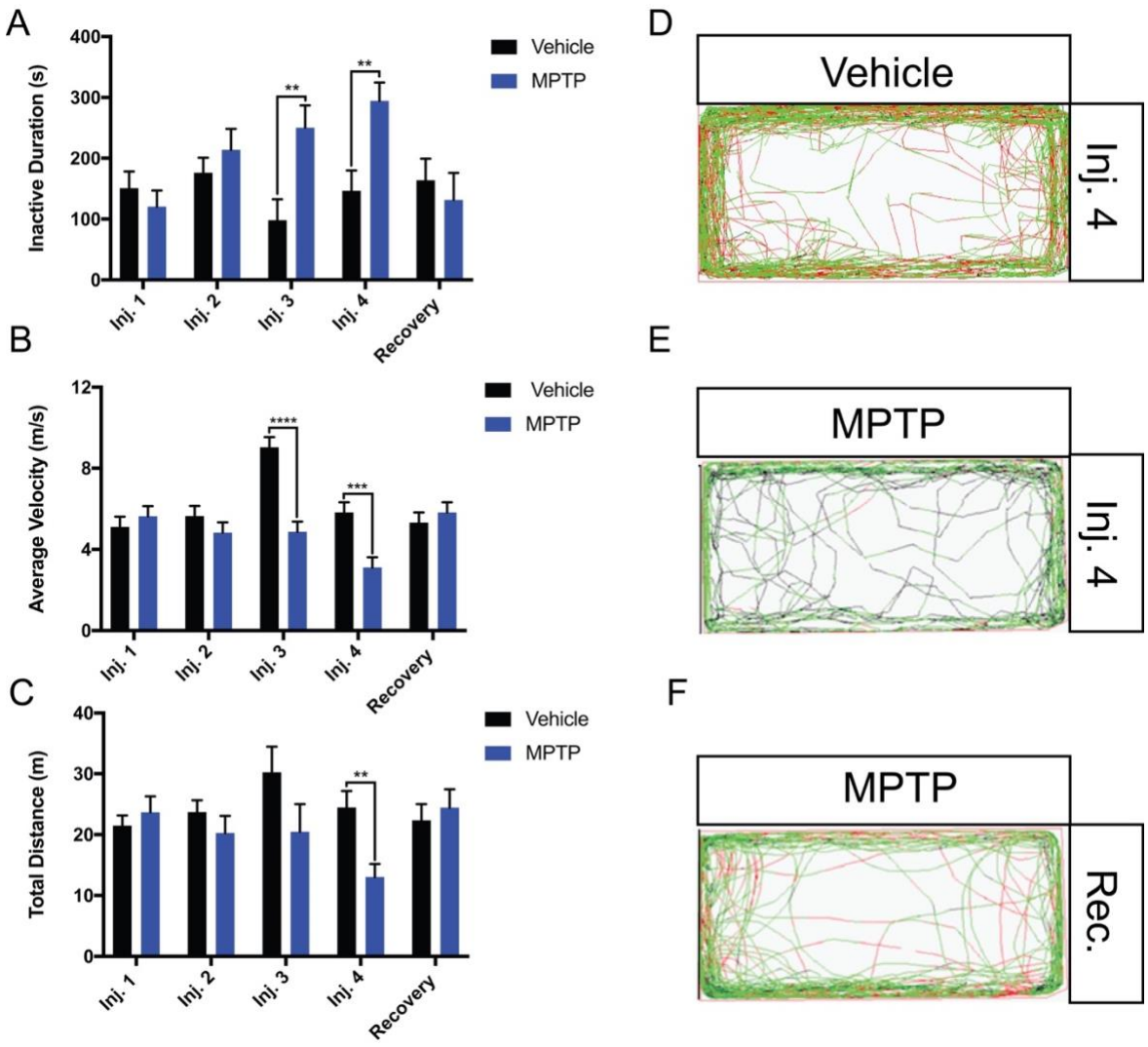

Figure 4.3. Impact of MPTP on adult zebrafish swimming behavior. Fish were acclimated to the apparatus for 15 minutes prior to behavioral analyses. 7-minute trials were performed. A-C) Analysis of inactive durations (proxy for freezing bouts), average velocity and total distance for MPTP injected zebrafish and vehicle controls. Respective path images are as follows; injection 4 vehicle control D), injection 4 MPTP E) and 2-week recovered MPTP treated zebrafish F). Red lines represent fast movement, green lines represent slow movement and black lines represent inactive movement below the slow threshold. (n = 10 for all groups). Bars represent the Mean ± the SEM. **($p<0.01$), ***($p<0.001$) and ****($p<0.0001$).

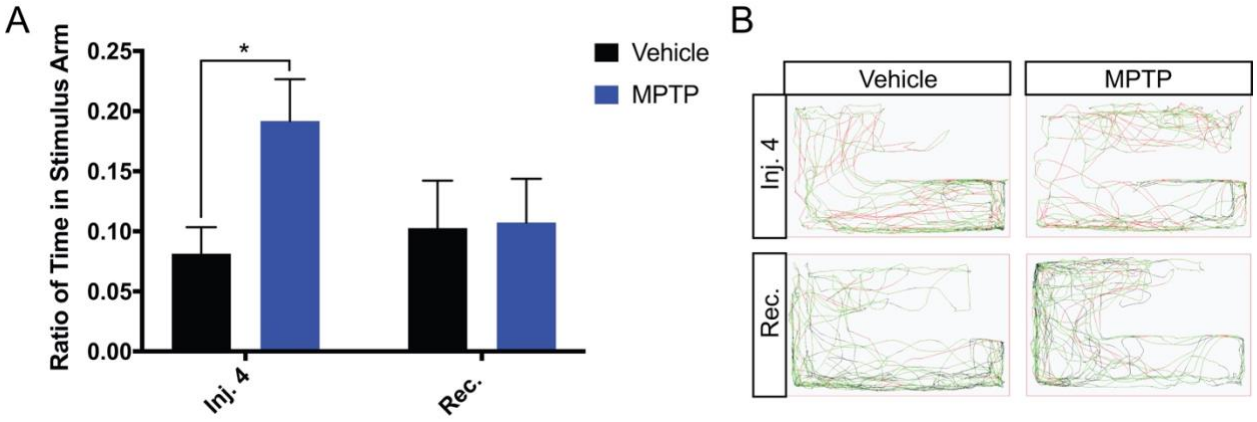

Figure 4.4. Impact of MPTP on olfactory response in adult zebrafish. A) Ratio of time spent in the stimulus arm following the fourth injection and two-week recovery. B) Respective path images for MPTP injected zebrafish and vehicle controls after the fourth injection and a two-week recovery. Red lines represent fast movement, green lines represent slow movement and black lines represent inactive movement below the slow threshold. (*n*=10). Bars represent the Mean ± the SEM. *($p<0.05$).

4.5. Discussion

4.5.1. The efficiency of CVMI for DAnergic cell death

Techniques to administer drugs will vary depending on the nature of the drug, the site of action and properties of the experimental animal. Popular administration methods include direct immersion, intraabdominal/intraperitoneal (IP) and intramuscular (IM) injections. However, each method comes with evident pitfalls. The largest downfall to IP injections is the primary route of absorption being through mesenteric vessels. Dosages are generally increased in this case to overcome the potential of the drug undergoing hepatic metabolism prior to systemic circulation

(Abu-Hijleh et al. 1995; Turner et al. 2011). IM injections are commonly performed in mammalian models and are more difficult on zebrafish due to the reduced muscle mass and individual variability that poses the risk of differing drug absorption rates based on blood flow velocity (Manor and Sadeh 1989; Dowd 2017; Abbate et al. 2018). One must also be selective with the compound to be administered due to the potential for irritation and/or damage to the periphery nervous system that may result in paresis, paralysis or muscle necrosis (Rasmussen 1978). Similarly, the direct immersion method of drug delivery makes it difficult to assess the exact quantity of drug being absorbed and can cause variability between treatments groups due to differing sizes, swimming patterns and opercular movement speed (Cassar et al. 2020). The implementation of CVMI used in this study to administer MPTP did not result in any observable morphological abnormality nor systemic toxicity as observed using alternative methods (Bretaud et al. 2004; Kalyn et al. 2019).

MPTP is commonly known as the "gold standard" in Parkinsonian studies due to the selective targeting of DAnergic neurons. Alternative compounds may also act on other essential neuronal subtypes when injected in the absence of uptake inhibitors, such as 6-OHDA acting on both DAnergic and epinephrinergic neurons (Fulceri et al. 2006; Bové and Perier 2012). In zebrafish, the vast majority of MPTP studies were performed on embryos and/or larvae. However, these studies have laid the groundwork and outlined that MPTP affects ascending TH+ diencephalic (5, 6, 11) and pretectal clusters (7) more severely than others, while also decreasing *dat* and *th1* transcript and neurotransmitter levels (Sallinen et al. 2009; Kalyn et al. 2019). Moreover, MPTP and MPP+ have been shown to translate into motor perturbing phenotypes in 3dpf, 5dpf, 6dpf and 7dpf zebrafish (Lam et al. 2005; Sallinen et al. 2009; Díaz-Casado et al. 2016; Kalyn et al. 2019; Zhao et al. 2020). Larval studies have also identified a variety of compounds

that can be used in a pre-treatment exposure to mitigate some degree of MPTP induced DAnergic neurodegeneration. A few of these compounds include deprenyl, melatonin and rosmarinic acid which act to alleviate stress through MAO-B inhibition, anti-oxidation and/or anti-inflammation (Parng et al. 2006; Sallinen et al. 2009; Díaz-Casado et al. 2016; Zhao et al. 2020). In adults, reports primarily consist of behavioral assessment without much examination of DAnergic neurons and their mitochondria (Flinn et al. 2008; Selvaraj et al. 2019). However of the few that have investigated DAnergic health, Anichtchik and colleagues have shown that a systemic injection of MPTP resulted in decreases in dopamine and noradenaline concentrations in the brain without any effect on TH immunoreactivity, TH co-localization with TUNEL or any increase in caspase-3 activity (Anichtchik et al. 2004). Moreover, Bretaud et al. did not observe any DAnergic neuron ablation following IP injections of MPTP, rotenone or paraquat (other toxins implicated in PD studies)(Bretaud et al. 2004). Here we report that CVMI was a successful method to deliver MPTP into the adult zebrafish brain through the observed increases in DAnergic cell death within the telencephalic and olfactory regions of the adult brain, as well as, the spatial disorganization and slight reduction of DAnergic neurons in the PPv.

To assess the impact on DAnergic neurons and further support our findings, *th1*, *mao-b* and *dat* gene expression profiles were evaluated. Expression of *th1* was analyzed in contrast to *th2* as *th2* is exclusively expressed in non-mammalian vertebrates and present in only 4 hypothalamic neuronal clusters within the hypothalamic and posterior tubercular regions of the brain (Barrios et al. 2020). The increased MAO-B mRNA expression observed suggests the continuous conversion of MPTP into its active toxic form MPP+ even following the fourth injection point. MPP+ then exerts its effects on cells expressing *th1* and *dat*, as shown through decreases in respective gene mRNA levels. The >50% *dat* expression remaining can be explained by the remaining DAnergic

neurons expressing *dat* as a means to recycle synaptic dopamine into the cytosol of DAnergic neurons (Shimizu and Prasad 1991; Giros et al. 1992; Merhi et al. 2021). Although we cannot rule out the possibility of a transient downregulation in *dat*/*th1* expression that may contribute to the functional impairment and recovery of zebrafish behavior, the effect of MPTP on *tom20* expressing DAnergic neurons combined with the eGFP data are suggestive of neurodegeneration occurring.

Interestingly, increases in expression for neural proliferative genes and *shha* were observed immediately following the last injection of MPTP. Shh is a main signaling morphogen in the ventralization of vertebrate neural tubes (Hynes et al. 1995; Wang et al. 2009; Carballo et al. 2018). Particularly in zebrafish, *shha* expressing cells have been shown to give rise to preglomerular complex and posterior tubercular DAnergic neurons (Wullimann and Umeasalugo 2020). Given the activity of Shh in embryonic DAnergic neurogenesis and the increase in mRNA transcript levels observed in the present study, further analysis of Shh is warranted to determine its precise role in adult DAnergic neurogenesis following ablation.

4.5.2. Mitochondrial response to MPTP in DAnergic neurons

Mitochondrial dysfunction is a hallmark of neurodegeneration in PD patients. There are various processes (fission, biogenesis and mitophagy) that regulate mitochondrial quality within all cell types (Kobayashi et al. 2020). Fission is a mechanism that activates mitophagy and plays an adaptive role in the clearance of damaged mitochondria in response to oxidative stress or injury. Mitophagy is the process by which fragmented mitochondria are sequestered and degraded by lysosomes (Ding and Yin 2012). Regarding biogenesis, it is well characterized that mitochondria provide energy to the cell through two dominant pathways: glycolysis and oxidative

phosphorylation (Westermann 2012). The variations in energetic supply or metabolic cues can also influence mitochondrial morphology (Yu and Pekkurnaz 2018). Glycolytic mitochondria generally display a fragmented appearance with fission contributing to mitochondrial proliferation, while mitochondria undergoing oxidative phosphorylation display a more fused conformation (Rossignol et al. 2004; Westermann 2012; Youle and van der Bliek 2012; Seo et al. 2018). Dependent on the energetic requirements, highly active cells commonly rely on oxidative phosphorylation (Westermann 2012). DAnergic neurons fall into this category.

Many studies have outlined the mechanism of MPTP mediated cell death via the inhibition of the ETC (Przedborski et al. 2000, 2004a; Keane et al. 2011). However, a knowledge gap remains in visualizing these effects on mitochondrial conformational changes in the DAnergic neurons of adult zebrafish brain. Through performing injections on Tg(*dat:tom20 MLS:mCherry*) zebrafish, we were able to observe the direct consequences of MPTP on mitochondrial morphology. Twenty-four hours following the fourth injection, MPTP-injected zebrafish exhibited significant fragmentation in DAnergic neurons. Consistent with the results indicative of mitochondrial fission, there are significant increases in genes associated with this phenomenon: *fis1* (*mitochondrial fission protein 1*), *parkin* and *pink1 PTEN-induced kinase 1*). The Parkin/Pink1 pathway is active in all mitochondria of healthy cells to expel dysfunctional or damaged mitochondria through mitophagy. Thus, damaged mitochondria in highly energetic cells will display a fragmented morphology. Addressing this phenomenon, Park and colleagues found increased numbers of abnormal mitochondria within DAnergic neurons substantia nigra in macaques following MPTP exposure (Park et al. 2019). However, this study outlined the mechanism of fission through Drp1 and fis1 activation and not necessarily the subsequent cell death. Taken together with the decrease in eGFP+ expressing cells in our results, it is possible that the remaining DAnergic neurons are

degenerating via a mitophagy dominant mechanism inducing mitochondrial fission and neuronal death.

In addition to fragmentation as a response of oxidative stress and given that cellular bioenergetic demand can influence mitochondrial morphology, we cannot disregard that some DAnergic neurons may be undergoing metabolic reprogramming from oxidative phosphorylation to aerobic glycolysis following MPTP injections. Emerging studies have shown that similar modifications in mitochondrial networking and structure occur as a mechanism to bioenergetically adapt to stress and/or inflammation (Baker et al. 2014). Nair et al. tested this hypothesis by inducing fission and energetic reversion to glycolysis through lipopolysaccharide (LPS) exposure in microglia. They subsequently found that a Drp1 protein inhibitor, Mdivi-1, attenuates ROS production, fragmentation and pro-inflammatory responses following LPS treatment *in vivo* and *in vitro* (Nair et al. 2019). Further analysis of genes and/or proteins involved in the present study must be done to support this possibility of DAnergic mitochondrial metabolic reprogramming. One mechanism of interest was suggested by Zheng and colleagues who observed a loss of expression from lactate dehydrogenase and hexokinase, in parallel to the conversion in pyruvate kinase splicing from PKM2 to PKM1, that efficiently labels the transition from aerobic glycolysis in progenitor cells to oxidative phosphorylation in maturing neurons (Zheng et al. 2016).

4.5.3. Behavioral consequence following MPTP injections

The DAnergic system is critical to several biological functions that include reward, pleasure, movement and learning. Incidentally, the consequence of ablating dopamine producing cells can result in severe behavioral phenotypes. Microinjections of MPTP are shown to affect the DAnergic projectome that modulates movement through observed impaired swimming

parameters. MPTP-injected fish exhibited increased freezing bout duration, concurrent with decreases in both total distance and average velocity relative to the respective controls, resembling bradykinetic and dyskinetic symptoms (Vaz et al. 2018). MPTP-injected zebrafish displayed impaired olfactory response to the repulsive stimulus cadaverine. With the telencephalic and olfactory regions being two epicenters, in the zebrafish brain, that modulate behavior, this impact can be explained by the drastic decreases in eGFP+ cells residing within the olfactory bulbs and telencephalon in MPTP-injected zebrafish. These effects are greater than those observed in our group's previous work from Godoy et al., that used a chemogenetic approach to ablate DAnergic neurons (Godoy et al. 2020). The phenotypes observed in this study were transient as all motor and sensory functions were restored following a 2-week recovery period. This capacity for regeneration alone makes the zebrafish advantageous in neurodegenerative studies, however, this also poses a hindrance towards long-term therapeutic studies as it may be difficult to delineate any restorative effects between the therapeutic compound administered and the natural regeneration that occurs. Therapeutic studies using this model commonly treat the zebrafish prior to neuronal insult to evaluate the efficiency of varying neuroprotective compounds. Given the 2-week transiency of sensorimotor phenotypes, it would be beneficial to implement a short-term regenerative study following ablation to identify possible neurogenic drivers of DAnergic neurons in adult zebrafish to gain a better temporal understanding of behavioral restoration. As previously mentioned, identifying drivers, such as Shh, may serve as a foundation for gene-therapy application in higher vertebrate models.

4.6. Conclusions

Literature surrounding PD suffers from discrepancies among the degree of DAnergic ablation and behavioral phenotypes resulting from neurotoxin treatments. Here, we demonstrated that CVMI delivery of MPTP induces substantial DAnergic neuron death within the telencephalon and olfactory regions of the adult zebrafish brain. This reduction in DAnergic neurons resulted in transient sensory and motor phenotypes. Moreover, using the Tg(*dat:tom20 MLS:mCherry*) zebrafish, we were able to observe a significant increase in the proportion of fragmented mitochondria in MPTP-injected zebrafish. Supporting gene expression evidence suggests that the DAnergic cell death is activated via a mitophagy mechanism that results in increased fission and a more fragmented mitochondrial morphology. Taken together this study will ameliorate our understanding of chemically induced mitochondrial dysfunction in the neurodegeneration of DAnergic neurons and other PD pathologies.

CHAPTER 5: DIFFERENTIAL ROLES OF *NR4A2* (*NURR1*) PARALOGS IN THE BRAIN AND BEHAVIOR OF ZEBRAFISH

5.1. Abstract

Dopaminergic (DAnergic) dysfunction and imbalanced dopamine (DA) levels are known contributors to the pathogenesis of numerous psychiatric and neurodegenerative disorders. To better understand disease etiology, researchers have begun to investigate genetic predisposition that increases an individual's risk to developing DA-associated disorders. Many risk factors have since been identified, however one transcription factor involved in DAnergic differentiation, named *nuclear receptor subfamily 4 group A2* (*NR4A2*; or *nuclear receptor related-1* protein (*NURR1*)), has shown to influence a multitude of phenotypes reminiscent of attention deficit hyperactive disorder (ADHD) and Parkinson's disease. Studies surrounding *nr4a2* in zebrafish have been looked at with a narrow scope of tyrosine hydroxylase characterization and basic motility without much regard to the impact *nr4a2* has on other neurological systems, metabolism and more complex behaviors. Here, we knocked out *nr4a2* paralogs, *nr4a2a* and *nra2b*, in zebrafish to provide a more encompassing understanding of the roles for each paralog in the brain, oxidative respiration, regeneration and startle response in addition to confirming the predominant function in DAnergic homeostasis. We found complementary and contrasting results to what was observed in literature. *nr4a2a* mutants more closely recapitulated Parkinsonian phenotypes and was deleterious to neurotrophic health. Conversely, *nr4a2b* mutants displayed behavioral symptoms reminiscent of mice deficient in *Nr4a2* with an increase in neurotrophic output. *Nr4a2a* mutants also showed an increase in maximal respiration which may suggest a compensatory mechanism at play to meet the metabolic requirements of DAnergic health while possessing an impaired DAnergic system. Conversely, *nr4a2b* mutants displayed an increase in metabolic input

from non-mitochondrial sources indicative of high cytosolic reactive oxygen species and perturbed mitochondrial function. Lastly, we found *nr4a2a* to drive the differentiation of regenerated DAnergic neurons through shared expression patterns with *sonic hedgehog a* (*shha*) in an MPTP-model of PD. Interestingly, we found increases in *notch1*, *th1* and *nestin* prior to the largest increase of *shha* transcription which may suggest notch1a is the predominant driver of proliferating DAnergic neurons that shifts to shha signaling for cell specific differentiation from 3- to 5 days post-treatment (dpt). Overall, the knockout models generated in this study can be implemented for further use in uncovering mechanisms of DA-related disease pathologies, therapeutic investigation and in the regeneration of DAnergic neurons.

5.2. Introduction

Dopamine (DA) is a multifaceted catecholamine that modulates a wide range of central (CNS) and peripheral nervous system (PNS) function and behavior (Elsworth and Roth 1997; Ayano 2016). Consequently, impairments to DA neurotransmission can lead to a plethora of psychiatric and neurological diseases that include but are not restricted to attention deficit hyperactive disorder (ADHD), schizophrenia and Parkinson's disease (PD) that currently affect 5.3%, 0.75% and 1.4% of the global population respectively (Orrico-Sánchez et al. 2020; Simon et al. 2020; Espinet et al. 2022). In recent years, considerable research has been done to elucidate the molecular drivers behind DA homeostasis and have since revealed a complex interplay between morphogens (*SHH* and *WNT1A*), neurotrophins (*GDNF* and *BDNF*) and transcription factors (*LMX1A* and *PITX3*) (Roussa and Krieglstein 2004; Chinta and Andersen 2005; Filippi et al. 2007; Wong et al. 2021). One transcription factor that has been be shown to possess vast

influence over the nervous systems is *nuclear receptor subfamily 4 group A2* (*NR4A2*; alternatively named *nuclear receptor related-1* protein (*NURR1*)).

NR4A2 encodes a steroid orphan nuclear receptor belonging to a ligand activated superfamily of proteins and is primarily expressed within the substantia nigra, ventral tegmentum, nucleus accumbens, olfactory bulbs, hippocampus, cerebellum, habenula and hypothalamus of the CNS (Saucedo-Cardenas and Conneely 1996; Bäckman et al. 1999). Periphery expression of *NR4A2* is localized to endothelial cells, cardiomyocytes, intestine, bone, synovial tissues, adrenal glands and macrophages (Holla et al. 2011; Han and Cao 2012; Lallier et al. 2016; Ashraf et al. 2022). *NR4A2* has been shown to regulate a number of cellular processes such as cancer (Holla et al. 2011), cardiovascular health (Ashraf et al. 2022), gastrointestinal inflammation (Han and Cao 2012) and metabolism (Pearen and Muscat 2010). However, its predominant role remains as a putative transcription factor vital to the development and maintenance of DAnergic neurons (Luo et al. 2008). *NR4A2* carries out this function by interacting with and regulating the expression of various components essential for DA synthesis, storage and release that include tyrosine hydroxylase (TH), dopamine transporter (DAT) and aromatic amino acid decarboxylase (AADC) (Jankovic et al. 2005). Several polymorphic variants of NR4A2 have since been identified that contribute to DAnergic dysfunction and in the pathogenesis of human disease (Le et al. 2003). To model these disease states, loss-of-function studies targeting *Nr4a2* in mice were performed but homozygous mutants did not survive past postnatal day (P) 1 with a complete abolishment of midbrain DAnergic neurons (Zetterström et al. 1997). Subsequent experimentation and studies have been carried out using heterozygotes and yielded variable results that depend on the developmental stage of analysis. At 5-8-months post-fertilization (mpf), *Nr4a2*-null mice displayed hyperactive phenotypes reminiscent of schizophrenia and ADHD-like symptoms (Rojas

et al. 2007; Montarolo et al. 2019). However, the degeneration of midbrain DAnergic neurons appears to progress with age as striatal DA and motor output was observed to decrease in mice >15mpf (Zetterström et al. 1997). Despite these differences, DAnergic neurons of *Nr4a2*-deficient mice displayed an increased sensitivity to neurotoxins regardless of age suggesting that Nr4a2 can also act as a neuroprotectant in addition to its role in development. This effect was complemented in a study that observed reduced levels of NR4A2 in neurons dense in Lewy body aggregates collected from the brains of autopsied PD patients (Jankovic et al. 2005). Together, these findings implicate *NR4A2* as an attractive target for novel gene therapies, but also as a candidate for further investigation into the developmental discrepancies in behavior and cellular output.

Many researchers commonly adopt the use of rodent models to recapitulate various aspects of human disease. However, in recent years the zebrafish has emerged due to a number of experimental advantages. Zebrafish lay broodstocks of up to 200 optically clear embryos that are amendable to gene-editing, pharmacological screening and live-imaging at various developmental time points (Stewart et al. 2014). Catecholaminergic circuitry has been well characterized in zebrafish where functional analogs to various mammalian pathways have been described (Holzschuh et al. 2001b; Sallinen et al. 2009; Panula et al. 2010). One is the nigrostriatal pathway affected in PD and consists of projecting DAnergic efferents from the substantia nigra through the putamen and thalamus with branching arbors terminating in the striatum (Reeves et al. 2002; Prensa et al. 2009). The zebrafish counterpart originates with ascending DAnergic efferents from the posterior tuberculum (PT) to the ventral and dorsal pallium of the telencephalon in concert with subpallial born DAnergic neurons that locally project through to the dorsal pallium (Rink and Wullimann 2002b,a; Tay et al. 2011). The conserved nature between mammals and this teleost species is likely attributed to a genome that is 71% homologous to humans and includes 87% of

disease-related genes (Du et al. 2016). However, loss-of-function studies are more challenging in zebrafish due to an ancestral genome duplication event (Taylor et al. 2001). Because of this, zebrafish possess two *NR4A2* orthologs, *nr4a2a* and *nr4a2b*. In the literature there have been contradictory findings surrounding various aspects of expression, function and protection between *nr4a2a* and *nr4a2b*. One example of this comes from a study that first detailed no involvement of either paralog in PT DAnergic development (Filippi et al. 2007; Luo et al. 2008). However, this was later shown to be untrue through the co-localization of both *nr4a2a* and *nr4a2b* with TH in the PT and within preoptic and pretectal areas that were previously overlooked (Blin et al. 2008). These inconsistencies persist and, following morpholino-mediated knockdowns, varying (or undetected) degrees of TH+ neuronal loss were recorded (Filippi et al. 2007; Blin et al. 2008; Luo et al. 2008). Since, there has been limited studies that have come forth to better our understanding of *nr4a2a* and *nr4a2b* using a zebrafish model.

To resolve the discrepancies and broaden the scope of *nr4a2* beyond TH, we decided to knockout (KO) *nr4a2a* and *nr4a2b* using CRISPR-Cas9 genome editing. This was accomplished in Tg(*dat:eGFP*) zebrafish to validate the impact of the targeted mutations on DA circuitry and to examine the effects on cellular metabolism, escape behaviors, regeneration, neurotrophic factors and alternative neurotransmission. Following mutagenesis,both *nr4a2a* and *nr4a2b* homozygous mutants grew up viable and healthy. We found a significant effect on DAnergic precursors and transporters in *nr4a2a* and *nr4a2b* mutants, as predicted. To our surprise, we observed contrasting roles between paralogs that persisted throughout life. *nr4a2b* mutant zebrafish displayed a hyperactive behavior, increased neurotrophic input and global decreases in DA reminiscent of ADHD or schizophrenic phenotypes. Conversely, *nr4a2a* mutant zebrafish displayed reductions in motor performance, increased neurotrophic factor expression and decreased DAnergic health.

Furthermore, we found that the gene expression of *nr4a2a*, not *nr4a2b*, closely mirrored the patterns of *shha* during DAnergic regeneration following MPTP-induced neurotoxicity. Both *nr4a2a* and *nr4a2b* mutants displayed perturbed startle response and the loss of *nr4a2a* translated into minor metabolic consequences. Together, the zebrafish lines generated in this study reveal differential impacts on multiple facets of neurological health and behavior that can be used for further investigation into DA deficiencies.

5.3. Materials and methods

5.3.1. Zebrafish care and husbandry

Transgenic zebrafish (*Danio rerio*), Tg(*dat:eGFP*), were used and maintained in compliance with the University of Ottawa Animal Care Committee following guidelines of the Canadian Council on Animal Care (protocol number BL-2081). Embryos were collected by natural spawning and staged in days post-fertilization (dpf) and months post-fertilization (mpf). Larvae were selected for and sorted by fluorescent intensity detected at 4dpf. Populations were housed with water quality being continuously monitored to maintain the temperature (28°C), pH (7.4) and conductivity (μS) while also exposing zebrafish to 14-hour light/10-hour dark light cycling.

5.3.2. Single guide RNA (sgRNA) design and synthesis

sgRNAs were designed in accordance to Montague and colleagues (2014) using CHOPCHOP software from the coding regions of *nr4a2a* and *nr4a2b* in the current zebrafish genome annotation GRCZ11 on Ensembl (Montague et al. 2014). To avoid off-target mutagenic effects, target sequences of no more than three predicted mismatches effects were selected. A total

of four sgRNA target sequences were identified with two sgRNAs located at both upstream and downstream genomic regions. sgRNA synthesis followed the protocol outlined by Gagnon and colleagues (2014). Constant oligonucleotides containing the T7 promoter, PAM sequence and the chimeric sgRNA scaffold for Cas9 hybridization were annealed to a 20-base pair (bp; N_{20}) gene specific target site in the following orientation; ATTTAGGTGACACTATA-N_{20}-GTTTTAGAGCTAGAAATAGCAAG and amplified using PCR. Oligonucleotides and target sequences are listed in Table 1. PCR products were cleaned using the PCR purification kit (Qiagen), transcribed in vitro using T7 RNA polymerase activity (HiScribe^{TM} T7 Quick High yield RNA synthesis kit, E2050S; New England Biolab) and stored at -80°C for future use.

5.3.3. sgRNA-Cas9 complex assembly, preparation and microinjections

sgRNAs were thawed and concentrations were measured using the NanoDrop 1000 spectrophotometer (ThermoFisher). A microinjection cocktail was prepared using 40ng/µL of each sgRNA, 20ng/µL Cas9 (New England BioLabs, Ipswich, MA, USA) and 0.1% phenol red (Sigma) to track dispersion. The mix was incubated at room temperature (23°C) for 10min prior to microinjections and then microinjected into the cytoplasm of 1-cell stage Tg(*dat:eGFP*) embryos.

5.3.4. Genetic screening of *nr4a2a* and *nr4a2b* mutant lines

To genotype each mutant, three primers were designed with one forward primer sequence located upstream of the 3' cut site, another forward primer nested in the coding region (WT) and one reverse primer located downstream of the 5' cut site to detect all three genotypes in one PCR (Fig. 5.1). The primers used for *nr4a2a* genotyping are F1W: CGTCCCTCAACCACAGTAAAA, F2M: GAGACAGCAAAAGAAGCAGAG and R1: CCTGGCTAAATACAGAGCTCA. The

primers used for *nr4a2b* genotyping are: F1M: GTGGTCACTGACAATTCTCCA, F2W: GGATTCATGAGCCTCAGATCA and R1: GAAATGCGTTGTCTATGGTGC. All primer sequences are listed in 5' to 3' orientation.

To perform the PCR, fin clips were collected to extract genomic DNA by incubating the clipping in 100μL of 50mM NaOH at 98°C that was then neutralized by adding 10μL of 1M Tris-HCl. If collecting genomic DNA from embryos then 20μL of 50mM NaOH was used with 2μL of 1M Tris-HCl. Additional reagents necessary to amplify the target region was included in a GoTaq PCR master mix that contains the dNTPs, $MgCl_2$, reaction buffer and DNA polymerase (Promega).

5.3.5. RNA extraction and quantitative RT-PCR (qRT-PCR)

Adult zebrafish were euthanized using ice and system water. Following 5-10 mins in the ice bath the zebrafish were collected, decapitated and their brains were dissected out. Whole brains of three zebrafish per genotype were flash frozen in liquid nitrogen and homogenized in TriZol (InVitrogen) using a pestel for RNA extractions according to manufacturer's protocols. RNA purity was evaluated using the NanoDrop 1000 spectrophotometer to assure A260/280 ratios were within the 1.8-2.1 range. The integrity of RNA was determined through visualization of 28S and 18S ribosomal RNA bands at a ratio of 2:1 through bleached gel electrophoresis. cDNA synthesis was carried out using the iScript cDNA synthesis kit (Bio-Rad) following manufacturer's protocol with 500ng of RNA. Technical triplicates of qRT-PCR were performed using two references genes, *elongation factor 1 alpha* (*ef1a*) and *ribosomal protein l13a* (*rpl13a*), to calculate the comparative Cq method of relative expression for the gene of interest. Normalized expression was determined for the following genes: *dat, th1, gdnf, bdnf, cdnf, manf, serta, gad1b, d1* and *d2*.

Primer sequences are listed in Table 5.1. Each reaction mix consisted of 5µL of SsoFast™ EvaGreen Supermix (Bio-Rad), 0.4µL of forward primer, 0.4µL of reverse primer, 0.2µL of nuclease free water and 4µL of cDNA. Reactions were run using the Bio-Rad CFX96 thermocycler with Maestro software.

Table 5.1. Primer sequences designed for qRT-PCR.

Primer	Forward Sequence (5'-3')	Reverse Sequence (5'-3')	Reference
rpl13a	TCTGGAGGACTGTAAGAGGTATGC	AGACGCACAATCTTGAGAGCAG	(Tang et al. 2007)
ef1a	CTGGAGGCCAGCTCAAACAT	ATCAAGAAGAGTAGTACCGCTAGCATTAC	
dat	AGACATCTGGGAAGGTGGTG	ACCTGAGCATCATACAGGCG	(Barreto-Valer et al. 2012)
th1	GACGGAAGATGATCGGAGACA	CCGCCATGTTCCGATTTCT	(Chen et al. 2016)
Gdnf	TGTCCACACGTCCCCTTTTC	TCCCGTTAGGTCATATTGTTCCTC	
bdnf	CGAGGAATAGACAAGCGGCA	ATCCGTATAAACCGCCAGCC	(Blanco et al. 2020)
manf	ACCATGTGCCAGTGGAAAAGA	TCGACGGAGCTCAAGTCAAC	(Chen et al. 2020)
cdnf	TTCTGCAGCCAAAGTGACCG	TCTGTGCTCCAGTCAAGAACC	
gad1b	GGCCAAGGGCACGATTGGGT	GCATGCCACGCAGACTCGGT	
serta	ACAACCGATGGAACACTCCC	CAACACCTGCCGGACATAAA	
d1	ACGCTGTCCATCCTTATCTC	TGTCCGATTAAGGCTGGAG	(Barreto-Valer et al. 2012)
d2	TGTGATTGCGAATCCTGCCT	CGGGATGGGTGCATTTCTTT	(Thörnqvist et al. 2019)

5.3.6. Brain preparation, immunohistochemistry and imaging

Adult zebrafish were euthanized using the same method as for RNA collection. However, following decapitation the heads were placed in ice cold PBS for 5 mins and then 4% PFA

overnight at 4°C to fix the tissue. Dissections were carried out the following day in PBS, brains were placed in 4% PFA at room temperature for 10 mins and then washed in 1XPBS-T three times prior to overnight incubation in 30% sucrose. The brains were then immersed in Tissue-tek OCT (VWR) for 5 mins then placed into cryomolds to be flash frozen in liquid nitrogen. Coronal cryosections of 14 µm and sagittal cryosections of 20 µm were obtained using the CM3050S cryostat (Leica) for immunohistochemical staining.

Sections were thawed and antibody incubation followed the methods detailed in Kalyn and Ekker (2019) with slight modifications. Primary and secondary antibody incubations were performed using mouse anti-GFP (InVitrogen and anti-mouse Alexa 488 (InVitrogen) respectively. Images were captured using either the Olympus FV1000 or Nikon A1 confocal microscope. Relative eGFP+ neuronal counts were automated using Fiji (ImageJ) software plug-ins (following the optimization of detection threshold, unit specification and circularity to analyze particles) of maximum projection images processed from z-stacks taken in 0.3µm intervals. 3-D renditions of each image were also generated to validate maximum projected data.

5.3.7. Behavioral assays

Larval and adult total distance and freezing bout activities were analyzed using the ZebraLab and ZebraCube tracking instruments and software (ViewPoint Life Sciences). Zebrafish were allocated into 24-well plates for larval (5dpf) evaluation or a static tank for adults (3-6mpf) to acclimate 10 mins prior to recording captured through infrared illumination, a mounted camera and LED lights.

Light/dark behavioral analysis was captured using the same ZebraLab tracking apparatus and software. The experimental design and set up consisted of distributing zebrafish larvae (5dpf)

into 96-well plates with 250uL of system water and capturing swimming activity over a 50-minute period. The first 20 mins are an acclimatory period followed by 5-minute cycles of light and dark for the next 30 mins.

5.3.8. Evaluation of oxidative metabolism and mitochondrial respiration

Real-time metabolic measurements were detected in live zebrafish larvae using the Seahorse XFe 24 analyzer (Agilent). Seven dechorionated 2dpf WT, *nr4a2a* KO and *nr4a2b* KO larvae were loaded into Seahorse XFe 24 islet capture FluxPak plates to be exposed to 12.5µM oligomycin, 5µM FCCP, 1.5µM rotenone/antimycin A injected at staggered cycles to calculate basal oxygen consumption rate (OCR), ATP OCR, proton leak, maximal OCR and non-mitochondrial OCR respectively. All genotypes were exposed to 0.1% DMSO from 4-48 hours post-fertilization (hpf) as SeaHorse reagents are insoluble in water and are reconstituted in DMSO.

5.3.9. Neurotoxin exposure and recovery

1-methyl-4-phenyl-1,2,3,6-tetrahydropyridine hydrochloride (MPTP; Sigma) was reconstituted in distilled water to a stock concentration of 500 mM that was then diluted into the working concentration of 0.25 mM. Exposures were carried out from 3dpf to 7dpf using 6-well plates with 25 Tg(*dat:eGFP*) larvae loaded per well. MPTP and media for non-treated controls (NTC) were refreshed daily. The recovery time-points selected for regenerative analysis were 0-, 3- and 5 days post-treatment (dpt). Pools of 7 larvae were collected for qRT-PCR quantification to compare target gene expression of MPTP-treated larvae with the controls.

5.3.10. Statistical analysis

All statistical analyses and data quantification were done using GraphPad Prism v.6 software. Significance for relative gene expression and behavior between genotypes was calculated with an ordinary one-way ANOVA for multiple comparisons using the Tukey's method. OCR and mitochondrial respiration was quantified using a one-way ANOVA for multiple comparisons using the Dunnett method.

Total swimming distance, average swimming velocity and gene expression data for the regenerative assessment were analyzed using two-tailed unpaired Student's t-test with significance determined using the Holm–Sidak method. Results demonstrated statistical significance when *p*-value < 0.05 and significance was indicated as * $p < 0.05$, ** $p < 0.01$, *** $p < 0.001$. Data bars are shown as the mean ± the standard error of the mean (SEM).

5.4. Results

5.4.1. Generation of stable *nr4a2a* and *nr4a2a* homozygous mutant zebrafish lines

Primary injected Tg(*dat:eGFP*) zebrafish were grown into adulthood and out-crossed with wild-type (WT) to identify founders (F_0). Deletions of 9178bp and 6743bp were detected in *nr4a2a* and *nr4a2b* F_2 mutants respectively, as outlined below. Heterozygote F_1 progeny were raised into adulthood and in-crossed to establish sibling WT, KO and heterozygote populations for both *nr4a2a* and *nr4a2b* (Fig. 5.1).

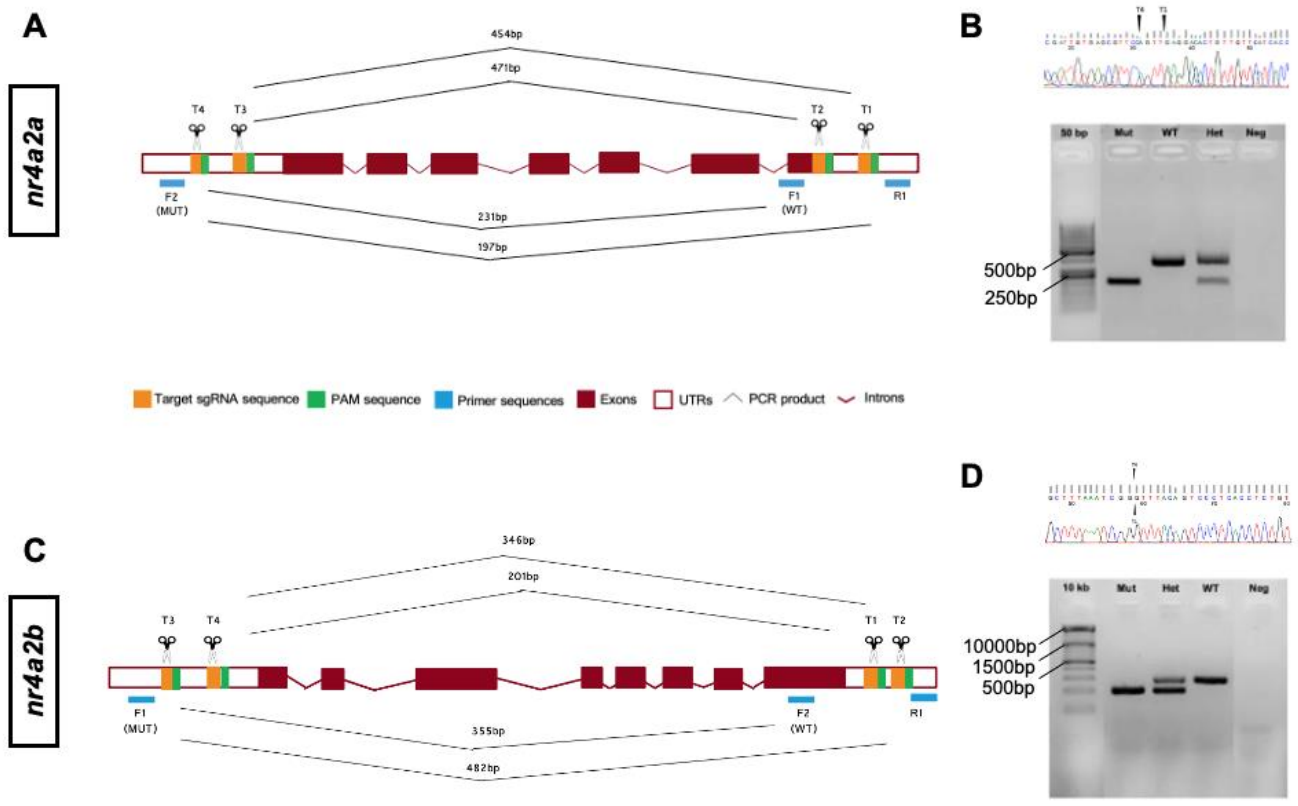

Figure 5.1. CRISPR-Cas9 mediated gene KO of *nr4a2a* and *nr4a2b*. A) Schematic representation of sgRNAs targeting 5' and 3' UTR regions of *nr4a2a*. B) Sequencing and genotyping confirmation of *nr4a2a* mutagenesis. C) Schematic representation of sgRNAs targeting 5' and 3' UTR regions of *nr4a2b*. D) Confirmation of *nr4a2b* mutagenesis through genotyping and sequencing.

5.4.1. Impact of *nr4a2a* and *nr4a2b* on adult DAnergic systems

In line to what was observed among murine models where heterozygotes expressing *Nr4a2* on one allele survived, single KOs targeting *nr4a2a* and *nr4a2b* did not result in lethality. Immunostaining of eGFP revealed similar global effects from the loss of each paralogue on DAnergic neurons in the adult zebrafish brain. Reductions of 35-45% in numbers were observed in the olfactory bulbs, telencephalon and periventricular pretectal nucleus (PPv) of *nr4a2b*

mutants, but numbers in the hypothalamus were unaffected (Fig. 5.2). These data were complemented by detecting 33% and 18% decreases in *dat* and *th1* mRNA transcript levels.

Similarly, 30%, 55% and 13% fewer eGFP+ neurons were observed in the olfactory bulbs, PT and hypothalamus respectively in *nr4a2a* mutants (Fig. 5.2). However, the cell counts within the telencephalon surprisingly remained unaffected. Supporting gene expression analyses revealed a larger effect at the level of transcription following the loss *nr4a2a* than *nr4a2b* where *dat* and *th1* expression was reduced by 32% and 60% respectively.

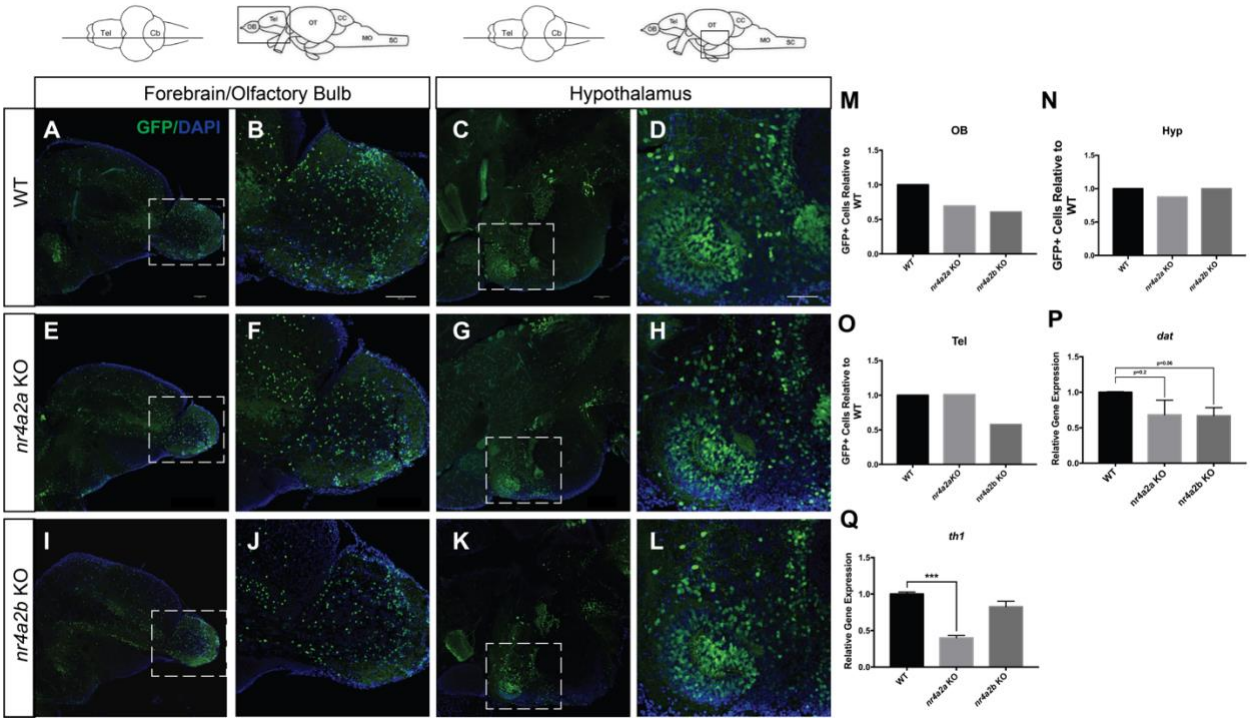

Figure 5.2. Impact on DAnergic neurons following the loss of *nr4a2a* and *nr4a2b*. A-L) Schematic representation of OB and Hyp brain regions and the immunostaining of eGFP (green) and DAPI (blue) using sagittal cryosections. M-O) Quantification of eGFP+ neurons in the OB, Hyp and Tel detecting using coronal cryosections (n=1). P-Q) *dat* and *th1* gene expression levels

in *nr4a2a* and *nr4a2b* mutants relative to WT (*n*=3 brains). Bars represent the Mean ± the SEM. ***($p<0.001$). (Scale bar = 100 μm). OB, olfactory bulbs; Hyp, hypothalamus; Tel, telencephalon.

5.4.2. *nr4a2a* and *nr4a2b* activity during DAnergic regeneration

The function of *nr4a2a* and *nr4a2b* throughout DAnergic development is well understood, however, the activities throughout the regeneration of DAnergic neurons had yet to be examined. Thus, we exposed Tg(*dat:eGFP*) zebrafish larvae to the LC50 dose of MPTP from 3dpf to 7dpf. Exposed larvae were then collected and pooled at 0dpt, 3dpt and 5dpt to assess motor performance, *nr4a2a* and *nr4a2b* expression levels along with other neurogenic and proliferative markers.

Swimming activities were significantly affected at 0dpt in MPTP-treated zebrafish, but gradually recovered to comparable levels observed in NTC by 5dpt (Fig. 5.3I-K). *dat* and *th1* expression levels were then examined to confirm the ablative effects of MPTP on the DAnergic system. A 40% decrease of *dat* was detected at 0dpt that gradually became more severe with 70% fewer neurons than the control by 5dpt. Surprisingly, neuron numbers then showed a 24% increase at 5dpt (Fig. 5.3A). *th1* was also immediately downregulated by 82% at 0dpt, spiked 111% at 3dpt and reduced back down to 28% of the control by 5dpt (Fig. 5.3D). The transcript levels of neural stem cell marker *sry-box* 2 (*sox2*) and *nestin* were then assessed to validate the activation of neurogenesis and progenitor proliferation following neurotoxic injury. *Sox2* was already upregulated by 93% at 0dpt and that increase slowly diminished to 55% expression at 5dpt (Fig. 5.3E). Similarly, *nestin* was shown to increase 75% at 0dpt, spike to 400% at 3dpt and decrease down to 100% more expression than the control at 5dpt (Fig. 5.3B). Despite an initial decrease of 41% in *nr4a2b* levels at 0dpt, no change *nr4a2b* expression was observed at 3dpt or 5dpt between MPTP-treated larvae and controls (Fig. 5.3F). *Nr4a2a* expression was also reduced at 0dpt by

50%, however, a 22% and 49% increase in mRNA was detected at 3dpt and 5dpt respectively (Fig. 5.3C). This trend resembled the changes in *shha* expression during DAnergic regeneration where a 63% reduction of expression was first observed at 0dpt but then *shha* was upregulated by 11% at 3dpt and 33% at 5dpt relative to the control (Fig. 5.3G). The expression of *notch1a* throughout recovery mirrored that of *nestin* and *th1* as increases of 37%, 300% and 15% were detected at 0-, 3- and 5dpt (Fig. 5.3H).

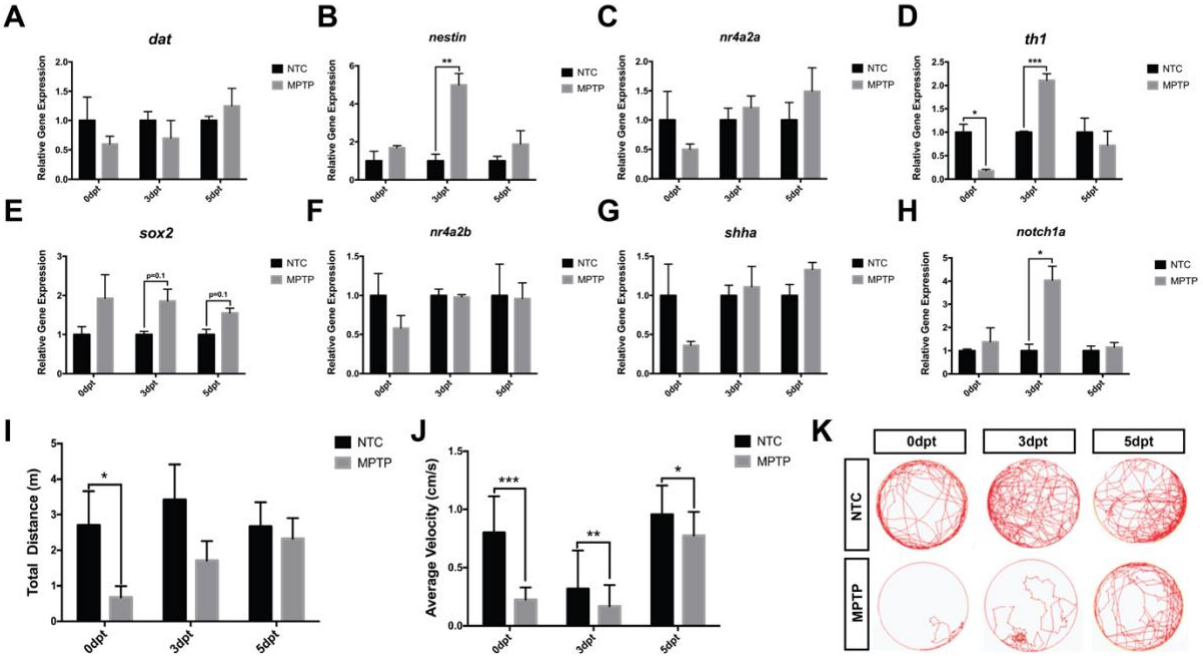

Figure 5.3. *nr4a2* response following MPTP-induced neurodegeneration. A-H) Relative gene expression is also provided for markers of regeneration, neurogenesis, DAnergic transcription and synthesis throughout larval recovery (*n*=2-3 pools of 7 larvae). I-J) Total distance travelled and average velocity of MPTP-treated and NTC controls from 0- to 5dpt (*n*=30). K) Representative path images. Bars represent the Mean ± the SEM. *($p<0.05$), **($p<0.01$) and ***($p<0.001$).

5.4.3. Impaired *nr4a2a* and *nr4a2b* function affects a family of neurotrophic factors and alternative neurotransmission

To further our insight into the role of *nr4a2a* and *nr4a2b* in various processes involved in neurological homeostasis, we analysed gene expression for biomarkers of neurotrophic factor family members, alternative neurotransmitting systems and DA receptors.

To our surprise, we found considerable differences between the loss of *nr4a2a* and *nr4a2b* on the expression profiles of certain neurotrophic factors. In *nr4a2b* mutants, *glial-derived neurotrophic factor* (*gdnf*) and *brain-derived neurotrophic factor* (*bdnf*) showed 30% and 24% increases in expression respectively, whereas *cerebral dopamine neurotrophic factor* (*cdnf*) and *mesencephalic astrocyte-derived neurotrophic factor* (*manf*) expression did not differ from WT levels (Fig. 5.4A-D). Conversely, the loss of *nr4a2a* resulted in a 49% and 35% decreases in *gdnf* and *bdnf* expression, while *manf* and *cdnf* were also decreased by 80% and 22% relative to WT.

Due to the critical role that DA and the DAnergic system play in the neurodevelopment of differing neurotransmitting pathways, the relative expression of *glutamate decarboxylase 1b* (*gad1b*, a precursor to GABA) and *serotonin receptor a* (*serta*), as well as, DA receptors *d1* and *d2* were examined. *Nr4a2b* mutants did not show any change in *gad1b* expression, but a 41% decrease in the expression of *serta* (Fig. 5.4G-H). Reductions of 42% and 23% were also detected in *d1* and *d2* mRNA levels (Fig. 5.4E-F). A similar effect was observed in *nr4a2a* mutants as *serta* and *gad1b* were downregulated and upregulated 23% and 5-fold respectively. The expression of *d1* was unaffected, while *d2* expression was decreased 63% relative to the controls.

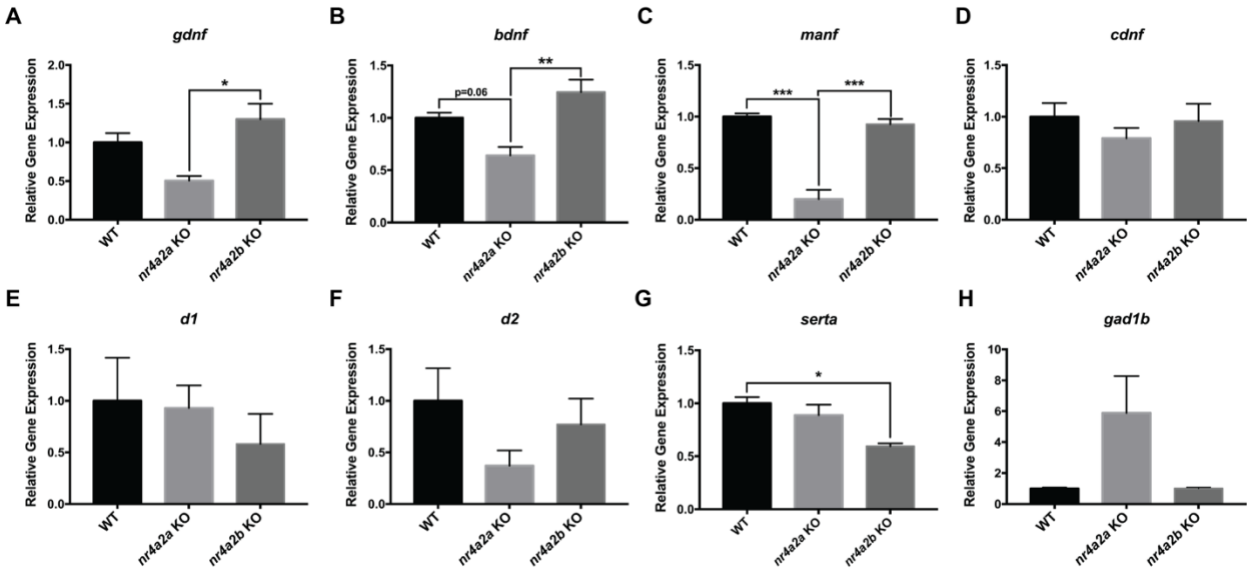

Figure 5.4. Whole brain transcriptional changes in *nr4a2a* and *nr4a2b* mutants. A-H) Relative gene expression for neurotrophic factors, DA receptors and other neurotransmitting systems. (*n*=2-3 brains) Bars represent the Mean ± the SEM. *($p<0.05$), **($p<0.01$) and ***($p<0.001$).

5.4.4. Metabolic impact from the loss of *nr4a2a* and *nr4a2b*

We sought to evaluate the role of *nr4a2a* and *nr4a2a* in mitochondrial biogenesis measured in real-time using the SeaHorse assay. We found that the loss of *nr4a2a* exerted the largest metabolic changes in basal and maximal respiration with minimal effect to ATP-linked and non-mitochondrial OCR. Conversely, *nr4a2b* mutants displayed the largest impact on ATP-linked and non-mitochondrial OCR without affecting basal or maximal respiration (Fig. 5.5A-E).

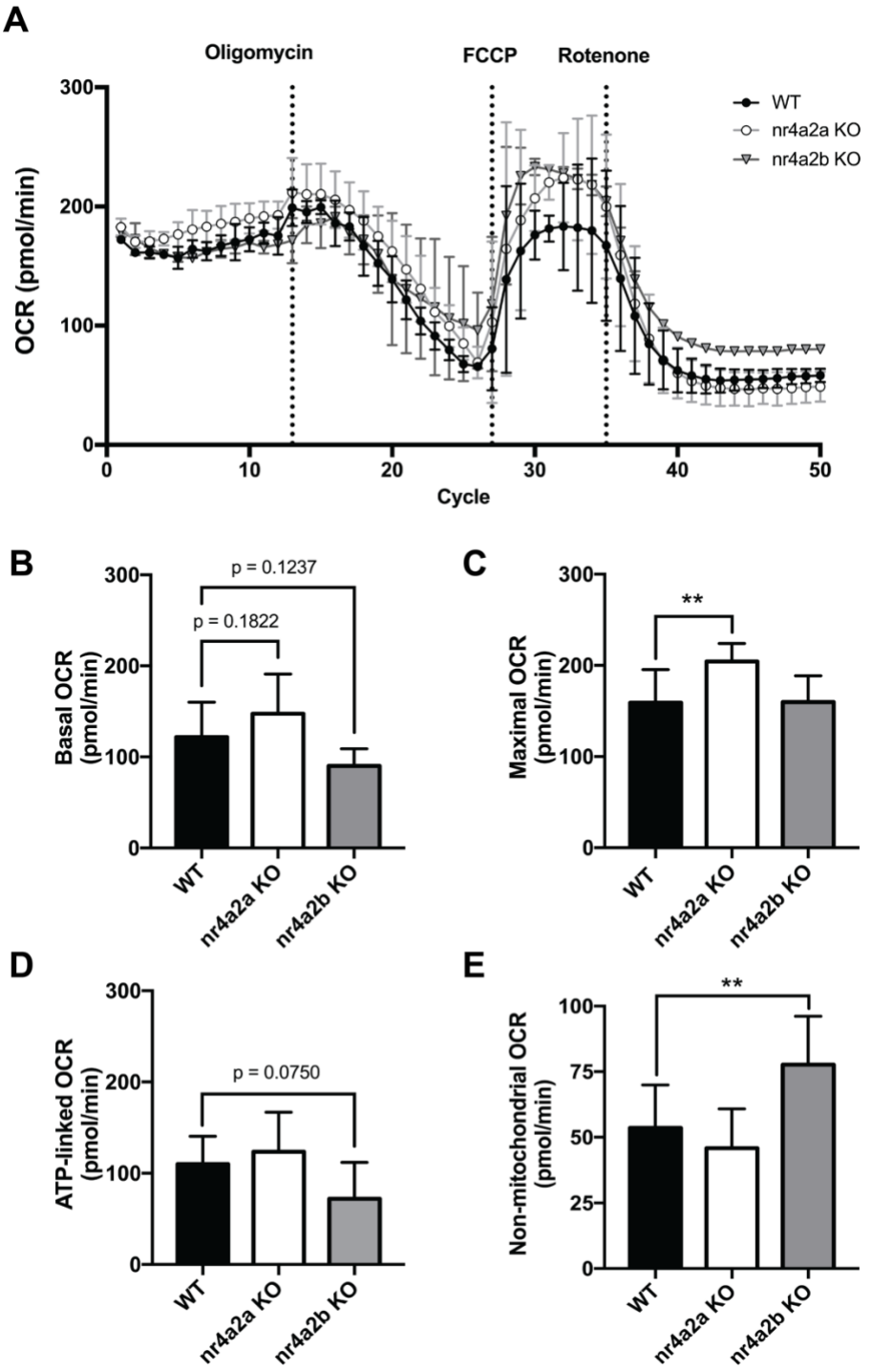

Figure 5.5. Metabolism in WT, *nr4a2a* and *nr4a2b* mutant larval zebrafish. A) Experimental design and overview of the genotypic response to the addition of oligomycin, FCCP and rotenone. B-E) Average basal OCR, maximal OCR, ATP-linked OCR and non-mitochondrial OCR for *nr4a2* mutant zebrafish relative to the WT controls. (*n*=9-13). Bars represent the Mean ± the SEM.

5.4.5. *nr4a2a* and *nr4a2b* differentially impact locomotion and behavior

Motor perturbance is a hallmarked feature of PD that arises only after considerable DAnergic cell death. To determine if there are any behavioral or locomotor consequences following the loss of *nr4a2a* and *nr4a2b*, several assays were carried out. Total distance and freezing bout activities were first recorded in both larval and adult zebrafish mutants to compare to WT siblings. We only observed a slight change in motor performance following the KO of *nr4a2b*. There was a large variance without a distinct pattern observed at 5dpf, but this did not persist into adulthood where 3mpf mutants consistently swam with a minor hyperactive phenotype . Consequently, *nr4a2b* mutant adults displayed reduced freezing bouts (Fig. 5.6A-C). *nr4a2a* mutants swam 45% less far at 5dpf than the WT control, but that reduction diminished to 33% less than controls in adults (Fig. 5.6A-B). Freezing bout durations followed a similar trend that decreased relative to controls in adult *nr4a2a* mutants (Fig. 5.6C).

Anxiety is also a common underlying factor to many neurodegenerative diseases including Alzheimer's, Parkinson's and Huntington's (Ferretti et al. 2001; Duff et al. 2007; Broen et al. 2016). To evaluate the behavioral implications of *nr4a2a* and *nr4a2b* KOs on anxiety or fear response in zebrafish we performed a light/dark stimulus test. We found *nr4a2a* mutants displayed a significantly increased freezing response in both light and darkness, whereas *nr4a2b* mutants were primarily affected in darkness (Fig. 5.7A-C). This trend was consistent when evaluating the total distance, average velocity and active duration of all groups.

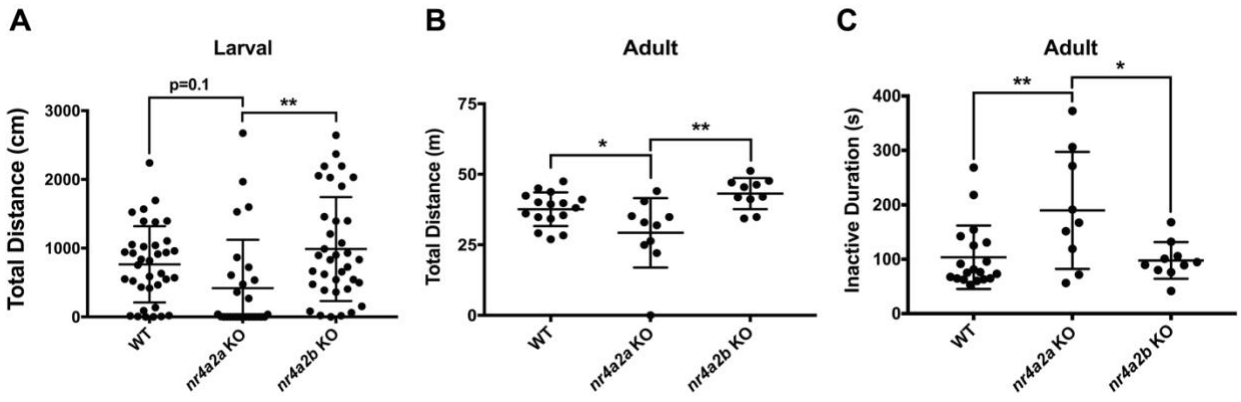

Figure 5.6. Impact on swimming activities following the loss of *nr4a2a* and *nr4a2b*. Locomotor changes between WT, *nr4a2a* and *nr4a2b* mutants at larval (5dpf) and adult (3-6mpf) developmental stages. The parameters analyzed were A-B) total distance travelled and C) inactivity duration. (*n*=28-36 for larvae and 9-16 for adults). Bars represent the Mean ± the SD. *(p<0.05) and **(p<0.01).

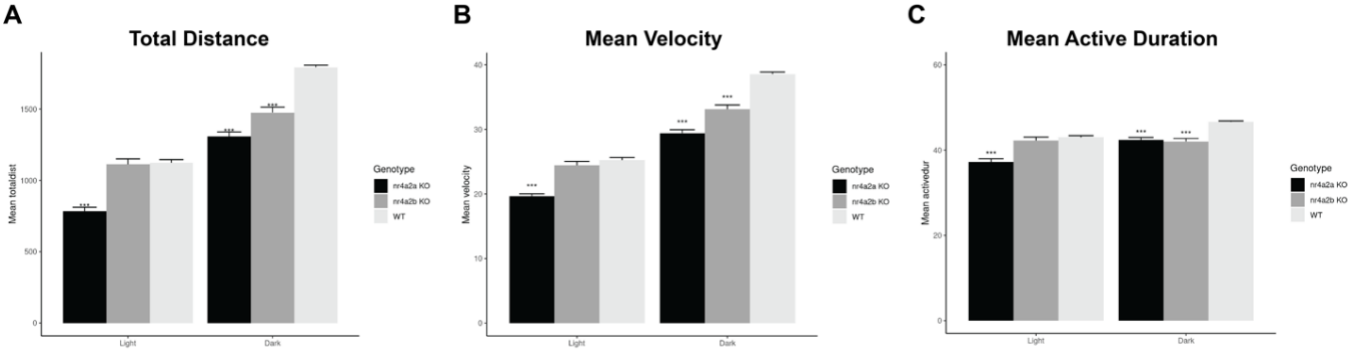

Figure 5.7. Anxiety and stress response to light/dark cycling in *nr4a2a* and *nr4a2b* mutant 5dpf zebrafish larvae. Startle response following light/dark cycling analyzed using A) total distance swam, B) mean velocity and C) active duration. (n=24). Bars represent the Mean ± SEM for light/dark behavior. ***(p<0.001).

5.5. Discussion

NR4A2 is a transcription factor essential for the development and protection of midbrain DAnergic neurons in a wide array of vertebrate and invertebrate species (Chinta and Andersen 2005; Jankovic et al. 2005; Filippi et al. 2007; Luo et al. 2008). Because of this, any dysfunction to *NR4A2* activity can be consequential and lead to the pathogenesis of DA-associated diseases such as PD, ADHD and schizophrenia (Jiang et al. 2005; Rojas et al. 2007; Montarolo et al. 2019).

Here we present the first single KO model targeting *nr4a2a* and *nr4a2b* paralogs using zebrafish. Despite the apparently normal development of homozygous mutants into adults, we found that zebrafish lacking either *nr4a2a* or *nr4a2b* present degeneration of DAnergic neurons detected through reduced eGFP+ cells in mutants relative to WT controls. It was important to use Tg(*dat:eGFP*) zebrafish for precise DAnergic quantification as *dat* expression is localized to DAnergic neurons while *th1* is also expressed in adrenergic and noradrenergic cells types. Moreover, *th1* and *th2* paralogs also possess distinct expression patterns where *th2* is only expressed in the PT and hypothalamus of non-mammalian vertebrates thus proper delineation is crucial when comparing results (Barrios et al. 2020).

Intriguingly, we found the loss of *nr4a2a* and *nr4a2b* to translate into differing effects on locomotion and on various components essential to neurological homeostasis. *nr4a2b* mutants displayed a slight hyperactivity that followed a similar behavioral trend recorded in heterozygote mice mediated through increased DA turnover (Le et al. 1999; Rojas et al. 2007). *th1* and *dat* gene expression data suggest that a similar turnover mechanism may be at play to compensate for the global losses of DAnergic neurons. We continued to explore DA signalling impairments that contribute to the observed phenotype by analyzing *d1* and *d2* activity as several studies have highlighted their roles in behavior and motor response (Korchounov 2008; Korchounov et al.

2010). We found a drastic decrease in *d1* that is reminiscent of a KO mouse line deficient of *D1* and following the pharmacological disruption of *d1* in zebrafish that resulted in increases in spontaneous movement and locomotion respectively (Xu et al. 1994; Scerbina et al. 2012). *Dat* expression was also significantly lower than *nr4a2a* mutants which likely acts to potentiate the hyperactivity as observed within a *dat* KO zebrafish model where mutants displayed increased average swimming and anxiety-associated behaviors (Kacprzak et al. 2017). These effects, however, manifested themselves in a more age-dependent manner, thus the additional impacts on *th1*, *d1* and *d2* following *nr4a2b* KO may synergistically drive the swimming defects observed throughout development. When exposed to a light/dark fear provoking assay, *nr4a2b* mutants displayed increased freezing bouts in the darkness. Zebrafish are generally more active in darkness, thus the observed effect on startle response complements literature surrounding *Nr4a2* deficiencies to induce anxiety phenotypes. *nr4a2a* mutants displayed similar anxious behaviors in both lightness and darkness consistent with cognitive symptoms that arise in PD pathologies (Broen et al. 2016). However, *nr4a2a* mutants also exhibited significantly reduced motility throughout their lifespan similar to heterozygous mice >15mpf. These contrast what was reported in previous morpholino studies that observed hyperactive phenotypes using the rudimentary parameters of total distance and inactivity following the single and double knockdown of *nr4a2b* and *nr4a2* respectively in wild-type zebrafish larvae (Blin et al. 2008). However, the transient and cytotoxic nature of morpholinos do not give the full picture as CRISPR-mediated KOs affect every cell from birth until death. Consequently, neurotrophic pathways that are involved in locomotion and complex behaviors such as stress and anxiety were also significantly impacted following the loss of *nr4a2a* and *nr4a2b* that were previously overlooked. Of which, *nr4a2a* mutants displayed drastic reductions for both *gdnf* and *bdnf* transcript levels. KO zebrafish were recently generated

for *gdnf* and *bdnf* where mutants swam far less on average than their WT siblings observed as early as 7dpf in *gdnf* mutants and 4dpf in *bdnf* mutants (Wong et al. 2021; D'Agostino et al. 2022). The neurotrophic impact along with the widespread depletion of DAnergic neurons detected through eGFP+ quantification are the probable source for the deleterious impacts observed on locomotion.

Neurotrophins interact with receptors in the brain to modulate many aspects of neurological health including inflammation, development, movement and neurotransmission (Henderson 1996; Lima Giacobbo et al. 2019). GDNF and BDNF have gotten much attention in the past decade for their robust roles in DAnergic protection and maintenance (Hyman et al. 1991; Choi-Lundberg et al. 1997) with GDNF being pursued in clinical trials for symptomic relief in PD to varying success (Gash et al. 2020). In vitro, silencing *Nr4a2* led to reduced TH and BDNF levels within cultured rat midbrain neurons that is mediated though CREB activation and NMDAR stimulation (Volpicelli et al. 2007; Barneda-Zahonero et al. 2012). Nr4a2 has also been shown to regulate GDNF activity by interacting with GDNF receptor Ret (Kambey et al. 2021). Surprisingly, we found zebrafish lacking *nr4a2a* and *nr4a2b* displayed opposite effects on *bdnf* and *gdnf* expression. The decreases in *gdnf* and *bdnf* transcripts found in *nr4a2a* mutants resembled more of what is reported in literature than *nr4a2b* mutants. Conversely, we found both *gdnf* and *bdnf* to be increased following the KO of *nr4a2b*. One study recently observed that *Nr4a2* did not impact BDNF activity in certain brain tissues, however, no increase of BDNF has yet been observed in the absence of functional *Nr4a2* (Abdollahi and Fahnestock 2022). Further investigation into *Ret*, *CREB* and *NMDA* activity will be needed to validate the mechanistic understanding of this pro-survival effect limited to *nr4a2b* but not *nr4a2a* mutants.

Expanding on the neurotrophic effects, various studies have come forth highlighting MANF and CDNF as two components critical to neural health (Airavaara et al. 2012; Chen et al.

2012). Of which, Chen and colleagues (2014) demonstrated this by using *nr4a2b* morphant zebrafish whose DAnergic phenotype was rescued following exogenous administration of *manf,* in addition to an observed upregulation of *nr4a2b* in *manf* morphants (Chen et al. 2012). Our findings verify the interplay between *manf* and *nr4a2*, however, differ in the sense that it was the KO of *nr4a2a* that translated into the largest change in *manf* expression. Similarly, *nr4a2a* KO resulted in the downregulation of *cdnf.* Despite its name, impaired CDNF function has been shown to display limited effects on DA levels in deficient mice without exposure to supplemental stress (Pakarinen et al. 2022). Under pathological conditions, however, CDNF and MANF activity has been reported to regulate the endoplasmic reticular stress-induced unfolded protein response activated in the clearance of disease-associated cellular defects (Lindholm and Saarma 2022; Pakarinen et al. 2022). The reductions detected in *nr4a2a* mutants may indicate an increased susceptibility relative to *nr4a2b* mutants to mitochondrial and ER associated stress and neurodegeneration. Recently, a KO line was generated for *cdnf* using zebrafish that confirmed the minimal impact on DA populations, but the loss of *cdnf* evoked widespread change in other neurotransmitting systems that translated into behavioral defects reminiscent of epilepsy (Chen et al. 2020). Because of this interconnectivity, we sought to examine the consequence of *nr4a2a* and *nr4a2b* on neurotransmitting systems essential in the modulation of complex behaviors such as GABA and serotonin.

Serotonin and serotoninergic dysfunction have long been known to contribute to the onset of DA-associated psychiatric disease states such as schizophrenia and depression (Abi-Dargham 2007). This comes to no surprise given the similarity in efferent projection trajectories within limbic and nigrostriatal regions in the brain (Niederkofler et al. 2015). The impact following the loss of *nr4a2a* and *nr4a2b* was in line to the reduced serotonergic output observed within the

striatum of heterozygous mice deficient in *Nr4a2* used to model schizophrenia (Rojas et al. 2007). With reduced *Nr4a2* detected in the prefrontal cortex of brains from patients of schizophrenia as well (Xing et al. 2006), we can propose that the *nr4a2b* line is more suitable to model this disease from the telencephalic insult observed in this study relative to *nr4a2a* mutants. The telencephalon or pallium is proposed to be the functional analog to the mammalian cortex (Rink and Wullimann 2002b; Panula et al. 2010; Mueller et al. 2011), thus quantifying receptor activity to calculate DA and serotonin turnover in this structure will validate the regional discrepancies observed within the *Nr4a2*-deficient mouse model for schizophrenia. Regarding *nr4a2* influence over GABAergic circuitry, there was a negative correlation between the two documented in mice where *Nr4a2* suppression resulted in increased GABAergic differentiation and calbindin inhibition in amacrine populations (Jiang and Xiang 2009). These effects may be consistent to what was observed in *nr4a2a* mutants, however, further immunohistochemical and transcriptomic analysis of other GABAergic receptors and subtypes are required to support this claim.

Although previously unexplored outside of a protective environment, our findings support the hypothesis of *nr4a2* involvement in DAnergic regeneration following MPTP-induced neurodegeneration. To our surprise, *nr4a2a*, not *nr4a2b*, predominantly shared a similar expression pattern with *shha*. The initial reduction and gradual increase in transcript levels may be explained by an initial inhibition in cell-fate differentiation, assuming that hedgehog signaling retains the role described throughout mouse embryogenesis (Roussa and Krieglstein 2004; Carballo et al. 2018). In the affirmative, the gradual increases observed at 3- and 5dpt could potentially be correlated to the induction of the differentiation stage of neurogenesis, particularly DAnergic cells given the selective cytotoxicity of MPTP. We found another complimentary trend between *nestin*, *th1* and *notch1a* gene expression levels. Understanding that *nestin* is active during

the proliferative stage of neurogenesis we can hypothesize that *notch1a* is driving the proliferation of DAnergic neurons primarily at 3dpt. However, at 5dpt we find all mRNA levels to drop thus the we can hypothesize that differentiation into a DAnergic cell fate requires the shift from *notch1a* to *shha* signaling activation between 3- and 5dpt. Further investigation into pharmacological antagonists targeting *shha* and *notch1a*, in addition to, the expression levels of alternative DAnergic transcription factors will be useful in further delineating the functional roles of *nr4a2a*, *nr4a2b*, *notch1a* and *shha* in DAnergic regeneration.

In PD, it is known that DAnergic neurons of the substantia nigra are more susceptible to oxidative stress than DAnergic neurons located in other brain regions; ventral tegmentum and OB (Pacelli et al. 2015). Researchers attribute this disproportional vulnerability to the bioenergetic requirements necessary to produce the vast striatal arborization observed within this population of DAnergic neurons . Aside from its function in DAnergic development, *Nr4a2* has also been shown to regulate the expression of numerous nuclear-encoded mitochondrial genes (Kadkhodaei et al. 2013). Based on the OCR data, we can hypothesize that the reduced growth of the DAnergic system within *nr4a2a* mutants triggered a maximal respiratory response to in the surviving neurons in parallel to the slight increase in basal OCR. Inversely, the increase in non-mitochondrial OCR observed in *nr4a2b* mutants could be from the contribution of other intracellular organelles that possess oxidase activity (endoplasmic reticulum and plasma membrane). Moreover, decreases in ATP-linked OCR suggest a larger presence of reactive oxygen species in the *nr4a2b* mutants. The non-mitochondrial response may act as a protective mechanism to clear oxygen when approaching harmful concentrations in aim to prevent further insult from oxidative stress as described in previous studies surrounding non-mitochondrial OCR and antioxidation (Bishop and Brand 2000; Arzuaga and Elskus 2010; Raftery et al. 2017). With our *gdnf* and *bdnf* data suggestive of a pro-

survival effect at play, further inquiry into ATP-turnover, ROS clearance and alternative organelle activity in *nr4a2b* mutants is required to support this claim and to elucidate the molecular mechanism driving this response.

5.6. Conclusion

Collectively, we have shown that the genetic KO of *nr4a2a* and *nr4a2b* induces similar effects on DAnergic neurodegeneration, but this loss translated into variable consequences on other neurological systems and behavior between genotypes. *nr4a2a* mutants displayed symptoms more reminiscent of PD-related pathologies, whereas *nr4a2b* mutants displayed symptoms associated DA-related hyperactive disorders such as schizophrenia and ADHD. Further investigation into the mechanistic understanding behind these differences is warranted to establish the *nr4a2a* and *nr4a2b* mutant zebrafish lines as viable models for DA-associated diseases.

CHAPTER 6: GENERAL DISCUSSION AND PERSPECTIVES

The primary objectives of my thesis were to further our understanding of neurotoxin-induced PD, to screen naturally derived phytochemicals for DAnergic neuroprotection and to elucidate alternative neurological insult following impaired DAnergic development. We found it crucial to evaluate the multiple facets of disease pathogenesis due to the idiopathic nature of PD and the onset being likely attributed to a combination of both genetic predisposition and environmental exposure.

6.1. Comparative analysis and establishment of a neurotoxin-induced model of Parkinson's disease

Chemo-ablative studies of PD commonly rely on the administration of 6-OHDA, MPP+, MPTP, paraquat or rotenone to elicit widespread DAnergic loss. To date, there have been conflicting reports surrounding the degree of cell death, the effects of locomotion, the development of morphological abnormalities and the method of delivery. We tested the viability of each neurotoxic model by exposing Tg(*dat:eGFP*) to the LC50 dose under standardized conditions to determine the optimal compound to model PD without any undesired side effects. We found that MPTP and MPP+ exposures resulted in the largest deleterious effects on DAnergic populations within the vDC and on motor performance. The vDC region is of particular importance for its proposed analogous function to the human nigrostriatal pathway implicated in PD. These effects were validated through *th1*, *dat* and *p53* gene expression, in addition to eGFP+ quantification of clusters 8, 12 and 13. Swimming activities were assessed using the proxies of average velocities, distance swam and freezing bout duration. MPP+ was ultimately selected as the choice neurotoxin

to model PD through water immersion using larval zebrafish as MPTP regularly induced cardiac edemas and morphological defects. Interestingly, we observed the upregulation of *p53* following the administration of MPTP and MPP+ unseen by the other neurotoxins. We can propose that the MPTP-induced increase of expression is attributed to systemic apoptosis and defects resulting from water exposures. It would be interesting to investigate the increase observed in MPP+ treatment groups as MPTP was shown to activate mitophagy directed mechanisms of cell death in chapter 4.

Future studies can adopt this experimental model to analyze the spatiotemporal regeneration of DAnergic neurons following injury. The zebrafish has also emerged as a powerful tool for high-throughput pharmacological screening (Ali et al. 2011), thus the establishment of this model will be helpful for the therapeutic investigation of compounds that can be used to alleviate oxidative stress-mediated symptoms of PD.

6.2. Neuroprotective screening of natural phytochemicals to alleviate Parkinsonian symptoms

Over the decades, much advancement has been made researching treatments to alleviate the symptomatic suffering associated with PD as there remains to be a definitive cure (Pedrosa and Timmermann 2013). These treatments are often only available after the considerable loss of midbrain DA and have been correlated to the onset of negative side effects. Thus is it imperative to seek alternative approaches to prevent or ameliorate the progression of PD.

Building on the foundation laid in chapter 1, we performed an extensive comparison of naturally derived phenols that are known to possess antioxidizing properties in aim to mitigate some of the mitochondrial damage observed in PD pathologies. From this, AA, FA and VA were

selected to contrast neuroprotective efficacies in an MPTP-induced model of PD using larval zebrafish that was previously unexplored. MPTP was selected for this study instead of MPP+ as we wanted to explore the possibility of protecting against the most severe morphological defects in addition to DAnergic neurotransmission. We analyzed *th1* and *fis1* mRNA transcript levels to determine which phytoconstituent relays the largest DAnergic and mitochondrial protective effects respectively as *fis1* and *th1* are both upregulated and downregulated in an adult zebrafish model of MPTP-induced PD respectively. Swimming activities were also measured to determine if AA, FA or VA pretreatment translates into any preserved motor function relative to the MPTP-treated positive control. We found FA to be the optimal phenol to protect against all proxies of analysis. Surprisingly, we observed differential effects between AA and VA pretreatment groups. Larvae exposed to AA maintained some gene function relative to the control without any rescued movement, whereas VA resulted in some protective effect on locomotion but not on the level of gene expression.

It will be interesting to first validate these findings at the protein level through immunohistochemical analyses of DAnergic and mitochondrial biomarkers such as TH, Dat, Tom20 and Pink1. Alternatively, treatments performed on Tg(*dat:eGFP*) and Tg(*dat:tom20 MLS:mCherry*) transgenic zebrafish lines will facilitate the labeling of DA neurons and their mitochondria with GFP and mCherry for precise quantification. Given the complex I targeting and free radical scavenging activities of MPTP and the tested phenols respectively, it would be useful to implement ROS detection assays and analyze the gene expression for markers of oxidative stress to build a comprehensive mechanistic profile of each phytochemical in an MPTP-induced model of PD.

6.3. Establishment of a novel model for sporadic Parkinson's disease using adult zebrafish

The onset of Parkinsonian motor symptoms arise only following considerable depletion of midbrain DA (DeMaagd and Philip 2015). Previous studies using zebrafish have reported discrepancies in reproducing a similar loss of DA to that in humans to translate into consistent motor phenotypes. Moreover, the mitochondrial impact in these models have frequently been overlooked. Much of these inconsistencies can likely be attributed to conventional drug delivery techniques that introduce the neurotoxin into the water or through intra-abdominal injections that both pose the risk of developing undesired side effects and make monitoring the absorption rate across replicates difficult in some cases. To overcome these hurdles, we generated a reliable MPTP-induced model of PD using adult zebrafish to evaluate mitochondrial dynamics and sensory impairments in addition to the well characterized motor defects. To administer MPTP, we adopted the cerebroventricular microinjection (CVMI) technique to locally distribute MPTP into the cerebroventricular fluid that surrounds the brain of the zebrafish. Microinjections were performed on Tg(*dat:eGFP*) and Tg(*dat:tom20 MLS:mCherry*) transgenic zebrafish lines to visualize DAnergic neurons and their mitochondria respectively.

We found a widespread loss of DAnergic neurons that was supported through reductions in *th1* and *dat* gene expression without affected alternative neurotransmitting systems (Appendix A.1-2.). We then sought to evaluate the mitochondrial impact and found vast fragmentation within the OBs of MPTP-injected zebrafish relative to the controls. To elucidate the mechanism of cell death activated in this model, we evaluated gene expression to find increases in *pink1* and *parkin* transcript levels, but not *opa1*. These data suggest mitophagy to be the predominant driver of this phenotype and to potentiate MPTP-induced neurodegeneration. Furthermore, the DAnergic loss within the sensorimotor epicenters of the zebrafish brain following MPTP-injections was shown

to translate into perturbed locomotion and olfaction. These behavioral consequences, however, were corrected within a 2-week recovery period.

5-bromo-2-deoxyuridine (BrdU) intrabdominal injections have since been performed to investigate the functional regeneration of DAnergic neurons within this model. BrdU is a thymidine analogue that is integrated into the DNA of dividing cells during the S-phase of mitosis and commonly implemented as a marker for proliferation (Gratzner 1982). No striking changes between MPTP-injected zebrafish and controls were observed at 7- and 14dpi (Appendix A.3.). Previous work in our laboratory has shown that DAnergic neurons regenerate in the OB following chemogenetic ablation and are detectable at 45dpi (Godoy et al. 2020). It would be interesting to contrast the regenerative capacity of this model with what was observed in the chemogenetic model as MPTP-injections had a more prominent impact on behavior and larger degree of cell loss (Godoy et al. 2020). Moreover, we can hypothesize that we will observe an increase in BrdU+/GFP+ neurons at later time points than 14dpi. It would also be useful to explore different brain regions other than the OB that can regenerate DAnergic neurons in the adult brain, as well as, tracing the migratory paths of newly formed neurons to see if there are local or distal pressures following MPTP-injections. Furthermore, it is known that fission is not only mediated by the mitochondria but the ER also depicts cleavage spots and interacts with the dysfunctional mitochondrion during fragmentation (Korobova et al. 2013; Marchi et al. 2014). Examining MPTP-injected zebrafish cryosections with anti-mCherry and immunogold staining for electron microscopy will allow us to observe mitochondrial cristae in better resolution to provide more precise measurements of cristae remodelling and ER activity. Furthermore, it would be worthwhile to investigate the impaired olfactory observed in this study to determine if it is due to a lack of fear response or from suppressed olfaction as cadaverine is also known to provoke habenular mediated

escape behaviors in zebrafish (Choi et al. 2021). In doing so, we will be able to provide a more comprehensive understanding of the physiological and functional consequences observed within sporadic PD, in addition to exploring mechanisms of DAnergic regeneration.

6.4. *nr4a2a* and *nr4a2b* mutants can be used to model dopamine-associated neurological disorders

Chapter 5 shifted from sporadic PD modeling to explore avenues of genetic predisposition that potentiate PD and other the DA-associated neurological disorders. Targeting DAnergic transcription factor *NR4A2* paralogues, *nr4a2a* and *nr4a2b*, for CRISPR-Cas9 mediated mutagenesis resulted in effects that both contrast and coincide with literature. *nr4a2a* mutants displayed reduced locomotion, impaired startle response, overactive metabolic output, reduced neurotrophic factor expression in addition to the predicted widespread loss of DA. *nr4a2b* KO induced the widespread depletion of DA, however, mutants were hyperactive, could startle, displayed normal metabolism and increased the expression of neurotrophins *gdnf* and *bdnf* relative to WT controls. Previous studies have shown homozygosity to be lethal in mice and heterozygotes to be hyperactive throughout their lifespan until over a year when Parkinsonian symptoms appear. These mice display impaired DA production, increased DA turnover and a rapid degeneration of DAnergic neurons at later developmental time points. Due to the array of distinct phenotypes, *Nr4a2*-deficient mice have been used to model numerous DA-associated disorders such as schizophrenia, ADHD and PD (Zetterström et al. 1997; Rojas et al. 2007; Montarolo et al. 2019).

The *nr4a2a* mutants more strongly recapitulated symptoms of PD that persisted throughout their lifespan, whereas *nr4a2b* mutants displayed similar effects to what was observed in heterozygous mice and reminiscent of hyperactive disorders. It would be interesting to examine

the swimming activities in older zebrafish adults to determine if locomotor impairments arise in an age-dependent similar to what was observed in the mice. It is also important to consider that zebrafish have a range of complex behaviors such as memory, social interaction and cognition (Saverino and Gerlai 2008; Roberts et al. 2013). Further experimentation will be required to validate if *nr4a2b* mutants are a suitable model for ADHD and schizophrenia in addition to the learning and function impairments associated with PD such as olfactory loss and anxiety. Given the role of cortisol in anxiety, it would be useful to compare the levels of cortisol in *nr4a2a* and *nr4a2b* mutants with their WT siblings through high-performance liquid chromatography, in addition to DA, DOPAC and serotonin. Furthermore, performing FACS to isolate GFP+ neurons for RNA sequencing will help uncover if any other DAnergic transcription factors are compensating for the loss of *nr4a2a* or *nr4a2b* and would also generate transcriptomic profiles for other cellular processes such as neuroinflammation and metabolism. Lastly, it will be useful to perform lethality studies using double *nr4a2* mutants. We have detected double homozygotes in embryological stages, however, we have yet to observe any that reached 14dpf. Designing a developmental time-sensitive study to uncover the exact stage and mechanism of death will contribute significantly to our understanding of *nr4a2* in the disease pathologies.

6.5. Conclusions

In sum, we have shown that MPP+ is the most robust neurotoxin to recapitulate PD-related symptoms without systemic defects relative to rotenone, MPTP, paraquat and 6-OHDA. In search of plant derived antioxidants, we have shown FA to produce the largest neuroprotective effect against MPTP-induced neurodegeneration. Furthermore, we have generated a reliable model for PD using adult zebrafish through the CVMI administration of MPTP that can be used to explore

mechanisms of DAnergic regeneration and more a detailed assessment of mitochondrial impact using Tg(*dat:tom20 MLS:mCherry*) zebrafish. The *nr4a2* mutants will also be a valuable tool to investigate various aspects of DA-associated diseases, therapeutics and to better our understanding of their role in regeneration and sensitivities to environmental exposures. Overall, the neurotoxic and genetic zebrafish models we generated in this study will serve as a platform to further our knowledge of PD and other disorders related to DA deficiencies.

APPENDIX A: SUPPLEMENTAL DATA

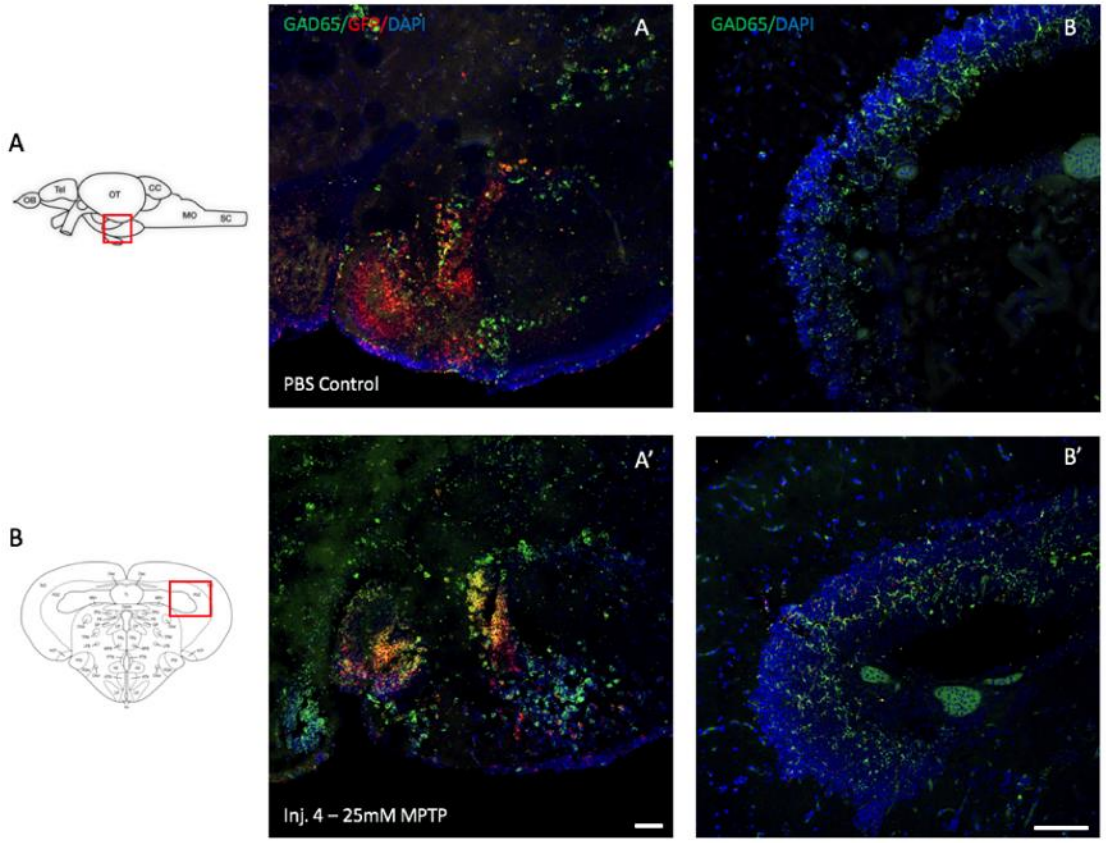

Figure A.1. MPTP injections do not impact GABAergic neurons. Fluorescent in situ hybridization of A) sagittal and B) coronal cryosections. *gad65*probe was used to label GABA and eGFP for DAnergic cells. A) Expression was imaged in the hypothalamic region and B) the periventricular grey zone (PGZ). A-B) PBS vehicle treated zebrafish. A'-B') MPTP-treated zebrafish (n = 1-2). (Scale bars = 150 μm).

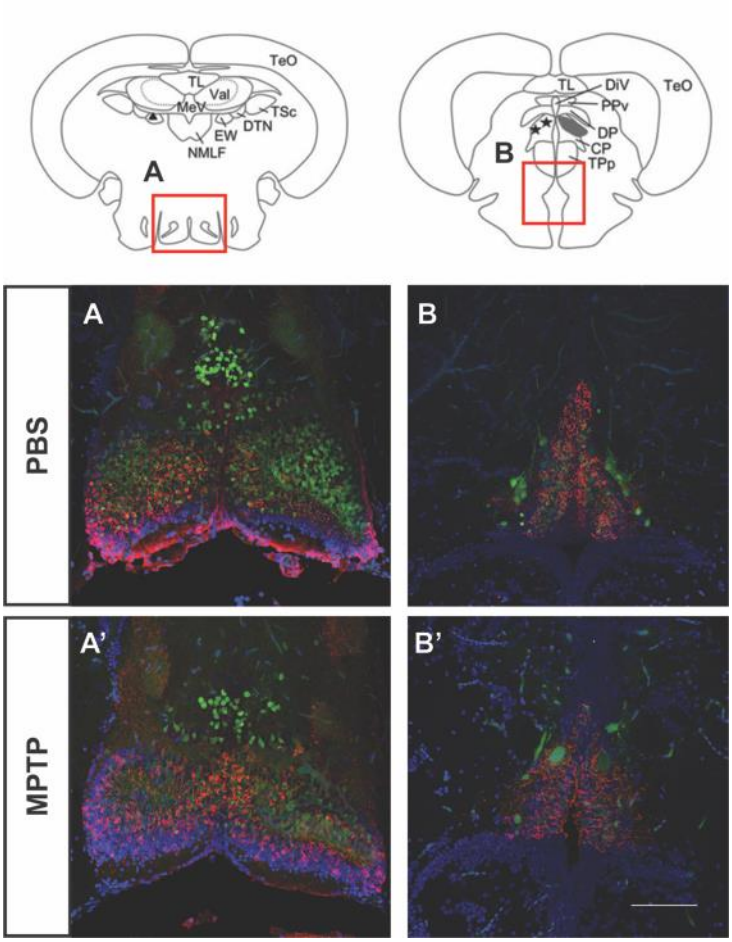

Figure A.2. MPTP does not impact serotonin dense nuclei in the adult zebrafish brain. Coronal cryosections were used to label serotonin+ cells within the A) hypothalamic and B) posterior tuberculum regions of the brain. A-B) PBS-treated control. A'-B') MPTP-treated zebrafish ($n = 2$). (Scale bar = 100 μm)

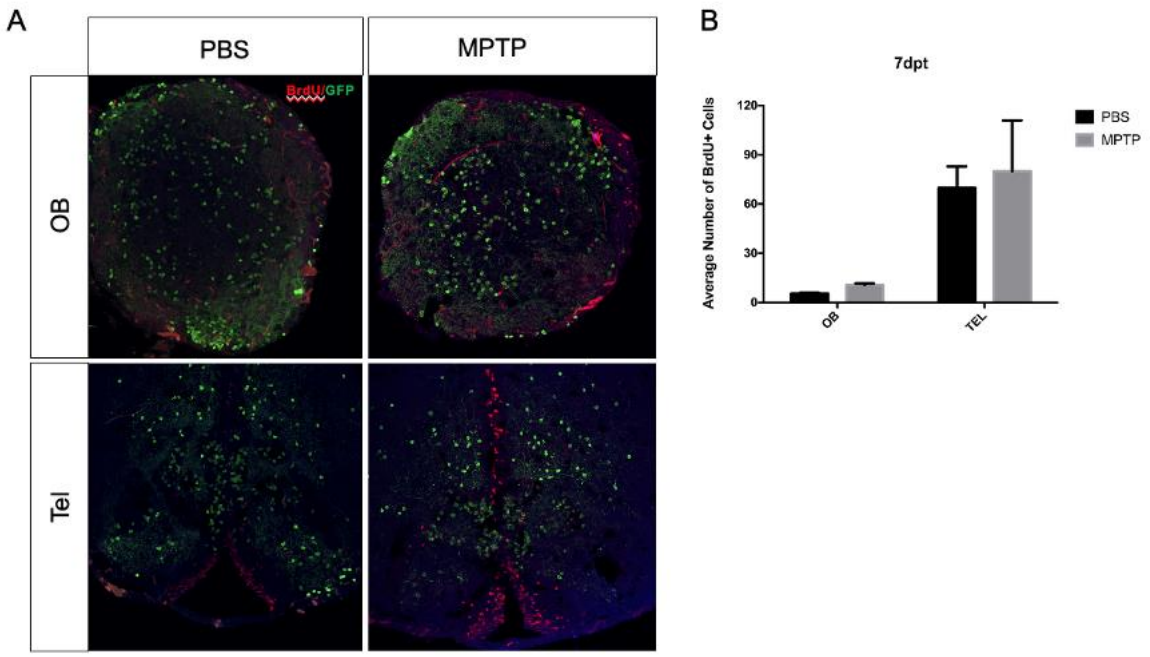

Figure A.3. Neurogenesis in the forebrain following MPTP-injections in adult zebrafish. A) IHC of BrdU (red) and GFP (green) in the olfactory bulbs (OB) and telencephalon (Tel). B) Quantification of BrdU+ in each region. Bars ± the SEM.

APPENDIX B: LIST OF CONTRIBUTIONS

B.1. Contributions to additional publications

B1.1. Godoy, R., Hua, K., **Kalyn, M.**, Cusson, V-M., Anisman, H., Ekker, M. Dopaminergic neurons regenerate following chemogenetic ablation in the olfactory bulb of adult Zebrafish (*Danio rerio*). *Scientific Reports* 10, 12825. (2020). https://doi.org/10.1038/s41598-020-69734-0.

- I collected and analyzed all behavioral data.
- I generated the figure for publication and critically proof-read the manuscript.

B1.2. Merhi, R., **Kalyn, M.**, Zhu-Pawlowsky, A., Ekker, M. Loss of *parla* Function Results in Inactivity, Olfactory Impairment, and Dopamine Neuron Loss in Zebrafish. *Biomedicines 9*, 205. (2021). https://doi.org/10.3390/biomedicines9020205.

- I performed the immunohistochemistry, confocal imaging and collected behavioral data
- I critically proof-read the manuscript for publication.

B.2. Unpublished

B2.1. Kalyn, M., Curry, J., Mennigen, J., Lee, H., Ekker, M. "Deleterious effects of PFOS, OBS and F53B on dopaminergic health, metabolism and behavior using zebrafish (*Danio rerio*)"

- I am first author of the study.
- Dr. Jan Mennigen and I conceptualized the study

- I performed exposure gradient experiments, RNA extraction, qRT-PCR, whole-mount immunohistochemistry, confocal imaging and collected the behavioral data for analysis.

REFERENCES

Abbate, A., P. L. Almasio, M. Mongitore, G. Di Vita, and R. Patti. 2018. Necrotizing Soft Tissue Fasciitis after Intramuscular Injection. Case Rep. Surg. 2018:3945497. Hindawi.

Abdollahi, M., and M. Fahnestock. 2022. Nurr1 Is Not an Essential Regulator of BDNF in Mouse Cortical Neurons. Int. J. Mol. Sci. 23:6853. MDPI.

Abi-Dargham, A. B. T.-I. R. of N. 2007. Alterations of Serotonin Transmission in Schizophrenia. Pp. 133–164 *in* Integrating the Neurobiology of Schizophrenia. Academic Press.

Abu-Hijleh, M. F., O. A. Habbal, and S. T. Moqattash. 1995. The role of the diaphragm in lymphatic absorption from the peritoneal cavity. J. Anat. 186 (Pt 3:453–467.

Adinoff, B. 2004. Neurobiologic processes in drug reward and addiction. Harv. Rev. Psychiatry 12:305–320.

Airavaara, M., B. K. Harvey, M. H. Voutilainen, H. Shen, J. Chou, P. Lindholm, M. Lindahl, R. K. Tuominen, M. Saarma, B. Hoffer, and Y. Wang. 2012. CDNF Protects the Nigrostriatal Dopamine System and Promotes Recovery after MPTP Treatment in Mice. Cell Transplant. 21:1213–1223. SAGE Publications Inc.

Ali, S., D. L. Champagne, H. P. Spaink, and M. K. Richardson. 2011. Zebrafish embryos and larvae: A new generation of disease models and drug screens. Birth Defects Res. Part C Embryo Today Rev. 93:115–133. John Wiley & Sons, Ltd.

Amalric, M., and G. F. Koob. 1987. Depletion of dopamine in the caudate nucleus but not in nucleus accumbens impairs reaction-time performance in rats. J. Neurosci. 7:2129–2134. Soc Neuroscience.

Ang, S.-L. 2006. Transcriptional control of midbrain dopaminergic neuron development. Oxford

University Press for The Company of Biologists Limited.

Anichtchik, O., H. Diekmann, A. Fleming, A. Roach, P. Goldsmith, and D. C. Rubinsztein. 2008. Loss of PINK1 function affects development and results in neurodegeneration in zebrafish. J. Neurosci. 28:8199–8207. Soc Neuroscience.

Anichtchik, O. V, J. Kaslin, N. Peitsaro, M. Scheinin, and P. Panula. 2004. Neurochemical and behavioural changes in zebrafish Danio rerio after systemic administration of 6-hydroxydopamine and 1-methyl-4-phenyl-1,2,3,6-tetrahydropyridine. J. Neurochem. 88:443–453. John Wiley & Sons, Ltd.

Anis, E., M. F. Zafeer, F. Firdaus, S. N. Islam, A. Anees Khan, A. Ali, and M. M. Hossain. 2020. Ferulic acid reinstates mitochondrial dynamics through PGC1α expression modulation in 6-hydroxydopamine lesioned rats. Phyther. Res. 34:214–226. John Wiley & Sons, Ltd.

Aoyama-Ishiwatari, S., and Y. Hirabayashi. 2021. Endoplasmic Reticulum–Mitochondria Contact Sites—Emerging Intracellular Signaling Hubs. Front. Cell Dev. Biol. 1040. Frontiers.

Arias-Carrión, O., M. Stamelou, E. Murillo-Rodríguez, M. Menéndez-González, and E. Pöppel. 2010. Dopaminergic reward system: a short integrative review. Int. Arch. Med. 3:24. BioMed Central.

Arrigoni, O., and M. C. De Tullio. 2002. Ascorbic acid: much more than just an antioxidant. Biochim. Biophys. Acta - Gen. Subj. 1569:1–9.

Aryal, B., and Y. Lee. 2019. Disease model organism for Parkinson disease: Drosophila melanogaster. BMB Rep. 52:250–258.

Arzuaga, X., and A. Elskus. 2010. Polluted-site killifish (Fundulus heteroclitus) embryos are resistant to organic pollutant-mediated induction of CYP1A activity, reactive oxygen

species, and heart deformities. Environ. Toxicol. Chem. An Int. J. 29:676–682. Wiley Online Library.

Ashraf, S., H. Taegtmeyer, and R. Harmancey. 2022. Prolonged cardiac NR4A2 activation causes dilated cardiomyopathy in mice. Basic Res. Cardiol. 117:33.

Ay, M. 2022. Vanillic acid induces mitochondrial biogenesis in SH-SY5Y cells. Mol. Biol. Rep. 49:4443–4449.

Ayano, G. 2016. Dopamine: receptors, functions, synthesis, pathways, locations and mental disorders: review of literatures. J Ment Disord Treat 2:2.

Bäckman, C., T. Perlmann, Å. Wallén, B. J. Hoffer, and M. Morales. 1999. A selective group of dopaminergic neurons express Nurr1 in the adult mouse brain. Brain Res. 851:125–132. Elsevier.

Baker, B., U. Maitra, S. Geng, and L. Li. 2014. Molecular and cellular mechanisms responsible for cellular stress and low-grade inflammation induced by a super-low dose of endotoxin. J. Biol. Chem. 289:16262–16269. American Society for Biochemistry and Molecular Biology.

Baliga, B., and S. Kumar. 2003. Apaf-1/cytochrome c apoptosome: an essential initiatorof caspase activation or just a sideshow? Cell Death Differ. 10:16–18.

Ban, T., T. Ishihara, H. Kohno, S. Saita, A. Ichimura, K. Maenaka, T. Oka, K. Mihara, and N. Ishihara. 2017. Molecular basis of selective mitochondrial fusion by heterotypic action between OPA1 and cardiolipin. Nat. Cell Biol. 19:856–863. Nature Publishing Group.

Barbeau, A., L. Dallaire, N. T. Buu, J. Poirier, and E. Rucinska. 1985. Comparative behavioral, biochemical and pigmentary effects of MPTP, MPP+ and paraquat in rana pipiens. Life Sci. 37:1529–1538.

Barneda-Zahonero, B., J.-M. Servitja, N. Badiola, A. J. Miñano-Molina, R. Fadó, C. A. Saura,

and J. Rodríguez-Alvarez. 2012. Nurr1 Protein Is Required for N-Methyl-d-aspartic Acid (NMDA) Receptor-mediated Neuronal Survival *. J. Biol. Chem. 287:11351–11362. Elsevier.

Barreto-Valer, K., R. López-Bellido, F. Macho Sánchez-Simón, and R. E. Rodríguez. 2012. Modulation by Cocaine of Dopamine Receptors through miRNA-133b in Zebrafish Embryos. PLoS One 7:e52701. Public Library of Science.

Barrios, J. P., W. C. Wang, R. England, E. Reifenberg, and A. D. Douglass. 2020. Hypothalamic Dopamine Neurons Control Sensorimotor Behavior by Modulating Brainstem Premotor Nuclei in Zebrafish. Curr. Biol. 1–13. Elsevier Ltd.

Bartel, W. P., V. S. Van Laar, and E. A. Burton. 2020. Chapter 23 - Parkinson's disease. Pp. 377–412 *in* R. T. B. T.-B. and N. G. of Z. Gerlai, ed. Academic Press.

Best, J. D., and W. K. Alderton. 2008a. Zebra fish : An in vivo model for the study of neurological diseases. 4:567–576.

Best, J. D., and W. K. Alderton. 2008b. Zebrafish: An in vivo model for the study of neurological diseases. Neuropsychiatr. Dis. Treat. 4:567–576. Dove Medical Press.

Betarbet, R., T. B. Sherer, G. MacKenzie, M. Garcia-Osuna, A. V Panov, and J. T. Greenamyre. 2000. Chronic systemic pesticide exposure reproduces features of Parkinson's disease. Nat. Neurosci. 3:1301–1306.

Bhurtel, S., N. Katila, S. Srivastav, S. Neupane, and D.-Y. Choi. 2019. Mechanistic comparison between MPTP and rotenone neurotoxicity in mice. Neurotoxicology 71:113–121.

Billingsley, K. J., S. Bandres-Ciga, S. Saez-Atienzar, and A. B. Singleton. 2018. Genetic risk factors in Parkinson's disease. Cell Tissue Res. 373:9–20.

Birling, M.-C., Y. Herault, and G. Pavlovic. 2017. Modeling human disease in rodents by

CRISPR/Cas9 genome editing. Mamm. Genome 28:291–301.

Bishop, T., and M. D. Brand. 2000. Processes contributing to metabolic depression in hepatopancreas cells from the snail Helix aspersa. J. Exp. Biol. 203:3603–3612. Company of Biologists The Company of Biologists, Bidder Building, 140 Cowley ….

Blaess, S., S. R. W. Stott, and S.-L. Ang. 2020. Chapter 17 - The generation of midbrain dopaminergic neurons. Pp. 369–398 *in* J. Rubenstein, P. Rakic, B. Chen, and K. Y. B. T.-P. and C. T. S. in the D. C. N. S. and P. N. S. (Second E. Kwan, eds. Academic Press.

Blanco, A. M., J. I. Bertucci, A. Hatef, and S. Unniappan. 2020. Feeding and food availability modulate brain-derived neurotrophic factor, an orexigen with metabolic roles in zebrafish. Sci. Rep. 10:10727.

Blesa, J., S. Phani, V. Jackson-Lewis, and S. Przedborski. 2012. Classic and new animal models of Parkinson's disease. J. Biomed. Biotechnol. 2012:845618. Hindawi Publishing Corporation.

Blin, M., W. Norton, L. Bally-Cuif, and P. Vernier. 2008. NR4A2 controls the differentiation of selective dopaminergic nuclei in the zebrafish brain. Mol. Cell. Neurosci. 39:592–604.

Bonifati, V., P. Rizzu, M. J. van Baren, O. Schaap, G. J. Breedveld, E. Krieger, M. C. J. Dekker, F. Squitieri, P. Ibanez, M. Joosse, J. W. van Dongen, N. Vanacore, J. C. van Swieten, A. Brice, G. Meco, C. M. van Duijn, B. A. Oostra, and P. Heutink. 2003. Mutations in the DJ-1 Gene Associated with Autosomal Recessive Early-Onset Parkinsonism. Sci. 299:256–259.

Bortolotto, J., G. Cognato, R. Rilo Christoff, L. Nery, C. Leite, L. Kist, M. Bogo, M. Vianna, and C. Bonan. 2014. Long-Term Exposure to Paraquat Alters Behavioral Parameters and Dopamine Levels in Adult Zebrafish (Danio Rerio). Zebrafish 11.

Bové, J., and C. Perier. 2012. Neurotoxin-based models of Parkinson's disease. Neuroscience

211:51–76.

Bretaud, S., C. Allen, P. W. Ingham, and O. Bandmann. 2007. p53-dependent neuronal cell death in a DJ-1-deficient zebrafish model of Parkinson's disease. J. Neurochem. 100:1626–1635. John Wiley & Sons, Ltd.

Bretaud, S., S. Lee, and S. Guo. 2004. Sensitivity of zebrafish to environmental toxins implicated in Parkinson's disease. Neurotoxicol. Teratol. 26:857–64.

Brodie, M. S., and T. V Dunwiddie. 1990. Cocaine effects in the ventral tegmental area: evidence for an indirect dopaminergic mechanism of action. Naunyn. Schmiedebergs. Arch. Pharmacol. 342:660–665. Germany.

Broen, M. P. G., N. E. Narayen, M. L. Kuijf, N. N. W. Dissanayaka, and A. F. G. Leentjens. 2016. Prevalence of anxiety in Parkinson's disease: A systematic review and meta-analysis. Mov. Disord. 31:1125–1133. John Wiley & Sons, Ltd.

Bromilow, R. H. 2004. Paraquat and sustainable agriculture. Pest Manag. Sci. 60:340–349. John Wiley & Sons, Ltd.

Broughton, J. P., X. Deng, G. Yu, C. L. Fasching, V. Servellita, J. Singh, X. Miao, J. A. Streithorst, A. Granados, A. Sotomayor-Gonzalez, K. Zorn, A. Gopez, E. Hsu, W. Gu, S. Miller, C.-Y. Pan, H. Guevara, D. A. Wadford, J. S. Chen, and C. Y. Chiu. 2020. CRISPR–Cas12-based detection of SARS-CoV-2. Nat. Biotechnol. 38:870–874.

Brown, S. J., I. Boussaad, J. Jarazo, J. C. Fitzgerald, P. Antony, M. Keatinge, J. Blechman, J. C. Schwamborn, R. Krüger, M. Placzek, and O. Bandmann. 2021. PINK1 deficiency impairs adult neurogenesis of dopaminergic neurons. Sci. Rep. 11:6617.

Burré, J., M. Sharma, T. Tsetsenis, V. Buchman, M. R. Etherton, and T. C. Südhof. 2010. α-Synuclein promotes SNARE-complex assembly in vivo and in vitro. Science (80-.).

329:1663–1667. American Association for the Advancement of Science.

Cabezas, R., M. Fidel, D. Torrente, R. Santos El-Bach, L. Morales, J. Gonzalez, and G. E. 2013. Astrocytes Role in Parkinson: A Double-Edged Sword. P. *in* Neurodegenerative Diseases.

Cameron, H. A., and R. D. G. Mckay. 2001. Adult neurogenesis produces a large pool of new granule cells in the dentate gyrus. J. Comp. Neurol. 435:406–417. Wiley Online Library.

Cankaya, S., B. Cankaya, U. Kilic, E. Kilic, and B. Yulug. 2019. The therapeutic role of minocycline in Parkinson's disease. Drugs Context 8:212553.

Cannon, J. R., V. Tapias, H. M. Na, A. S. Honick, R. E. Drolet, and J. T. Greenamyre. 2009. A highly reproducible rotenone model of Parkinson's disease. Neurobiol. Dis. 34:279–290. Elsevier.

Carballo, G. B., J. R. Honorato, G. P. F. de Lopes, and T. C. L. de S. e Spohr. 2018. A highlight on Sonic hedgehog pathway. Cell Commun. Signal. 16:1. BioMed Central.

Casarejos, M. J., S. Canals, S. De Bernardo, M. A. Mena, and E. Rodrı. 2002. Thiolic antioxidants protect from nitric oxide-induced toxicity in fetal midbrain cultures. 43:877–888.

Cassar, S., I. Adatto, J. L. Freeman, J. T. Gamse, I. Iturria, C. Lawrence, A. Muriana, R. T. Peterson, S. Van Cruchten, and L. I. Zon. 2020. Use of Zebrafish in Drug Discovery Toxicology. Chem. Res. Toxicol. 33:95–118.

Chartier-Harlin, M.-C., J. Kachergus, C. Roumier, V. Mouroux, X. Douay, S. Lincoln, C. Levecque, L. Larvor, J. Andrieux, M. Hulihan, N. Waucquier, L. Defebvre, P. Amouyel, M. Farrer, and A. Destée. 2004. α-synuclein locus duplication as a cause of familial Parkinson's disease. Lancet 364:1167–1169.

Chaudhuri, K. R., and A. H. V Schapira. 2009. Non-motor symptoms of Parkinson's disease:

dopaminergic pathophysiology and treatment. Lancet Neurol. 8:464–474.

Chaudhury, D., J. J. Walsh, A. K. Friedman, B. Juarez, S. M. Ku, J. W. Koo, D. Ferguson, H.-C. Tsai, L. Pomeranz, D. J. Christoffel, A. R. Nectow, M. Ekstrand, A. Domingos, M. S. Mazei-Robison, E. Mouzon, M. K. Lobo, R. L. Neve, J. M. Friedman, S. J. Russo, K. Deisseroth, E. J. Nestler, and M.-H. Han. 2013. Rapid regulation of depression-related behaviours by control of midbrain dopamine neurons. Nature 493:532–536.

Chen, H., S. A. Detmer, A. J. Ewald, E. E. Griffin, S. E. Fraser, and D. C. Chan. 2003. Mitofusins Mfn1 and Mfn2 coordinately regulate mitochondrial fusion and are essential for embryonic development. J. Cell Biol. 160:189–200.

Chen, Y.-C., D. Baronio, S. Semenova, S. Abdurakhmanova, and P. Panula. 2020. Cerebral Dopamine Neurotrophic Factor Regulates Multiple Neuronal Subtypes and Behavior. J. Neurosci. Off. J. Soc. Neurosci. 40:6146–6164.

Chen, Y.-C., S. Semenova, S. Rozov, M. Sundvik, J. L. Bonkowsky, and P. Panula. 2016. A Novel Developmental Role for Dopaminergic Signaling to Specify Hypothalamic Neurotransmitter Identity. J. Biol. Chem. 291:21880–21892. American Society for Biochemistry and Molecular Biology.

Chen, Y.-C., M. Sundvik, S. Rozov, M. Priyadarshini, and P. Panula. 2012. MANF regulates dopaminergic neuron development in larval zebrafish. Dev. Biol. 370:237–249.

Cheng, C.-Y., T.-Y. Ho, E.-J. Lee, S.-Y. Su, N.-Y. Tang, and C.-L. Hsieh. 2008. Ferulic acid reduces cerebral infarct through its antioxidative and anti-inflammatory effects following transient focal cerebral ischemia in rats. Am. J. Chin. Med. 36:1105–1119. World Scientific.

Cheng, H.-C., C. M. Ulane, and R. E. Burke. 2010. Clinical progression in Parkinson disease and

the neurobiology of axons. Ann. Neurol. 67:715–725.

Chinta, S. J., and J. K. Andersen. 2005. Dopaminergic neurons. Int. J. Biochem. Cell Biol. 37:942–946.

Cho, J.-Y., H.-S. Kim, D.-H. Kim, J.-J. Yan, H.-W. Suh, and D.-K. Song. 2005. Inhibitory effects of long-term administration of ferulic acid on astrocyte activation induced by intracerebroventricular injection of β-amyloid peptide (1–42) in mice. Prog. Neuro-Psychopharmacology Biol. Psychiatry 29:901–907. Elsevier.

Choi-Lundberg, D. L., Q. Lin, Y.-N. Chang, Y. L. Chiang, C. M. Hay, H. Mohajeri, B. L. Davidson, and M. C. Bohn. 1997. Dopaminergic neurons protected from degeneration by GDNF gene therapy. Science (80-.). 275:838–841. American Association for the Advancement of Science.

Choi, J.-H., E. R. Duboue, M. Macurak, J.-M. Chanchu, and M. E. Halpern. 2021. Specialized neurons in the right habenula mediate response to aversive olfactory cues. Elife 10:e72345. eLife Sciences Publications, Ltd.

Cicchetti, F., N. Lapointe, A. Roberge-Tremblay, M. Saint-Pierre, L. Jimenez, B. W. Ficke, and R. E. Gross. 2005. Systemic exposure to paraquat and maneb models early Parkinson's disease in young adult rats. Neurobiol. Dis. 20:360–371. United States.

Collins, A. L., T. J. Aitken, V. Y. Greenfield, S. B. Ostlund, and K. M. Wassum. 2016. Nucleus Accumbens Acetylcholine Receptors Modulate Dopamine and Motivation. Neuropsychopharmacol. Off. Publ. Am. Coll. Neuropsychopharmacol. 41:2830–2838.

Contreras, L., I. Drago, E. Zampese, and T. Pozzan. 2010. Mitochondria: The calcium connection. Biochim. Biophys. Acta - Bioenerg. 1797:607–618.

Coulom, H., and S. Birman. 2004. Chronic Exposure to Rotenone Models Sporadic

Parkinson's Disease in Drosophila melanogaster J. Neurosci. 24:10993 LP – 10998.

Covarrubias-Pinto, A., A. I. Acuña, F. A. Beltrán, L. Torres-Díaz, and M. A. Castro. 2015. Old Things New View: Ascorbic Acid Protects the Brain in Neurodegenerative Disorders. Int. J. Mol. Sci. 16:28194–28217.

Crews, L., H. Mizuno, P. Desplats, E. Rockenstein, A. Adame, C. Patrick, B. Winner, J. Winkler, and E. Masliah. 2008. α-Synuclein Alters Notch-1 Expression and Neurogenesis in Mouse Embryonic Stem Cells and in the Hippocampus of Transgenic Mice. J. Neurosci. 28:4250 LP – 4260.

Cummings, J. L. 1991. Behavioral Complications of Drug Treatment of Parkinson's Disease. J. Am. Geriatr. Soc. 39:708–716. John Wiley & Sons, Ltd.

D'Agostino, Y., E. Frigato, T. M. R. Noviello, M. Toni, F. Frabetti, L. Cigliano, M. Ceccarelli, P. Sordino, L. Cerulo, C. Bertolucci, and S. D'Aniello. 2022. Loss of circadian rhythmicity in bdnf knockout zebrafish larvae. iScience 25:104054.

D'Costa, A., and I. T. Shepherd. 2009. Zebrafish development and genetics: introducing undergraduates to developmental biology and genetics in a large introductory laboratory class. Zebrafish 6:169–177.

Danial, N. N., and S. J. Korsmeyer. 2004. Cell Death: Critical Control Points. Cell 116:205–219.

Daubner, S. C., T. Le, and S. Wang. 2011. Tyrosine hydroxylase and regulation of dopamine synthesis. Arch. Biochem. Biophys. 508:1–12.

Dauer, W., and S. Przedborski. 2003. Parkinson's Disease: Mechanisms and Models. Neuron 39:889–909.

Dawson, T. M., and V. L. Dawson. 2010. The role of parkin in familial and sporadic Parkinson's

disease. Mov. Disord. 25 Suppl 1:S32–S39.

de Juan Romero, C., I. Reillo, V. Borrell, and M. Á. García-Cabezas. 2010. A Role for Intermediate Radial Glia in the Tangential Expansion of the Mammalian Cerebral Cortex. Cereb. Cortex 21:1674–1694.

de Lau, L. M. L., and M. M. B. Breteler. 2006. Epidemiology of Parkinson's disease. Lancet Neurol. 5:525–535.

De Rienzo, G., J. A. Bishop, Y. Mao, L. Pan, T. P. Ma, C. B. Moens, L. Tsai, and H. Sive. 2011. Disc1 regulates both β-catenin-mediated and noncanonical Wnt signaling during vertebrate embryogenesis. FASEB J. 25:4184–4197. Wiley Online Library.

Decressac, M., B. Mattsson, M. Lundblad, P. Weikop, and A. Björklund. 2012. Progressive neurodegenerative and behavioural changes induced by AAV-mediated overexpression of α-synuclein in midbrain dopamine neurons. Neurobiol. Dis. 45:939–953. Elsevier.

DeMaagd, G., and A. Philip. 2015. Parkinson's Disease and Its Management: Part 1: Disease Entity, Risk Factors, Pathophysiology, Clinical Presentation, and Diagnosis. Pharm. Ther. 40:504–532. MediMedia USA, Inc.

Dexter, D. T., and P. Jenner. 2013. Parkinson disease: from pathology to molecular disease mechanisms. Free Radic. Biol. Med. 62:132–144.

Dhillon, A. S., G. L. Tarbutton, J. L. Levin, G. M. Plotkin, L. K. Lowry, J. T. Nalbone, and S. Shepherd. 2008. Pesticide/Environmental Exposures and Parkinson's Disease in East Texas. J. Agromedicine 13:37–48. Taylor & Francis.

Di Fonzo, A., C. Tassorelli, M. De Mari, H. F. Chien, J. Ferreira, C. F. Rohe, G. Riboldazzi, A. Antonini, G. Albani, A. Mauro, R. Marconi, G. Abbruzzese, L. Lopiano, E. Fincati, M. Guidi, P. Marini, F. Stocchi, M. Onofrj, V. Toni, M. Tinazzi, G. Fabbrini, P. Lamberti, N.

Vanacore, G. Meco, P. Leitner, R. J. Uitti, Z. K. Wszolek, T. Gasser, E. J. Simons, G. J. Breedveld, S. Goldwurm, G. Pezzoli, C. Sampaio, E. Barbosa, E. Martignoni, B. A. Oostra, and V. Bonifati. 2005. Comprehensive analysis of the LRRK2 gene in sixty families with Parkinson's disease. Eur J Hum Genet 14:322–331.

Di Fonzo, A., C. Tassorelli, M. De Mari, H. F. Chien, J. Ferreira, C. F. Rohé, G. Riboldazzi, A. Antonini, G. Albani, A. Mauro, R. Marconi, G. Abbruzzese, L. Lopiano, E. Fincati, M. Guidi, P. Marini, F. Stocchi, M. Onofrj, V. Toni, M. Tinazzi, G. Fabbrini, P. Lamberti, N. Vanacore, G. Meco, P. Leitner, R. J. Uitti, Z. K. Wszolek, T. Gasser, E. J. Simons, G. J. Breedveld, S. Goldwurm, G. Pezzoli, C. Sampaio, E. Barbosa, E. Martignoni, B. A. Oostra, V. Bonifati, and T. I. P. G. Network. 2006. Comprehensive analysis of the LRRK2 gene in sixty families with Parkinson's disease. Eur. J. Hum. Genet. 14:322–331.

Díaz-Casado, M. E., E. Lima, J. A. García, C. Doerrier, P. Aranda, R. K. Sayed, A. Guerra-Librero, G. Escames, L. C. López, and D. Acuña-Castroviejo. 2016. Melatonin rescues zebrafish embryos from the parkinsonian phenotype restoring the parkin/PINK1/DJ-1/MUL1 network. J. Pineal Res. 61:96–107. England.

Ding, W.-X., and X.-M. Yin. 2012. Mitophagy: mechanisms, pathophysiological roles, and analysis. Biol. Chem. 393:547–564.

Dowd, F. J. 2017. Pharmacokinetics: The Absorption, Distribution, and Fate of Drugs. Seventh Ed. Elsevier Inc.

Doyle, J. M., and R. P. Croll. 2022. A Critical Review of Zebrafish Models of Parkinson's Disease. Front. Pharmacol. 13:835827.

Du, Y., Q. Guo, M. Shan, Y. Wu, S. Huang, H. Zhao, H. Hong, M. Yang, X. Yang, L. Ren, J. Peng, J. Sun, H. Zhou, S. Li, and B. Su. 2016. Spatial and Temporal Distribution of

Dopaminergic Neurons during Development in Zebrafish. Front. Neuroanat. 10:115. Frontiers Media S.A.

Duff, K., J. S. Paulsen, L. J. Beglinger, D. R. Langbehn, and J. C. Stout. 2007. Psychiatric Symptoms in Huntington’s Disease before Diagnosis: The Predict-HD Study. Biol. Psychiatry 62:1341–1346. Elsevier.

Dukes, A. A., Q. Bai, V. S. Van Laar, Y. Zhou, V. Ilin, C. N. David, Z. S. Agim, J. L. Bonkowsky, J. R. Cannon, S. C. Watkins, C. M. S. Croix, E. A. Burton, and S. B. Berman. 2016. Live imaging of mitochondrial dynamics in CNS dopaminergic neurons in vivo demonstrates early reversal of mitochondrial transport following MPP(+) exposure. Neurobiol. Dis. 95:238–249.

Dunlop, B. W., and C. B. Nemeroff. 2007. The role of dopamine in the pathophysiology of depression. Arch. Gen. Psychiatry 64:327–337. American Medical Association.

E Moore, K., and S. M Wuerthele. 1979. Regulation of nigrostriatal and tuberoinfundibular hypophyseal dopamine neurons.

Edson, A. J., H. A. Hushagen, A. K. Frøyset, I. Elda, E. A. Khan, A. Di Stefano, and K. E. Fladmark. 2019. Dysregulation in the Brain Protein Profile of Zebrafish Lacking the Parkinson’s Disease-Related Protein DJ-1. Mol. Neurobiol. 56:8306–8322.

Elsworth, J. D., and R. H. Roth. 1997. Dopamine Synthesis, Uptake, Metabolism, and Receptors: Relevance to Gene Therapy of Parkinson’s Disease. Exp. Neurol. 144:4–9.

Espinet, S. D., G. Graziosi, M. E. Toplak, J. Hesson, and P. Minhas. 2022. A Review of Canadian Diagnosed ADHD Prevalence and Incidence Estimates Published in the Past Decade. Brain Sci. 12.

Farrell, T. C., C. L. Cario, C. Milanese, A. Vogt, J.-H. Jeong, and E. A. Burton. 2011. Evaluation

of spontaneous propulsive movement as a screening tool to detect rescue of Parkinsonism phenotypes in zebrafish models. Neurobiol. Dis. 44:9–18.

Fei, Q., A. L. McCormack, D. A. Di Monte, and D. W. Ethell. 2008. Paraquat neurotoxicity is mediated by a Bak-dependent mechanism. J. Biol. Chem. 283:3357–3364. ASBMB.

Feng, C.-W., Z.-H. Wen, S.-Y. Huang, H.-C. Hung, C.-H. Chen, S.-N. Yang, N.-F. Chen, H.-M. Wang, C.-D. Hsiao, and W.-F. Chen. 2014. Effects of 6-hydroxydopamine exposure on motor activity and biochemical expression in zebrafish (Danio rerio) larvae. Zebrafish 11:227–239. Mary Ann Liebert, Inc.

Feng, C., and C. Chen. 2014. Effects of 6-Hydroxydopamine Exposure on Motor Activity and Biochemical Expression in Zebrafish (Danio Rerio) Larvae. 11.

Ferretti, L., S. M. McCurry, R. Logsdon, L. Gibbons, and L. Teri. 2001. Anxiety and Alzheimer's disease. J. Geriatr. Psychiatry Neurol. 14:52–58. Sage Publications Sage CA: Thousand Oaks, CA.

Filippi, A., K. Dürr, S. Ryu, M. Willaredt, J. Holzschuh, and W. Driever. 2007. Expression and function of nr4a2, lmx1b, and pitx3 in zebrafish dopaminergic and noradrenergic neuronal development. BMC Dev. Biol. 7:135.

Fitzgerald, P., and T. G Dinan. 2008. Prolactin and dopamine: What is the connection? A Review Article.

Fleming, A., H. Diekmann, and P. Goldsmith. 2013. Functional characterisation of the maturation of the blood-brain barrier in larval zebrafish. PLoS One 8:e77548–e77548. Public Library of Science.

Flinn, L., S. Bretaud, C. Lo, P. W. Ingham, and O. Bandmann. 2008. Zebrafish as a new animal model for movement disorders. J. Neurochem. 106:1991–1997. John Wiley & Sons, Ltd.

Flinn, L., M. Keatinge, S. Bretaud, H. Mortiboys, H. Matsui, E. De Felice, H. Woodroof, L. Brown, A. McTighe, R. Soellner, C. Allen, P. Heath, M. Milo, M. Muqit, A. Reichert, R. Köster, P. Ingham, and O. Bandmann. 2013. TigarB Causes Mitochondrial Dysfunction and Neuronal Loss in PINK1 Deficiency. Ann. Neurol. 74.

Flinn, L., H. Mortiboys, K. Volkmann, R. W. Köster, P. W. Ingham, and O. Bandmann. 2009. Complex I deficiency and dopaminergic neuronal cell loss in parkin-deficient zebrafish (Danio rerio). Brain 132:1613–1623. Oxford University Press.

Fornai, F., O. M. Schlüter, P. Lenzi, M. Gesi, R. Ruffoli, M. Ferrucci, G. Lazzeri, C. L. Busceti, F. Pontarelli, and G. Battaglia. 2005. Parkinson-like syndrome induced by continuous MPTP infusion: convergent roles of the ubiquitin-proteasome system and α-synuclein. Proc. Natl. Acad. Sci. 102:3413–3418. National Acad Sciences.

Forno, L. S., J. W. Langston, L. E. DeLanney, I. Irwin, and G. A. Ricaurte. 1986. Locus ceruleus lesions and eosinophilic inclusions in MPTP-treated monkeys. Ann. Neurol. Off. J. Am. Neurol. Assoc. Child Neurol. Soc. 20:449–455. Wiley Online Library.

Fraga, D. B., A. P. Costa, G. Olescowicz, A. Camargo, F. L. Pazini, A. E. Freitas, M. Moretti, P. S. Brocardo, and A. L. S. Rodrigues. 2020. Ascorbic acid presents rapid behavioral and hippocampal synaptic plasticity effects. Prog. Neuro-Psychopharmacology Biol. Psychiatry 96:109757. Elsevier.

Fulceri, F., F. Biagioni, P. Lenzi, A. Falleni, M. Gesi, S. Ruggieri, and F. Fornai. 2006. Nigrostriatal Damage with 6-OHDA: Validation of Routinely Applied Procedures. Ann. N. Y. Acad. Sci. 1074:344–348. Wiley Online Library.

Funayama, M., K. Hasegawa, H. Kowa, M. Saito, S. Tsuji, and F. Obata. 2002. A new locus for Parkinson's disease (PARK8) maps to chromosome 12p11.2-q13.1. Ann. Neurol. 51:296–

301. United States.

Gagnon, D., S. Petryszyn, M. G. Sanchez, C. Bories, J. M. Beaulieu, Y. De Koninck, A. Parent, and M. Parent. 2017. Striatal Neurons Expressing D1 and D2 Receptors are Morphologically Distinct and Differently Affected by Dopamine Denervation in Mice. Sci. Rep. 7:41432.

Gahr, M., S. Leitner, L. Fusani, and F. Rybak. 2002. What is the adaptive role of neurogenesis in adult birds? Prog. Brain Res. 138:233–254. Elsevier.

Gao, S., and J. Hu. 2021. Mitochondrial Fusion: The Machineries In and Out. Trends Cell Biol. 31:62–74.

Garcia-Miralles, M., J. Coomaraswamy, K. Haebig, M. C. Herzig, N. Funk, F. Gillardon, M. Maisel, M. Jucker, T. Gasser, and D. Galter. 2015. No dopamine cell loss or changes in cytoskeleton function in transgenic mice expressing physiological levels of wild type or G2019S mutant LRRK2 and in human fibroblasts. PLoS One 10:e0118947. Public Library of Science San Francisco, CA USA.

Gardner, E. L., and C. R. Ashby. 2000. Heterogeneity of the mesotelencephalic dopamine fibers: physiology and pharmacology. Neurosci. Biobehav. Rev. 24:115–118.

Gash, D. M., G. A. Gerhardt, L. H. Bradley, R. Wagner, and J. T. Slevin. 2020. GDNF clinical trials for Parkinson’s disease: a critical human dimension. Cell Tissue Res. 382:65–70. Springer.

Ghaddar, B., L. Lübke, D. Couret, S. Rastegar, and N. Diotel. 2021. Cellular Mechanisms Participating in Brain Repair of Adult Zebrafish and Mammals after Injury.

Gilbert, S. 2000. Developmental Biology. Sixth. Sinauer Associates.

Ginter, E. 1975. Ascorbic acid in cholesterol and bile acid metabolism. Ann. N. Y. Acad. Sci.

258:410–421.

Giros, B., S. El Mestikawy, N. Godinot, K. Zheng, H. Han, T. Yang-Feng, and M. G. Caron. 1992. Cloning, pharmacological characterization, and chromosome assignment of the human dopamine transporter. Mol. Pharmacol. 42:383–390.

Gispert, S., F. Ricciardi, A. Kurz, M. Azizov, H.-H. Hoepken, D. Becker, W. Voos, K. Leuner, W. E. Müller, and A. P. Kudin. 2009. Parkinson phenotype in aged PINK1-deficient mice is accompanied by progressive mitochondrial dysfunction in absence of neurodegeneration. PLoS One 4:e5777. Public Library of Science San Francisco, USA.

Godoy, R., K. Hua, M. Kalyn, V.-M. Cusson, H. Anisman, and M. Ekker. 2020. Dopaminergic neurons regenerate following chemogenetic ablation in the olfactory bulb of adult Zebrafish (Danio rerio). Sci. Rep. 10:12825.

Gómez-Benito, M., N. Granado, P. García-Sanz, A. Michel, M. Dumoulin, and R. Moratalla. 2020. Modeling Parkinson's Disease With the Alpha-Synuclein Protein. Front. Pharmacol. 11:356.

Grandel, H., J. Kaslin, J. Ganz, I. Wenzel, and M. Brand. 2006. Neural stem cells and neurogenesis in the adult zebrafish brain: Origin, proliferation dynamics, migration and cell fate. Dev. Biol. 295:263–277.

Grattan, D. R. 2015. 60 YEARS OF NEUROENDOCRINOLOGY: The hypothalamo-prolactin axis. J. Endocrinol. 226:T101–T122. Bioscientifica Ltd, Bristol, UK.

Gratzner, H. G. 1982. Monoclonal antibody to 5-bromo-and 5-iododeoxyuridine: a new reagent for detection of DNA replication. Science (80-.). 218:474–475. American Association for the Advancement of Science.

Greenamyre, J. T., R. Betarbet, and T. B. Sherer. 2003. The rotenone model of Parkinson's

disease: genes, environment and mitochondria. Parkinsonism Relat. Disord. 9:59–64. Elsevier.

Grimes, D. A., F. Han, M. Panisset, L. Racacho, F. Xiao, R. Zou, K. Westaff, and D. E. Bulman. 2006. Translated mutation in the Nurr1 gene as a cause for Parkinson's disease. Mov. Disord. 21:906–909. John Wiley & Sons, Ltd.

Han, Y.-F., and G.-W. Cao. 2012. Role of nuclear receptor NR4A2 in gastrointestinal inflammation and cancers.

Hare, D. J., P. A. Adlard, P. A. Doble, and D. I. Finkelstein. 2013. Metallobiology of 1-methyl-4-phenyl-1,2,3,6-tetrahydropyridine neurotoxicity. Metallomics 5:91–109. The Royal Society of Chemistry.

Hatano, Y., Y. Li, K. Sato, S. Asakawa, Y. Yamamura, H. Tomiyama, H. Yoshino, M. Asahina, S. Kobayashi, S. Hassin-Baer, C.-S. Lu, A. R. Ng, R. L. Rosales, N. Shimizu, T. Toda, Y. Mizuno, and N. Hattori. 2004. Novel PINK1 mutations in early-onset parkinsonism. Ann. Neurol. 56:424–427. United States.

Hauser, T. U., E. Eldar, and R. J. Dolan. 2017. Separate mesocortical and mesolimbic pathways encode effort and reward learning signals. Proc. Natl. Acad. Sci. 114:E7395 LP-E7404.

Hawkes, C. H., K. Del Tredici, and H. Braak. 2009. Parkinson's disease: the dual hit theory revisited. Ann. N. Y. Acad. Sci. 1170:615–622. Wiley Online Library.

Henderson, C. E. 1996. Role of neurotrophic factors in neuronal development. Curr. Opin. Neurobiol. 6:64–70. Elsevier.

Hodson, D. J., M. Schaeffer, N. Romanò, P. Fontanaud, C. Lafont, J. Birkenstock, F. Molino, H. Christian, J. Lockey, and D. Carmignac. 2012. Existence of long-lasting experience-dependent plasticity in endocrine cell networks. Nat. Commun. 3:1–10. Nature Publishing

Group.

Holla, V. R., H. Wu, Q. Shi, D. G. Menter, and R. N. DuBois. 2011. Nuclear orphan receptor NR4A2 modulates fatty acid oxidation pathways in colorectal cancer. J. Biol. Chem. 286:30003–30009.

Holzschuh, J., S. Ryu, F. Aberger, and W. Driever. 2001a. Dopamine transporter expression distinguishes dopaminergic neurons from other catecholaminergic neurons in the developing zebra ® sh embryo. 101:237–243.

Holzschuh, J., S. Ryu, F. Aberger, and W. Driever. 2001b. Dopamine transporter expression distinguishes dopaminergic neurons from other catecholaminergic neurons in the developing zebrafish embryo. Mech. Dev. 101:237–243.

Hoppins, S., and J. Nunnari. 2009. The molecular mechanism of mitochondrial fusion. Biochim. Biophys. Acta - Mol. Cell Res. 1793:20–26.

Howe, K., M. D. Clark, C. F. Torroja, J. Torrance, C. Berthelot, M. Muffato, J. E. Collins, S. Humphray, K. McLaren, L. Matthews, S. McLaren, I. Sealy, M. Caccamo, C. Churcher, C. Scott, J. C. Barrett, R. Koch, G.-J. Rauch, S. White, W. Chow, B. Kilian, L. T. Quintais, J. A. Guerra-Assunção, Y. Zhou, Y. Gu, J. Yen, J.-H. Vogel, T. Eyre, S. Redmond, R. Banerjee, J. Chi, B. Fu, E. Langley, S. F. Maguire, G. K. Laird, D. Lloyd, E. Kenyon, S. Donaldson, H. Sehra, J. Almeida-King, J. Loveland, S. Trevanion, M. Jones, M. Quail, D. Willey, A. Hunt, J. Burton, S. Sims, K. McLay, B. Plumb, J. Davis, C. Clee, K. Oliver, R. Clark, C. Riddle, D. Elliott, G. Threadgold, G. Harden, D. Ware, S. Begum, B. Mortimore, G. Kerry, P. Heath, B. Phillimore, A. Tracey, N. Corby, M. Dunn, C. Johnson, J. Wood, S. Clark, S. Pelan, G. Griffiths, M. Smith, R. Glithero, P. Howden, N. Barker, C. Lloyd, C. Stevens, J. Harley, K. Holt, G. Panagiotidis, J. Lovell, H. Beasley, C. Henderson, D.

Gordon, K. Auger, D. Wright, J. Collins, C. Raisen, L. Dyer, K. Leung, L. Robertson, K. Ambridge, D. Leongamornlert, S. McGuire, R. Gilderthorp, C. Griffiths, D. Manthravadi, S. Nichol, G. Barker, S. Whitehead, M. Kay, J. Brown, C. Murnane, E. Gray, M. Humphries, N. Sycamore, D. Barker, D. Saunders, J. Wallis, A. Babbage, S. Hammond, M. Mashreghi-Mohammadi, L. Barr, S. Martin, P. Wray, A. Ellington, N. Matthews, M. Ellwood, R. Woodmansey, G. Clark, J. D. Cooper, A. Tromans, D. Grafham, C. Skuce, R. Pandian, R. Andrews, E. Harrison, A. Kimberley, J. Garnett, N. Fosker, R. Hall, P. Garner, D. Kelly, C. Bird, S. Palmer, I. Gehring, A. Berger, C. M. Dooley, Z. Ersan-Ürün, C. Eser, H. Geiger, M. Geisler, L. Karotki, A. Kirn, J. Konantz, M. Konantz, M. Oberländer, S. Rudolph-Geiger, M. Teucke, C. Lanz, G. Raddatz, K. Osoegawa, B. Zhu, A. Rapp, S. Widaa, C. Langford, F. Yang, S. C. Schuster, N. P. Carter, J. Harrow, Z. Ning, J. Herrero, S. M. J. Searle, A. Enright, R. Geisler, R. H. A. Plasterk, C. Lee, M. Westerfield, P. J. de Jong, L. I. Zon, J. H. Postlethwait, C. Nüsslein-Volhard, T. J. P. Hubbard, H. R. Crollius, J. Rogers, and D. L. Stemple. 2013. The zebrafish reference genome sequence and its relationship to the human genome. Nature 496:498. The Author(s).

Huang, F., H.-M. Deng, M.-M. Zhu, F. Xiao, L. Yang, and Z.-J. Zhang. 2011. Inhibitory effect of ferulic acid on in? ammatory response in microglia induced by lipopolysaccharides. Zool. Res. 32:311–316. Zoological Research.

Hussain, A., L. R. Saraiva, D. M. Ferrero, G. Ahuja, V. S. Krishna, S. D. Liberles, and S. I. Korsching. 2013. High-affinity olfactory receptor for the death-associated odor cadaverine. Proc. Natl. Acad. Sci. 110:19579 LP – 19584.

Hwang, O. 2013. Role of oxidative stress in Parkinson's disease. Exp. Neurobiol. 22:11. Korean Society for Brain and Neural Science.

Hwang, W. Y., Y. Fu, D. Reyon, M. L. Maeder, S. Q. Tsai, J. D. Sander, R. T. Peterson, J.-R. J. Yeh, and J. K. Joung. 2013. Efficient genome editing in zebrafish using a CRISPR-Cas system. Nat. Biotechnol. 31:227. Nature Publishing Group, a division of Macmillan Publishers Limited. All Rights Reserved.

Hyman, C., M. Hofer, Y.-A. Barde, M. Juhasz, G. D. Yancopoulos, S. P. Squinto, and R. M. Lindsay. 1991. BDNF is a neurotrophic factor for dopaminergic neurons of the substantia nigra. Nature 350:230–232. Nature Publishing Group.

Hynes, M., J. A. Porter, C. Chiang, D. Chang, M. Tessier-Lavigne, P. A. Beachy, and A. Rosenthal. 1995. Induction of midbrain dopaminergic neurons by Sonic hedgehog. Neuron 15:35–44. United States.

J., Y. R., and van der B. A. M. 2012. Mitochondrial Fission, Fusion, and Stress. Science (80-.). 337:1062–1065. American Association for the Advancement of Science.

Jabès, A., P. B. Lavenex, D. G. Amaral, and P. Lavenex. 2010. Quantitative analysis of postnatal neurogenesis and neuron number in the macaque monkey dentate gyrus. Eur. J. Neurosci. 31:273–285. Wiley Online Library.

Jankovic, J. 2008. Parkinson's disease: clinical features and diagnosis. J. Neurol. Neurosurg. & Psychiatry 79:368 LP – 376.

Jankovic, J., S. Chen, and W. D. Le. 2005. The role of Nurr1 in the development of dopaminergic neurons and Parkinson's disease. Prog. Neurobiol. 77:128–138. England.

Jia, C., H. Qi, C. Cheng, X. Wu, Z. Yang, H. Cai, S. Chen, and W. Le. 2020. α-Synuclein Negatively Regulates Nurr1 Expression Through NF-κB-Related Mechanism .

Jiang, C., X. Wan, Y. He, T. Pan, J. Jankovic, and W. Le. 2005. Age-dependent dopaminergic dysfunction in Nurr1 knockout mice. Exp. Neurol. 191:154–162.

Jiang, H., and M. Xiang. 2009. Subtype Specification of GABAergic Amacrine Cells by the Orphan Nuclear Receptor Nr4a2/Nurr1. J. Neurosci. 29:10449 LP – 10459.

Jinek, M., K. Chylinski, I. Fonfara, M. Hauer, J. A. Doudna, and E. Charpentier. 2012. A Programmable Dual-RNA–Guided DNA Endonuclease in Adaptive Bacterial Immunity. Science (80-.). 337:816–821. American Association for the Advancement of Science.

Kacprzak, V., N. A. Patel, E. Riley, L. Yu, J.-R. J. Yeh, and I. V Zhdanova. 2017. Dopaminergic control of anxiety in young and aged zebrafish. Pharmacol. Biochem. Behav. 157:1–8.

Kadkhodaei, B., A. Alvarsson, N. Schintu, D. Ramsköld, N. Volakakis, E. Joodmardi, T. Yoshitake, J. Kehr, M. Decressac, A. Björklund, R. Sandberg, P. Svenningsson, and T. Perlmann. 2013. Transcription factor Nurr1 maintains fiber integrity and nuclear-encoded mitochondrial gene expression in dopamine neurons. Proc. Natl. Acad. Sci. 110:2360 LP – 2365.

Kalyn, M., and M. Ekker. 2021. Cerebroventricular Microinjections of MPTP on Adult Zebrafish Induces Dopaminergic Neuronal Death, Mitochondrial Fragmentation, and Sensorimotor Impairments. Front. Neurosci. 1043. Frontiers.

Kalyn, M., K. Hua, S. Mohd Noor, C. E. D. Wong, and M. Ekker. 2019. Comprehensive Analysis of Neurotoxin-Induced Ablation of Dopaminergic Neurons in Zebrafish Larvae. Biomedicines 8. Switzerland.

Kambey, P. A., K. Kanwore, A. A. Ayanlaja, I. Nadeem, Y. Du, W. Buberwa, W. Liu, and D. Gao. 2021. Failure of Glial Cell-Line Derived Neurotrophic Factor (GDNF) in Clinical Trials Orchestrated By Reduced NR4A2 (NURR1) Transcription Factor in Parkinson's Disease. A Systematic Review .

Kari, G., U. Rodeck, and A. P. Dicker. 2007. Zebrafish: an emerging model system for human

disease and drug discovery. Clin. Pharmacol. Ther. 82:70–80. Wiley Online Library.

Kaslin, J., J. Ganz, and M. Brand. 2008. Proliferation, neurogenesis and regeneration in the non-mammalian vertebrate brain. Philos. Trans. R. Soc. London. Ser. B, Biol. Sci. 363:101–122.

Kastenhuber, E., C. F. Kratochwil, S. Ryu, J. Schweitzer, and W. Driever. 2010. Genetic dissection of dopaminergic and noradrenergic contributions to catecholaminergic tracts in early larval zebrafish. J. Comp. Neurol. 518:439–458. John Wiley & Sons, Ltd.

Kawabata, K., T. Yamamoto, A. Hara, M. Shimizu, Y. Yamada, K. Matsunaga, T. Tanaka, and H. Mori. 2000. Modifying effects of ferulic acid on azoxymethane-induced colon carcinogenesis in F344 rats. Cancer Lett. 157:15–21. Elsevier.

Keane, P. C., M. Kurzawa, P. G. Blain, and C. M. Morris. 2011. Mitochondrial Dysfunction in Parkinson's Disease. Park. Dis. 2011:716871. SAGE-Hindawi Access to Research.

Keow, J. 2016. Physiological and Behavioral Changes in a Rotenone Model of Dopamine Neurotoxicity and Neurodegeneration in Zebrafish.

Khoshnam, S. E., A. Sarkaki, M. Rashno, and Y. Farbood. 2018. Memory deficits and hippocampal inflammation in cerebral hypoperfusion and reperfusion in male rats: Neuroprotective role of vanillic acid. Life Sci. 211:126–132.

Kikugawa, M., H. Tsutsuki, T. Ida, H. Nakajima, H. Ihara, and T. Sakamoto. 2016. Water-soluble ferulic acid derivatives improve amyloid-β-induced neuronal cell death and dysmnesia through inhibition of amyloid-β aggregation. Biosci. Biotechnol. Biochem. 80:547–553. Oxford University Press.

Kim, Y., J. Park, S. Kim, S. Song, S.-K. Kwon, S.-H. Lee, T. Kitada, J.-M. Kim, and J. Chung. 2008. PINK1 controls mitochondrial localization of Parkin through direct phosphorylation.

Biochem. Biophys. Res. Commun. 377:975–980. Elsevier.

Kirik, D., C. Rosenblad, C. Burger, C. Lundberg, T. E. Johansen, N. Muzyczka, R. J. Mandel, and A. Björklund. 2002. Parkinson-like neurodegeneration induced by targeted overexpression of α-synuclein in the nigrostriatal system. J. Neurosci. 22:2780–2791. Soc Neuroscience.

Kitada, T., S. Asakawa, N. Hattori, H. Matsumine, Y. Yamamura, S. Minoshima, M. Yokochi, Y. Mizuno, and N. Shimizu. 1998. Mutations in the parkin gene cause autosomal recessive juvenile parkinsonism. Nature 392:605–608. England.

Kizil, C., and M. Brand. 2011. Cerebroventricular Microinjection (CVMI) into Adult Zebrafish Brain Is an Efficient Misexpression Method for Forebrain Ventricular Cells. PLoS One 6:e27395. Public Library of Science.

Klein, C., and A. Westenberger. 2012. Genetics of Parkinson's disease. Cold Spring Harb. Perspect. Med. 2:a008888–a008888. Cold Spring Harbor Laboratory Press.

Kobayashi, S., F. Zhao, Z. Zhang, T. Kobayashi, Y. Huang, B. Shi, W. Wu, and Q. Liang. 2020. Mitochondrial Fission and Mitophagy Coordinately Restrict High Glucose Toxicity in Cardiomyocytes .

Koh, P. 2013. Ferulic acid prevents cerebral ischemic injury-induced reduction of hippocalcin expression. Synapse 67:390–398. Wiley Online Library.

Korchounov, A. M. 2008. Role of D1 and D2 receptors in the regulation of voluntary movements. Bull. Exp. Biol. Med. 146:14–17. United States.

Korchounov, A., M. F. Meyer, and M. Krasnianski. 2010. Postsynaptic nigrostriatal dopamine receptors and their role in movement regulation. J. Neural Transm. 117:1359–1369.

Korobova, F., V. Ramabhadran, and H. N. Higgs. 2013. An actin-dependent step in

mitochondrial fission mediated by the ER-associated formin INF2. Science 339:464–467.

Kozol, R. A., H. N. Cukier, B. Zou, V. Mayo, S. De Rubeis, G. Cai, A. J. Griswold, P. L. Whitehead, J. L. Haines, and J. R. Gilbert. 2015. Two knockdown models of the autism genes SYNGAP1 and SHANK3 in zebrafish produce similar behavioral phenotypes associated with embryonic disruptions of brain morphogenesis. Hum. Mol. Genet. 24:4006–4023. Oxford University Press.

Krishnan, N., D. Kodrík, B. Kłudkiewicz, and F. Sehnal. 2009. Glutathione–ascorbic acid redox cycle and thioredoxin reductase activity in the digestive tract of Leptinotarsa decemlineata (Say). Insect Biochem. Mol. Biol. 39:180–188.

Kuida, K., T. F. Haydar, C. Y. Kuan, Y. Gu, C. Taya, H. Karasuyama, M. S. Su, P. Rakic, and R. A. Flavell. 1998. Reduced apoptosis and cytochrome c-mediated caspase activation in mice lacking caspase 9. Cell 94:325–337. United States.

Kumar, S., P. Prahalathan, and B. Raja. 2011. Antihypertensive and antioxidant potential of vanillic acid, a phenolic compound in l-NAME-induced hypertensive rats: A dose-dependence study. Redox Rep. 16:208–215. Taylor & Francis.

Lallier, S. W., A. E. Graf, G. R. Waidyarante, and L. K. Rogers. 2016. Nurr1 expression is modified by inflammation in microglia. Neuroreport 27:1120. Wolters Kluwer Health.

Lam, C. S., V. Korzh, and U. Strahle. 2005. SHORT COMMUNICATION Zebrafish embryos are susceptible to the dopaminergic neurotoxin MPTP. 21:1758–1762.

Lanciego, J. L., N. Luquin, and J. A. Obeso. 2012. Functional neuroanatomy of the basal ganglia. Cold Spring Harb. Perspect. Med. 2:a009621–a009621. Cold Spring Harbor Laboratory Press.

Langston, J. W., P. Ballard, J. W. Tetrud, and I. Irwin. 1983. Chronic Parkinsonism in humans

due to a product of meperidine-analog synthesis. Science (80-.). 219:979 LP – 980.

Le, W., O. M. Conneely, Y. He, J. Jankovic, and S. H. Appel. 1999. Reduced Nurr1 expression increases the vulnerability of mesencephalic dopamine neurons to MPTP-induced injury. J. Neurochem. 73:2218–2221. England.

Le, W., P. Xu, J. Jankovic, H. Jiang, S. H. Appel, R. G. Smith, and D. K. Vassilatis. 2003. Mutations in NR4A2 associated with familial Parkinson disease. Nat. Genet. 33:85–89.

Ledonne, A., and N. B. Mercuri. 2017. Current Concepts on the Physiopathological Relevance of Dopaminergic Receptors .

Lee, J. E., L. M. Westrate, H. Wu, C. Page, and G. K. Voeltz. 2016. Multiple dynamin family members collaborate to drive mitochondrial division. Nature 540:139–143.

Levecque, C., A. Destée, V. Mouroux, P. Amouyel, and M.-C. Chartier-Harlin. 2004. Assessment of Nurr1 nucleotide variations in familial Parkinson's disease. Neurosci. Lett. 366:135–138.

Li, P., D. Nijhawan, I. Budihardjo, S. M. Srinivasula, M. Ahmad, E. S. Alnemri, and X. Wang. 1997. Cytochrome c and dATP-Dependent Formation of Apaf-1/Caspase-9 Complex Initiates an Apoptotic Protease Cascade. Cell 91:479–489. Elsevier.

Li, X., J. Zhang, H. Rong, X. Zhang, and M. Dong. 2020. Ferulic Acid Ameliorates MPP+/MPTP-Induced Oxidative Stress via ERK1/2-Dependent Nrf2 Activation: Translational Implications for Parkinson Disease Treatment. Mol. Neurobiol. 57:2981–2995.

Li, Y., W. Liu, T. F. Oo, L. Wang, Y. Tang, V. Jackson-Lewis, C. Zhou, K. Geghman, M. Bogdanov, and S. Przedborski. 2009. Mutant LRRK2R1441G BAC transgenic mice recapitulate cardinal features of Parkinson's disease. Nat. Neurosci. 12:826–828. Nature

Publishing Group.

Liddle, R. A. 2018. Parkinson's disease from the gut. Brain Res. 1693:201–206.

Lidow, M. S. 1995. D1- and D2 dopaminergic receptors in the developing cerebral cortex of macaque monkey: A film autoradiographic study. Neuroscience 65:439–452.

Lima Giacobbo, B., J. Doorduin, H. C. Klein, R. A. J. O. Dierckx, E. Bromberg, and E. F. J. de Vries. 2019. Brain-derived neurotrophic factor in brain disorders: focus on neuroinflammation. Mol. Neurobiol. 56:3295–3312. Springer.

Lin, G., K. Zhang, and J. Li. 2015. Application of CRISPR/Cas9 Technology to HBV.

Lindholm, P., and M. Saarma. 2022. Cerebral dopamine neurotrophic factor protects and repairs dopamine neurons by novel mechanism. Mol. Psychiatry 27:1310–1321.

Liu, B., F. Fang, N. L. Pedersen, A. Tillander, J. F. Ludvigsson, A. Ekbom, P. Svenningsson, H. Chen, and K. Wirdefeldt. 2017. Vagotomy and Parkinson disease: A Swedish register-based matched-cohort study. Neurology 88:1996–2002.

Liu, H., and N. Song. 2016. Molecular Mechanism of Adult Neurogenesis and its Association with Human Brain Diseases. J. Cent. Nerv. Syst. Dis. 8:5–11.

Liu, Y., J.-D. Sun, L.-K. Song, J. Li, S.-F. Chu, Y.-H. Yuan, and N.-H. Chen. 2015. Environment-contact administration of rotenone: A new rodent model of Parkinson's disease. Behav. Brain Res. 294:149–161.

Lo Bianco, C., J. L. Ridet, B. L. Schneider, N. Deglon, and P. Aebischer. 2002. α-Synucleinopathy and selective dopaminergic neuron loss in a rat lentiviral-based model of Parkinson's disease. Proc. Natl. Acad. Sci. 99:10813–10818. National Acad Sciences.

Luo, G. R., Y. Chen, X. P. Li, T. X. Liu, and W. D. Le. 2008. Nr4a2 is essential for the differentiation of dopaminergic neurons during zebrafish embryogenesis. Mol. Cell.

Neurosci. 39:202–210. United States.

M., J. J., X. Zhihua, D. Quinn, E. Lisa, B. Dale, and R. J. C. 1998. Bax directly induces release of cytochrome c from isolated mitochondria. Proc. Natl. Acad. Sci. 95:4997–5002. Proceedings of the National Academy of Sciences.

Magistretti, P. J., and I. Allaman. 1999. Brain energy metabolism. Fundam. Neurosci. 3:271–293. Academic Press San Diego.

Mali, P., L. Yang, K. M. Esvelt, J. Aach, M. Guell, J. E. DiCarlo, J. E. Norville, and G. M. Church. 2013. RNA-Guided Human Genome Engineering via Cas9. Science (80-.). 339:823 LP – 826.

Manfredsson, F. P., N. K. Polinski, T. Subramanian, N. Boulis, D. R. Wakeman, and R. J. Mandel. 2020. The Future of GDNF in Parkinson's Disease .

Manning-Bog, A. B., A. L. McCormack, J. Li, V. N. Uversky, A. L. Fink, and D. A. Di Monte. 2002. The Herbicide Paraquat Causes Up-regulation and Aggregation of α-Synuclein in Mice: PARAQUAT AND α-SYNUCLEIN*. J. Biol. Chem. 277:1641–1644.

Manor, D., and M. Sadeh. 1989. Muscle fibre necrosis induced by intramuscular injection of drugs. Br. J. Exp. Pathol. 70:457–462.

Marchi, S., S. Patergnani, and P. Pinton. 2014. The endoplasmic reticulum–mitochondria connection: One touch, multiple functions. Biochim. Biophys. Acta - Bioenerg. 1837:461–469.

Margolis, E. B., G. O. Hjelmstad, W. Fujita, and H. L. Fields. 2014. Direct Bidirectional μ-Opioid Control of Midbrain Dopamine Neurons. J. Neurosci. 34:14707 LP – 14716.

Martel, S., J. Y. Keow, and M. Ekker. 2015. Rotenone Neurotoxicity Causes Dopamine Neuron Loss in Zebrafish. Univ. Ottawa J. Med. 5:16–21.

Matsuda, W., T. Furuta, K. C. Nakamura, H. Hioki, F. Fujiyama, R. Arai, and T. Kaneko. 2009. Single nigrostriatal dopaminergic neurons form widely spread and highly dense axonal arborizations in the neostriatum. J. Neurosci. 29:444–453. Soc Neuroscience.

Matsui, H., Y. Taniguchi, H. Inoue, K. Uemura, S. Takeda, and R. Takahashi. 2009. A chemical neurotoxin, MPTP induces Parkinson's disease like phenotype, movement disorders and persistent loss of dopamine neurons in medaka fish. Neurosci. Res. 65:263–271.

McCarty, N. S., A. E. Graham, L. Studená, and R. Ledesma-Amaro. 2020. Multiplexed CRISPR technologies for gene editing and transcriptional regulation. Nat. Commun. 11:1281.

McCormack, A. L., M. Thiruchelvam, A. B. Manning-Bog, C. Thiffault, J. W. Langston, D. A. Cory-Slechta, and D. A. Di Monte. 2002. Environmental risk factors and Parkinson's disease: selective degeneration of nigral dopaminergic neurons caused by the herbicide paraquat. Neurobiol. Dis. 10:119–127. Elsevier.

Meeusen, S., R. DeVay, J. Block, A. Cassidy-Stone, S. Wayson, J. M. McCaffery, and J. Nunnari. 2006. Mitochondrial inner-membrane fusion and crista maintenance requires the dynamin-related GTPase Mgm1. Cell 127:383–395. Elsevier.

Meiser, J., D. Weindl, and K. Hiller. 2013. Complexity of dopamine metabolism. Cell Commun. Signal. 11:34.

Meredith, G. E., and D. J. Rademacher. 2011. MPTP mouse models of Parkinson's disease: an update. J. Parkinsons. Dis. 1:19–33.

Merhi, R., M. Kalyn, A. Zhu-Pawlowsky, and M. Ekker. 2021. Loss of parla Function Results in Inactivity, Olfactory Impairment, and Dopamine Neuron Loss in Zebrafish. Biomedicines 9.

Milanese, C., J. J. Sager, Q. Bai, T. C. Farrell, J. R. Cannon, J. T. Greenamyre, and E. A. Burton.

2012. Hypokinesia and reduced dopamine levels in zebrafish lacking β-and γ1-synucleins. J. Biol. Chem. 287:2971–2983. ASBMB.

Ming, G.-L., and H. Song. 2011. Adult neurogenesis in the mammalian brain: significant answers and significant questions. Neuron 70:687–702.

Misgeld, T., and T. L. Schwarz. 2017. Mitostasis in neurons: maintaining mitochondria in an extended cellular architecture. Neuron 96:651–666. Elsevier.

Mojica, F. J. M., C. Díez-Villaseñor, J. García-Martínez, and E. Soria. 2005. Intervening Sequences of Regularly Spaced Prokaryotic Repeats Derive from Foreign Genetic Elements. J. Mol. Evol. 60:174–182.

Mojica, F. J. M., G. Juez, and F. Rodriguez-Valera. 1993. Transcription at different salinities of Haloferax mediterranei sequences adjacent to partially modified PstI sites. Mol. Microbiol. 9:613–621. John Wiley & Sons, Ltd.

Montague, T. G., J. M. Cruz, J. A. Gagnon, G. M. Church, and E. Valen. 2014. CHOPCHOP: a CRISPR/Cas9 and TALEN web tool for genome editing. Nucleic Acids Res. 42:W401–W407. Oxford University Press.

Montarolo, F., S. Martire, S. Perga, M. Spadaro, I. Brescia, S. Allegra, S. De Francia, and A. Bertolotto. 2019. NURR1 deficiency is associated to ADHD-like phenotypes in mice. Transl. Psychiatry 9:207.

Moss, J., and J. P. Bolam. 2008. A dopaminergic axon lattice in the striatum and its relationship with cortical and thalamic terminals. J. Neurosci. 28:11221–11230. Soc Neuroscience.

Muangpaisan, W., A. Mathews Mbbs, H. Hori, and D. Seidel Mphil. 2011. A Systematic Review of the Worldwide Prevalence and Incidence of Parkinson's Disease.

Mueller, T., Z. Dong, M. A. Berberoglu, and S. Guo. 2011. The dorsal pallium in zebrafish,

Danio rerio (Cyprinidae, Teleostei). Brain Res. 1381:95–105. Elsevier.

Müller, T. E., M. E. Nunes, C. C. Menezes, A. T. Marins, J. Leitemperger, A. C. L. Gressler, F. B. Carvalho, C. M. de Freitas, V. A. Quadros, R. Fachinetto, D. B. Rosemberg, and V. L. Loro. 2018. Sodium Selenite Prevents Paraquat-Induced Neurotoxicity in Zebrafish. Mol. Neurobiol. 55:1928–1941.

Musgrove, R. E. J., A. E. King, and T. C. Dickson. 2011. Neuroprotective Upregulation of Endogenous Alpha-Synuclein Precedes Ubiquitination in Cultured Dopaminergic Neurons. Neurotox. Res. 19:592–602.

Musgrove, R. E. J., A. E. King, and T. C. Dickson. 2013. α-Synuclein protects neurons from apoptosis downstream of free-radical production through modulation of the MAPK signalling pathway. Neurotox. Res. 23:358–369. United States.

Nagayama, H., M. Hamamoto, M. Ueda, C. Nito, H. Yamaguchi, and Y. Katayama. 2004. The Effect of Ascorbic Acid on the Pharmacokinetics of Levodopa in Elderly Patients with Parkinson Disease. Clin. Neuropharmacol. 27.

Nair, S., K. S. Sobotka, P. Joshi, P. Gressens, B. Fleiss, C. Thornton, C. Mallard, and H. Hagberg. 2019. Lipopolysaccharide-induced alteration of mitochondrial morphology induces a metabolic shift in microglia modulating the inflammatory response in vitro and in vivo. Glia 67:1047–1061. John Wiley & Sons, Ltd.

Nanda, N. B. P., P. C. Das, and J. Jena. 2009. Use of Rotenone as Piscicide: Toxicity Levels in a Few Common Freshwater Predatory and Weed Fishes. J. Appl. Aquac. 21:241–249. Taylor & Francis.

Naudet, N., E. Antier, D. Gaillard, E. Morignat, L. Lakhdar, T. Baron, and A. Bencsik. 2017. Oral Exposure to Paraquat Triggers Earlier Expression of Phosphorylated α-Synuclein in

the Enteric Nervous System of A53T Mutant Human α-Synuclein Transgenic Mice. J. Neuropathol. Exp. Neurol. 76:1046–1057.

Nellore, J., and N. P. 2015. Paraquat exposure induces behavioral deficits in larval zebrafish during the window of dopamine neurogenesis. Toxicol. reports 2:950–956. Elsevier.

Nguyen, A. P. T., E. Tsika, K. Kelly, N. Levine, X. Chen, A. B. West, S. Boularand, P. Barneoud, and D. J. Moore. 2020. Dopaminergic neurodegeneration induced by Parkinson's disease-linked G2019S LRRK2 is dependent on kinase and GTPase activity. Proc. Natl. Acad. Sci. 117:17296–17307. Proceedings of the National Academy of Sciences.

Niederkofler, V., T. E. Asher, and S. M. Dymecki. 2015. Functional Interplay between Dopaminergic and Serotonergic Neuronal Systems during Development and Adulthood. ACS Chem. Neurosci. 6:1055–1070.

Noble, S., R. Godoy, P. Affaticati, and M. Ekker. 2015. Transgenic Zebrafish Expressing mCherry in the Mitochondria of Dopaminergic Neurons. Zebrafish 12:349–356. Mary Ann Liebert, Inc., publishers.

Noble, S., A. Ismail, R. Godoy, Y. Xi, and M. Ekker. 2012. Zebrafish Parla- and Parlb-deficiency affects dopaminergic neuron patterning and embryonic survival. J. Neurochem. 122:196–207.

Nualart, F., L. Mack, A. García, P. Cisternas, E. R. Bongarzone, M. Heitzer, N. Jara, F. Martínez, L. Ferrada, and F. Espinoza. 2014. Vitamin C transporters, recycling and the bystander effect in the nervous system: SVCT2 versus gluts. J. Stem Cell Res. Ther. 4:209. NIH Public Access.

Ogiwara, T., K. Satoh, Y. Kadoma, Y. Murakami, S. Unten, T. Atsumi, H. Sakagami, and S. Fujisawa. 2002. Radical scavenging activity and cytotoxicity of ferulic acid. Anticancer

Res. 22:2711–2717.

Orrico-Sánchez, A., M. López-Lacort, C. Muñoz-Quiles, G. Sanfélix-Gimeno, and J. Díez-Domingo. 2020. Epidemiology of schizophrenia and its management over 8-years period using real-world data in Spain. BMC Psychiatry 20:149.

Ott, K. C., and P. D. 2006. Rotenone. A Brief Review of its Chemistry, Environmental Fate, and the Toxicity of Rotenone Formulations. Kevin C. Ott, Ph.D†. Fish.

Pacelli, C., N. Giguère, M.-J. Bourque, M. Lévesque, R. S. Slack, and L.-É. Trudeau. 2015. Elevated Mitochondrial Bioenergetics and Axonal Arborization Size Are Key Contributors to the Vulnerability of Dopamine Neurons. Curr. Biol. 25:2349–2360. Elsevier.

Paduraru, E., E.-I. Flocea, C. C. Lazado, I.-A. Simionov, M. Nicoara, A. Ciobica, C. Faggio, and R. Jijie. 2021. Vitamin C Mitigates Oxidative Stress and Behavioral Impairments Induced by Deltamethrin and Lead Toxicity in Zebrafish. Int. J. Mol. Sci. 22.

Pakarinen, E., P. Lindholm, M. Saarma, and M. Lindahl. 2022. CDNF and MANF regulate ER stress in a tissue-specific manner. Cell. Mol. Life Sci. 79:124.

Pan-Montojo, F., O. Anichtchik, Y. Dening, L. Knels, S. Pursche, R. Jung, S. Jackson, G. Gille, M. G. Spillantini, and H. Reichmann. 2010. Progression of Parkinson's disease pathology is reproduced by intragastric administration of rotenone in mice. PLoS One 5:e8762. Public Library of Science San Francisco, USA.

Panula, P., Y.-C. Chen, M. Priyadarshini, H. Kudo, S. Semenova, M. Sundvik, and V. Sallinen. 2010. The comparative neuroanatomy and neurochemistry of zebrafish CNS systems of relevance to human neuropsychiatric diseases. Neurobiol. Dis. 40:46–57.

Pardo, B., M. A. Mena, S. Fahn, and J. G. de Yébenes. 1993. Ascorbic acid protects against levodopa-induced neurotoxicity on a catecholamine-rich human neuroblastoma cell line.

Mov. Disord. Off. J. Mov. Disord. Soc. 8:278–284. Wiley Online Library.

Park, J., J. Seo, J. Won, H.-G. Yeo, Y.-J. Ahn, K. Kim, Y. B. Jin, B.-S. Koo, K. S. Lim, K.-J. Jeong, P. Kang, H.-Y. Lee, S. H. Baek, C.-Y. Jeon, J.-J. Hong, J.-W. Huh, Y.-H. Kim, S.-J. Park, S.-U. Kim, D.-S. Lee, S.-R. Lee, and Y. Lee. 2019. Abnormal Mitochondria in a Non-human Primate Model of MPTP-induced Parkinson's Disease: Drp1 and CDK5/p25 Signaling. Exp. Neurobiol. 28:414–424. The Korean Society for Brain and Neural Science.

Parng, C., C. Ton, Y.-X. Lin, N. M. Roy, and P. McGrath. 2006. A zebrafish assay for identifying neuroprotectants in vivo. Neurotoxicol. Teratol. 28:509–516.

Paterna, J.-C., A. Leng, E. Weber, J. Feldon, and H. Büeler. 2007. DJ-1 and Parkin Modulate Dopamine-dependent Behavior and Inhibit MPTP-induced Nigral Dopamine Neuron Loss in Mice. Mol. Ther. 15:698–704.

Pearen, M. A., and G. E. O. Muscat. 2010. Minireview: Nuclear Hormone Receptor 4A Signaling: Implications for Metabolic Disease. Mol. Endocrinol. 24:1891–1903.

Pedrosa, D. J., and L. Timmermann. 2013. Review: management of Parkinson's disease. Neuropsychiatr. Dis. Treat. 9:321–340.

Pickrell, A. M., and R. J. Youle. 2015. The roles of PINK1, parkin, and mitochondrial fidelity in Parkinson's disease. Neuron 85:257–273.

Pilsl, A., and K. F. Winklhofer. 2012. Parkin, PINK1 and mitochondrial integrity: emerging concepts of mitochondrial dysfunction in Parkinson's disease. Acta Neuropathol. 123:173–188.

Plaitakis, A., and P. Shashidharan. 2000. Glutamate transport and metabolism in dopaminergic neurons of substantia nigra: implications for the pathogenesis of Parkinson's disease. J. Neurol. 247:II25–II35. Springer.

Prabhudesai, S., F. Z. Bensabeur, R. Abdullah, I. Basak, S. Baez, G. Alves, N. G. Holtzman, J. P. Larsen, and S. G. Møller. 2016. LRRK2 knockdown in zebrafish causes developmental defects, neuronal loss, and synuclein aggregation. J. Neurosci. Res. 94:717–735. United States.

Prabhudesai, S., S. Sinha, A. Attar, A. Kotagiri, A. G. Fitzmaurice, R. Lakshmanan, M. I. Ivanova, J. A. Loo, F.-G. Klärner, and T. Schrader. 2012. A novel "molecular tweezer" inhibitor of α-synuclein neurotoxicity in vitro and in vivo. Neurotherapeutics 9:464–476. Springer.

Prensa, L., J. M. Giménez-Amaya, A. Parent, J. Bernácer, and C. Cebrián. 2009. The Nigrostriatal Pathway: Axonal Collateralization and Compartmental Specificity BT - Birth, Life and Death of Dopaminergic Neurons in the Substantia Nigra. Pp. 49–58 *in* G. Giovanni, V. Di Matteo, and E. Esposito, eds. Springer Vienna, Vienna.

Przedborski, S., P. Jackson-Lewis Vernice, R. Djaldetti, G. Liberatore, M. Vila, S. Vukosavic, and G. Almer. 2000. The parkinsonian toxin MPTP: Action and mechanism.

Przedborski, S., K. Tieu, C. Perier, and M. Vila. 2004a. MPTP as a mitochondrial neurotoxic model of Parkinson's disease. J. Bioenerg. Biomembr. 36:375–379. United States.

Przedborski, S., K. Tieu, C. Perier, and M. Vila. 2004b. MPTP as a mitochondrial neurotoxic model of Parkinson's disease. J. Bioenerg. Biomembr. 36:375–379.

Qian, W., S. Choi, G. A. Gibson, S. C. Watkins, C. J. Bakkenist, and B. Van Houten. 2012. Mitochondrial hyperfusion induced by loss of the fission protein Drp1 causes ATM-dependent G2/M arrest and aneuploidy through DNA replication stress. J. Cell Sci. 125:5745–5757.

Quessy, F., T. Bittar, L. J. Blanchette, M. Lévesque, and B. Labonté. 2021. Stress-induced

alterations of mesocortical and mesolimbic dopaminergic pathways. Sci. Rep. 11:11000.

Raftery, T. D., N. Jayasundara, and R. T. Di Giulio. 2017. A bioenergetics assay for studying the effects of environmental stressors on mitochondrial function in vivo in zebrafish larvae. Comp. Biochem. Physiol. Part C Toxicol. Pharmacol. 192:23–32.

Ramesh, T. M., P. J. Shaw, and J. McDearmid. 2014. A zebrafish model exemplifies the long preclinical period of motor neuron disease. J. Neurol. Neurosurg. & Psychiatry 85:1288 LP – 1289.

Ran, F. A., P. D. Hsu, C.-Y. Lin, J. S. Gootenberg, S. Konermann, A. E. Trevino, D. A. Scott, A. Inoue, S. Matoba, Y. Zhang, and F. Zhang. 2013. Double Nicking by RNA-Guided CRISPR Cas9 for Enhanced Genome Editing Specificity. Cell 154:1380–1389.

Rappold, P. M., M. Cui, A. S. Chesser, J. Tibbett, J. C. Grima, L. Duan, N. Sen, J. A. Javitch, and K. Tieu. 2011. Paraquat neurotoxicity is mediated by the dopamine transporter and organic cation transporter-3. Proc. Natl. Acad. Sci. U. S. A. 108:20766–20771. National Academy of Sciences.

Rasmussen, F. 1978. Tissue damage at the injection site after intramuscular injection of drugs. Vet. Sci. Commun. 2:173–182.

Reader, T. a., and K. M. Dewar. 1999. Review article Effects of denervation and hyperinnervation on dopamine and serotonin systems in the rat neostriatum: implications for human Parkinsons disease. Neurochem. Int. 34:1–21.

Reczek, C. R., K. Birsoy, H. Kong, I. Martínez-Reyes, T. Wang, P. Gao, D. M. Sabatini, and N. S. Chandel. 2017. A CRISPR screen identifies a pathway required for paraquat-induced cell death. Nat. Chem. Biol. 13:1274. Nature Publishing Group, a division of Macmillan Publishers Limited. All Rights Reserved.

Reeves, S., C. Bench, and R. Howard. 2002. Ageing and the nigrostriatal dopaminergic system. Int. J. Geriatr. Psychiatry 17:359–370. John Wiley & Sons, Ltd.

Reimer, M. M., V. Kuscha, C. Wyatt, I. Sörensen, R. E. Frank, M. Knüwer, T. Becker, and C. G. Becker. 2009. Sonic Hedgehog Is a Polarized Signal for Motor Neuron Regeneration in Adult Zebrafish. J. Neurosci. 29:15073 LP – 15082.

Ren, J., Y. Zhao, and X. Sun. 2009. Toxic influence of chronic oral administration of paraquat on nigrostriatal dopaminergic neurons in C57BL/6 mice. Chin. Med. J. (Engl). 122:2366–2371. Chinese Medical Journals Publishing House Co., Ltd. 42 Dongsi Xidajie ….

Ren, Z., R. Zhang, Y. Li, Y. Li, Z. Yang, and H. Yang. 2017. Ferulic acid exerts neuroprotective effects against cerebral ischemia/reperfusion-induced injury via antioxidant and anti-apoptotic mechanisms in vitro and in vivo. Int. J. Mol. Med. 40:1444–1456.

Richardson, J. R., Y. Quan, T. B. Sherer, J. T. Greenamyre, and G. W. Miller. 2005. Paraquat Neurotoxicity is Distinct from that of MPTP and Rotenone. 88:193–201.

Riederer, P., E. Sofic, W. Rausch, B. Schmidt, G. P. Reynolds, K. Jellinger, and M. B. H. Youdim. 1989. Transition Metals, Ferritin, Glutathione, and Ascorbic Acid in Parkinsonian Brains. J. Neurochem. 52:515–520. Wiley Online Library.

Rink, E., and M. F. Wullimann. 2002a. Connections of the ventral telencephalon and tyrosine hydroxylase distribution in the zebrafish brain (Danio rerio) lead to identification of an ascending dopaminergic system in a teleost. Brain Res. Bull. 57:385–387. United States.

Rink, E., and M. F. Wullimann. 2002b. Development of the catecholaminergic system in the early zebrafish brain: an immunohistochemical study. Dev. Brain Res. 137:89–100.

Robea, M.-A., I.-M. Balmus, A. Ciobica, S. Strungaru, G. Plavan, L. D. Gorgan, A. Savuca, and M. Nicoara. 2020. Parkinson’s Disease-Induced Zebrafish Models: Focussing on Oxidative

Stress Implications and Sleep Processes. Oxid. Med. Cell. Longev. 2020:1370837. Hindawi.

Roberts, A. C., B. R. Bill, and D. L. Glanzman. 2013. Learning and memory in zebrafish larvae. Front. Neural Circuits 7:126. Frontiers Media SA.

Rodríguez-Ortiz, R., and A. Martínez-Torres. 2021. Mutants of the Zebrafish K+ Channel Hcn2b Exhibit Epileptic-like Behaviors. Int. J. Mol. Sci. 22:11471. MDPI.

Rojas, P., E. Joodmardi, Y. Hong, T. Perlmann, and S. O. Ogren. 2007. Adult mice with reduced Nurr1 expression: an animal model for schizophrenia. Mol. Psychiatry 12:756–766. England.

Rossignol, R., R. Gilkerson, R. Aggeler, K. Yamagata, S. J. Remington, and R. A. Capaldi. 2004. Energy substrate modulates mitochondrial structure and oxidative capacity in cancer cells. Cancer Res. 64:985–993. United States.

Roussa, E., and K. Krieglstein. 2004. Induction and specification of midbrain dopaminergic cells: focus on SHH, FGF8, and TGF-β. Cell Tissue Res. 318:23–33.

Rubinstein, A. L. 2003. Zebrafish: from disease modeling to drug discovery. Curr. Opin. Drug Discov. Dev. 6:218–223. Citeseer.

Ryu, S., J. Mahler, D. Acampora, J. Holzschuh, S. Erhardt, D. Omodei, A. Simeone, and W. Driever. 2007. Orthopedia homeodomain protein is essential for diencephalic dopaminergic neuron development. Curr. Biol. 17:873–880. England.

Sailor, K. A., G.-L. Ming, and H. Song. 2006. Neurogenesis as a potential therapeutic strategy for neurodegenerative diseases. Expert Opin. Biol. Ther. 6:879–890.

Salau, V. F., O. L. Erukainure, C. U. Ibeji, T. A. Olasehinde, N. A. Koorbanally, and M. S. Islam. 2020. Vanillin and vanillic acid modulate antioxidant defense system via amelioration of metabolic complications linked to Fe2+-induced brain tissues damage.

Metab. Brain Dis. 35:727–738.

Saleem, S., and R. R. Kannan. 2018. Zebrafish: an emerging real-time model system to study Alzheimer's disease and neurospecific drug discovery. Cell Death Discov. 4:45.

Sallinen, V., V. Torkko, M. Sundvik, I. Reenilä, D. Khrustalyov, J. Kaslin, and P. Panula. 2009. MPTP and MPP+ target specific aminergic cell populations in larval zebrafish. J. Neurochem. 108:719–731. Wiley Online Library.

Santana, C., M. Rodriguez, D. Afonso, and R. Arevalo. 1992. Dopaminergic neuron development in rats: Biochemical study from prenatal life to adulthood. Brain Res. Bull. 29:7–13.

Sarath Babu, N., C. L. N. Murthy, S. Kakara, R. Sharma, C. V Brahmendra Swamy, and M. M. Idris. 2016. 1-Methyl-4-phenyl-1,2,3,6-tetrahydropyridine induced Parkinson's disease in zebrafish. Proteomics 16:1407–1420. John Wiley & Sons, Ltd.

Sassen, W. A., and R. W. Köster. 2015. A molecular toolbox for genetic manipulation of zebrafish. Adv. Genomics Genet. 5:151. Taylor & Francis Ltd.

Saucedo-Cardenas, O., and O. M. Conneely. 1996. Comparative distribution of NURR1 and NUR77 nuclear receptors in the mouse central nervous system. J. Mol. Neurosci. 7:51–63. Springer.

Saverino, C., and R. Gerlai. 2008. The social zebrafish: behavioral responses to conspecific, heterospecific, and computer animated fish. Behav. Brain Res. 191:77–87. Elsevier.

Scerbina, T., D. Chatterjee, and R. Gerlai. 2012. Dopamine receptor antagonism disrupts social preference in zebrafish: a strain comparison study. Amino Acids 43:2059–2072.

Schiffer, N. W., S. A. Broadley, T. Hirschberger, P. Tavan, H. A. Kretzschmar, A. Giese, C. Haass, F. U. Hartl, and B. Schmid. 2007. Identification of anti-prion compounds as efficient

inhibitors of polyglutamine protein aggregation in a zebrafish model. J. Biol. Chem. 282:9195–9203. ASBMB.

Schweitzer, J., and W. Driever. 2009. Development of the dopamine systems in zebrafish. Adv. Exp. Med. Biol. 651:1–14. United States.

Seitz, G., S. Gebhardt, J. F. Beck, W. Böhm, H. N. Lode, D. Niethammer, and G. Bruchelt. 1998. Ascorbic acid stimulates DOPA synthesis and tyrosine hydroxylase gene expression in the human neuroblastoma cell line SK-N-SH. Neurosci. Lett. 244:33–36. Ireland.

Selvaraj, V., H. Venkatasubramanian, K. Ilango, and K. Santhakumar. 2019. A simple method to study motor and non-motor behaviors in adult zebrafish. J. Neurosci. Methods 320:16–25.

Senoh, S., C. R. Creveling, S. Udenfriend, and B. Witkop. 1959. Chemical, enzymatic and metabolic studies on the mechanism of oxidation of dopamine1. J. Am. Chem. Soc. 81:6236–6240. ACS Publications.

Senoh, S., and B. Witkop. 1959. Non-enzymatic conversions of dopamine to norepinephrine and trihydroxyphenethylamines1. J. Am. Chem. Soc. 81:6222–6231. ACS Publications.

Seo, B. J., S. H. Yoon, and J. T. Do. 2018. Mitochondrial Dynamics in Stem Cells and Differentiation. Int. J. Mol. Sci. 19:3893. MDPI.

Sershen, H., M. E. A. Reith, A. Hashim, and A. Lajtha. 1985. Protection against 1-methyl-4-phenyl-1, 2, 3, 6-tetrahydropyridine neurotoxicity by the antioxidant ascorbic acid. Neuropharmacology 24:1257–1259. Elsevier.

Sha, D., L.-S. Chin, and L. Li. 2010. Phosphorylation of parkin by Parkinson disease-linked kinase PINK1 activates parkin E3 ligase function and NF-κB signaling. Hum. Mol. Genet. 19:352–363. Oxford University Press.

Sharma, N., N. Khurana, A. Muthuraman, and P. Utreja. 2021. Pharmacological evaluation of

vanillic acid in rotenone-induced Parkinson's disease rat model. Eur. J. Pharmacol. 903:174112.

Shimizu, I., and C. Prasad. 1991. Dopamine Transporter in Aging. Pp. 171–173 *in* S. Z. LANGER, A. M. GALZIN, and J. B. T.-P. R. and N. T. COSTENTIN, eds. Pergamon.

Shimizu, K., K. Ohtaki, K. Matsubara, K. Aoyama, T. Uezono, O. Saito, M. Suno, K. Ogawa, N. Hayase, K. Kimura, and H. Shiono. 2001. Carrier-mediated processes in blood–brain barrier penetration and neural uptake of paraquat. Brain Res. 906:135–142.

Sian, J., M. Youdim, P. Riederer, and M. Gerlach. 1999. MPTP-Induced Parkinsonian Syndrome. Basic Neurochem. Mol. Cell. Med. Asp. 6th Ed.

Sillitoe, R. V, and M. W. Vogel. 2008. Desire, Disease, and the Origins of the Dopaminergic System. Schizophr. Bull. 34:212–219.

Simon, D. K., C. M. Tanner, and P. Brundin. 2020. Parkinson Disease Epidemiology, Pathology, Genetics, and Pathophysiology. Clin. Geriatr. Med. 36:1–12.

Singleton, A. B., M. Farrer, J. Johnson, A. Singleton, S. Hague, J. Kachergus, M. Hulihan, T. Peuralinna, A. Dutra, R. Nussbaum, S. Lincoln, A. Crawley, M. Hanson, D. Maraganore, C. Adler, M. R. Cookson, M. Muenter, M. Baptista, D. Miller, J. Blancato, J. Hardy, and K. Gwinn-Hardy. 2003. α-Synuclein Locus Triplication Causes Parkinson's Disease. Science (80-.). 302:841 LP – 841.

Sinha, P., N. Ghosh, S. Mitra, and A. Bhattacharyya. 2016. Neuroinflammation During Parkinson's Disease: Key Cells and Molecules Involved in It. Pp. 185–208 *in* Inflammation: The Common Link in Brain Pathologies.

Smeets, W. J. A. J., and A. González. 2000. Catecholamine systems in the brain of vertebrates: new perspectives through a comparative approach. Brain Res. Rev. 33:308–379.

Son, M. J., C. W. Rico, S. H. Nam, and M. Y. Kang. 2010. Influence of oryzanol and ferulic acid on the lipid metabolism and antioxidative status in high fat-fed mice. J. Clin. Biochem. Nutr. 46:150–156. Society for Free Radical Research Japan.

Spillantini, M. G., M. L. Schmidt, V. M.-Y. Lee, J. Q. Trojanowski, R. Jakes, and M. Goedert. 1997. α-Synuclein in Lewy bodies. Nature 388:839–840.

Stanely Mainzen Prince, P., S. Rajakumar, and K. Dhanasekar. 2011. Protective effects of vanillic acid on electrocardiogram, lipid peroxidation, antioxidants, proinflammatory markers and histopathology in isoproterenol induced cardiotoxic rats. Eur. J. Pharmacol. 668:233–240.

Stewart, A. M., O. Braubach, J. Spitsbergen, R. Gerlai, and A. V Kalueff. 2014. Zebrafish models for translational neuroscience research: from tank to bedside. Trends Neurosci. 37:264–78.

Sulzer, D., S. J. Cragg, and M. E. Rice. 2016. Striatal dopamine neurotransmission: regulation of release and uptake. Basal Ganglia 6:123–148.

Suzzi, S., R. Ahrendt, S. Hans, S. A. Semenova, A. Chekuru, P. Wirsching, V. Kroehne, S. Bilican, S. Sayed, S. Winkler, S. Spieß, A. Machate, J. Kaslin, P. Panula, and M. Brand. 2021. Deletion of lrrk2 causes early developmental abnormalities and age-dependent increase of monoamine catabolism in the zebrafish brain. PLOS Genet. 17:e1009794. Public Library of Science.

Sveinbjornsdottir, S. 2016. The clinical symptoms of Parkinson’s disease. J. Neurochem. 139:318–324. John Wiley & Sons, Ltd (10.1111).

Swarnkar, S., S. Singh, R. Mathur, I. Patro, and C. Nath. 2010. A study to correlate rotenone induced biochemical changes and cerebral damage in brain areas with neuromuscular

coordination in rats. Toxicology 272:17–22.

Tanaka, A., M. M. Cleland, S. Xu, D. P. Narendra, D.-F. Suen, M. Karbowski, and R. J. Youle. 2010. Proteasome and p97 mediate mitophagy and degradation of mitofusins induced by Parkin. J. Cell Biol. 191:1367–1380. The Rockefeller University Press.

Tang, R., A. Dodd, D. Lai, W. C. McNabb, and D. R. Love. 2007. Validation of Zebrafish (Danio rerio) Reference Genes for Quantitative Real-time RT-PCR Normalization. Acta Biochim. Biophys. Sin. (Shanghai). 39:384–390.

Tay, T. L., O. Ronneberger, S. Ryu, R. Nitschke, and W. Driever. 2011. Comprehensive catecholaminergic projectome analysis reveals single-neuron integration of zebrafish ascending and descending dopaminergic systems. Nat. Commun. 2:1–12. Nature Publishing Group.

Taylor, J. S., Y. Van de Peer, I. Braasch, and A. Meyer. 2001. Comparative genomics provides evidence for an ancient genome duplication event in fish. Philos. Trans. R. Soc. London. Ser. B, Biol. Sci. 356:1661–1679.

Thiruchelvam, M., A. McCormack, E. K. Richfield, R. B. Baggs, A. W. Tank, D. A. Di Monte, and D. A. Cory-Slechta. 2003. Age-related irreversible progressive nigrostriatal dopaminergic neurotoxicity in the paraquat and maneb model of the Parkinson's disease phenotype. Eur. J. Neurosci. 18:589–600. Wiley Online Library.

Thörn Pérez, C., J. Ferraris, J. A. van Lunteren, A. Hellysaz, M. J. Iglesias, and C. Broberger. 2020. Adaptive Resetting of Tuberoinfundibular Dopamine (TIDA) Network Activity during Lactation in Mice. J. Neurosci. 40:3203 LP – 3216.

Thörnqvist, P.-O., S. McCarrick, M. Ericsson, E. Roman, and S. Winberg. 2019. Bold zebrafish (Danio rerio) express higher levels of delta opioid and dopamine D2 receptors in the brain

compared to shy fish. Behav. Brain Res. 359:927–934.

Tieu, K. 2011. A guide to neurotoxic animal models of Parkinson's disease. Cold Spring Harb. Perspect. Med. 1:a009316–a009316. Cold Spring Harbor Laboratory Press.

Truban, D., X. Hou, T. R. Caulfield, F. C. Fiesel, and W. Springer. 2017. PINK1, Parkin, and Mitochondrial Quality Control: What can we Learn about Parkinson's Disease Pathobiology? J. Parkinsons. Dis. 7:13–29. IOS Press.

Tsou, K., S. Brown, M. C. Sanudo-Pena, K. Mackie, and J. M. Walker. 1998. Immunohistochemical distribution of cannabinoid CB1 receptors in the rat central nervous system. Neuroscience 83:393–411. Elsevier.

Turner, P. V, T. Brabb, C. Pekow, and M. A. Vasbinder. 2011. Administration of substances to laboratory animals: routes of administration and factors to consider. J. Am. Assoc. Lab. Anim. Sci. 50:600–613. American Association for Laboratory Animal Science.

Ungerstedt, U. 1968. 6-Hydroxy-dopamine induced degeneration of central monoamine neurons. Eur. J. Pharmacol. 5:107–110. Elsevier.

Van Kampen, J. M., E. G. McGeer, and A. J. Stoessl. 2000. Dopamine transporter function assessed by antisense knockdown in the rat: Protection from dopamine neurotoxicity. Synapse 37:171–178. John Wiley & Sons, Ltd.

Vaz, R. L., T. F. Outeiro, and J. J. Ferreira. 2018. Zebrafish as an Animal Model for Drug Discovery in Parkinson's Disease and Other Movement Disorders: A Systematic Review .

Vijayakumar, K., and G.-W. Cho. 2019. Autophagy: An evolutionarily conserved process in the maintenance of stem cells and aging. Cell Biochem. Funct. 37:452–458. John Wiley & Sons, Ltd.

Vijayanathan, Y., F. T. Lim, S. M. Lim, C. M. Long, M. P. Tan, A. B. A. Majeed, and K.

Ramasamy. 2017. 6-OHDA-Lesioned Adult Zebrafish as a Useful Parkinson's Disease Model for Dopaminergic Neuroregeneration. Neurotox. Res. 32:496–508.

Visanji, N. P., P. L. Brooks, L.-N. Hazrati, and A. E. Lang. 2013. The prion hypothesis in Parkinson's disease: Braak to the future. Acta Neuropathol. Commun. 1:2.

Volkow, N. D., and M. Morales. 2015. The Brain on Drugs: From Reward to Addiction. Cell 162:712–725.

Volpicelli, F., M. Caiazzo, D. Greco, C. Consales, L. Leone, C. Perrone-Capano, L. C. D'Amato, and U. di Porzio. 2007. Bdnf gene is a downstream target of Nurr1 transcription factor in rat midbrain neurons in vitro. J. Neurochem. 102:441–453. John Wiley & Sons, Ltd.

Wang, X., X. Mao, L. Xie, D. A. Greenberg, and K. Jin. 2009. Involvement of Notch1 signaling in neurogenesis in the subventricular zone of normal and ischemic rat brain in vivo. J. Cereb. Blood Flow Metab. 29:1644–1654.

Wang, X., C. Souders II, Y. Zhao, and C. Martyniuk. 2017a. Exposure to paraquat affects mitochondrial bioenergetics, dopamine system expression, and locomotor activity in zebrafish (Danio rerio). Chemosphere 191.

Wang, X., D. Winter, G. Ashrafi, J. Schlehe, Y. L. Wong, D. Selkoe, S. Rice, J. Steen, M. J. LaVoie, and T. L. Schwarz. 2011. PINK1 and Parkin target Miro for phosphorylation and degradation to arrest mitochondrial motility. Cell 147:893–906. Elsevier.

Wang, Y., W. Liu, J. Yang, F. Wang, Y. Sima, Z.-M. Zhong, H. Wang, L.-F. Hu, and C.-F. Liu. 2017b. Parkinson's disease-like motor and non-motor symptoms in rotenone-treated zebrafish. Neurotoxicology 58:103–109. Netherlands.

Wen, L., W. Wei, W. Gu, P. Huang, X. Ren, Z. Zhang, Z. Zhu, S. Lin, and B. Zhang. 2008. Visualization of monoaminergic neurons and neurotoxicity of MPTP in live transgenic

zebrafish. Dev. Biol. 314:84–92. United States.

Westermann, B. 2012. Bioenergetic role of mitochondrial fusion and fission. Biochim. Biophys. Acta - Bioenerg. 1817:1833–1838.

Wills, J., J. Credle, A. W. Oaks, V. Duka, J.-H. Lee, J. Jones, and A. Sidhu. 2012. Paraquat, but Not Maneb, Induces Synucleinopathy and Tauopathy in Striata of Mice through Inhibition of Proteasomal and Autophagic Pathways. PLoS One 7:e30745. Public Library of Science.

Winklhofer, K. F., and C. Haass. 2010. Mitochondrial dysfunction in Parkinson's disease. Biochim. Biophys. Acta - Mol. Basis Dis. 1802:29–44.

Wise, R. A. 2004. Dopamine, learning and motivation. Nat. Rev. Neurosci. 5:483–494.

Wong, C. E. D., K. Hua, S. Monis, V. Saxena, A. Norazit, S. M. Noor, and M. Ekker. 2021. gdnf affects early diencephalic dopaminergic neuron development through regulation of differentiation-associated transcription factors in zebrafish. J. Neurochem. 156:481–498. John Wiley & Sons, Ltd.

Wong, D. L. 2006. Epinephrine Biosynthesis: Hormonal and Neural Control During Stress. Cell. Mol. Neurobiol. 26:889–898.

Wooten, G. F., L. J. Currie, V. E. Bovbjerg, J. K. Lee, and J. Patrie. 2004. Are men at greater risk for Parkinson's disease than women? J. Neurol. Neurosurg. Psychiatry 75:637–639. BMJ Publishing Group Ltd.

Wu, C., H. Lee, C. Liu, M. Korivi, H. Chen, and M. Chan. 2015. Protective role of L-ascorbic acid, N-acetylcysteine and apocynin on neomycin-induced hair cell loss in zebrafish. J. Appl. Toxicol. 35:273–279. Wiley Online Library.

Wullimann, M. F., and K. E. Umeasalugo. 2020. Sonic hedgehog expression in zebrafish forebrain identifies the teleostean pallidal signaling center and shows preglomerular

complex and posterior tubercular dopamine cells to arise from shh cells. J. Comp. Nfile///Users/michaelkalyn/Downloads/PMC6614070.riseurology 528:1321–1348. John Wiley & Sons, Ltd.

Xi, Y., S. Noble, and M. Ekker. 2011a. Modeling Neurodegeneration in Zebrafish. Curr. Neurol. Neurosci. Rep. 11:274–282.

Xi, Y., M. Yu, R. Godoy, G. Hatch, L. Poitras, and M. Ekker. 2011b. Transgenic zebrafish expressing green fluorescent protein in dopaminergic neurons of the ventral diencephalon. Dev. Dyn. 240:2539–2547. John Wiley & Sons, Ltd.

Xiang, Q., B. Xu, Y. Ding, X. Liu, Y. Zhou, and F. Ahmad. 2018. Oxidative stress response induced by butachlor in zebrafish Embryo/Larvae: The protective effect of vitamin C. Bull. Environ. Contam. Toxicol. 100:208–215. Springer.

Xing, G., L. Zhang, S. Russell, and R. Post. 2006. Reduction of dopamine-related transcription factors Nurr1 and NGFI-B in the prefrontal cortex in schizophrenia and bipolar disorders. Schizophr. Res. 84:36–56. Elsevier.

Xiong, N., J. Huang, Z. Zhang, Z. Zhang, J. Xiong, X. Liu, M. Jia, F. Wang, C. Chen, and X. Cao. 2009. Stereotaxical infusion of rotenone: a reliable rodent model for Parkinson's disease. PLoS One 4:e7878. Public Library of Science San Francisco, USA.

Xu, M., R. Moratalla, L. H. Gold, N. Hiroi, G. F. Koob, A. M. Graybiel, and S. Tonegawa. 1994. Dopamine D1 receptor mutant mice are deficient in striatal expression of dynorphin and in dopamine-mediated behavioral responses. Cell 79:729–742. United States.

Xu, P.-Y., R. Liang, J. Jankovic, C. Hunter, Y.-X. Zeng, T. Ashizawa, D. Lai, and W.-D. Le. 2002. Association of homozygous 7048G7049 variant in the intron six of Nurr1 gene with Parkinson's disease. Neurology 58:881–884. United States.

Yamada, K., and T. Iwatsubo. 2018. Extracellular α-synuclein levels are regulated by neuronal activity. Mol. Neurodegener. 13:1–8. BioMed Central.

Youle, R. J., and A. M. van der Bliek. 2012. Mitochondrial fission, fusion, and stress. Science 337:1062–1065.

Young, C., and J. Sonne. 2018. Neuroanatomy, Basal Ganglia. StatPearls Publishing, Treasure Island (FL).

Yu, R., S.-B. Jin, U. Lendahl, M. Nistér, and J. Zhao. 2019. Human Fis1 regulates mitochondrial dynamics through inhibition of the fusion machinery. EMBO J. 38.

Yu, S. B., and G. Pekkurnaz. 2018. Mechanisms Orchestrating Mitochondrial Dynamics for Energy Homeostasis. J. Mol. Biol. 430:3922–3941.

Zetterström, R. H., L. Solomin, L. Jansson, B. J. Hoffer, L. Olson, and T. Perlmann. 1997. Dopamine Neuron Agenesis in Nurr1-Deficient Mice. Science (80-.). 276:248 LP – 250.

Zhao, Y., Y. Han, Z. Wang, T. Chen, H. Qian, J. He, J. Li, B. Han, and T. Wang. 2020. Rosmarinic acid protects against 1-methyl-4-phenyl-1,2,3,6-tetrahydropyridine-induced dopaminergic neurotoxicity in zebrafish embryos. Toxicol. Vitr. 65:104823.

Zheng, X., L. Boyer, M. Jin, J. Mertens, Y. Kim, L. Ma, L. Ma, M. Hamm, F. H. Gage, and T. Hunter. 2016. Metabolic reprogramming during neuronal differentiation from aerobic glycolysis to neuronal oxidative phosphorylation. Elife 5:e13374. eLife Sciences Publications, Ltd.

Zimprich, A., S. Biskup, P. Leitner, P. Lichtner, M. Farrer, S. Lincoln, J. Kachergus, M. Hulihan, R. J. Uitti, D. B. Calne, A. J. Stoessl, R. F. Pfeiffer, N. Patenge, I. C. Carbajal, P. Vieregge, F. Asmus, B. Müller-Myhsok, D. W. Dickson, T. Meitinger, T. M. Strom, Z. K. Wszolek, and T. Gasser. 2004. Mutations in LRRK2 cause autosomal-dominant parkinsonism with

pleomorphic pathology. Neuron 44:601–607. United States.

Zorov, D. B., M. Juhaszova, and S. J. Sollott. 2014. Mitochondrial reactive oxygen species (ROS) and ROS-induced ROS release. Physiol. Rev. 94:909–950.

Zupanc, G. K. H., K. Hinsch, and F. H. Gage. 2005. Proliferation, migration, neuronal differentiation, and long-term survival of new cells in the adult zebrafish brain. J. Comp. Neurol. 488:290–319. John Wiley & Sons, Ltd.